Immunometabolic Factors Associated with Variations in Body Composition and Exercise Response in Diet-Sensitive and Diet-Resistant Women with Obesity

By:

Breana Grace Hooks

Research Thesis submitted to the University of Ottawa

in partial fulfillment of the requirements for a degree of

Master of Science in Biochemistry

Supervisor: Mary-Ellen Harper, PhD

Department of Biochemistry, Microbiology, Immunology

Faculty of Medicine, University of Ottawa

Abstract

Over the past 20 years, our collaborative research team at the Ottawa Hospital and the University of Ottawa have extensively investigated molecular and metabolic differences between individuals with obesity in the highest (DS) and lowest (DR) quintiles for rate of weight loss following 6 weeks of caloric restriction. Research on these cohorts of individuals with extreme phenotypes in diet-response has revealed that DS individuals have several skeletal muscle metabolic advantages, including increased proportions of type I oxidative fibres, increased mitochondrial proton leak, enhanced fatty acid metabolism, and a greater antioxidant capacity. Regular physical exercise provides a vast array of beneficial effects to metabolic health, including increases in skeletal muscle mitochondrial bioenergetic capacity and muscle cross-sectional area, leading to the hypothesis that exercise may be particularly beneficial to women with diet-resistant obesity. The overall aim of this thesis was to determine whether six weeks of exercise training improves skeletal muscle mitochondrial function and attenuates chronic low-grade inflammation in women with obesity previously identified as diet-sensitive (DS) and diet-resistant (DR). Here, we demonstrate that exercise training improves body composition, enhances cellular maximal respiration, and increases mitochondrial length preferentially in DR women. Contrary to our hypothesis, exercise training increased skeletal muscle IKK-NFκB inflammatory signaling to a greater extent in DR individuals, despite improvements in systemic cytokine concentrations. In response to an inflammatory challenge, LPS-treated primary myotubes derived from DR and DS skeletal muscle responded similarly and respiratory capacity was preserved. Taken together, these findings suggest that exercise can be especially beneficial as part of a treatment plan for DR individuals, and that DS and DR skeletal muscle have systemic and mechanistic differences in inflammatory responses.

Acknowledgements

First and foremost, I would like to thank Dr. Mary-Ellen Harper for accepting me into her lab and for being such a welcoming and supportive supervisor. You have given me the opportunity to experience and appreciate research in a new light – your passion and knowledge are inspiring. You truly allowed me to grow as a scientist and develop my interests in the fields of metabolism and immunometabolics. Your support allowed me to succeed and thrive throughout my Honour's and Master's programs.

I would like to thank Dr. Chantal Pileggi for her continuous support and valuable guidance throughout this project. You gave me the fundamental knowledge and confidence to work independently. Thank you for being the best teacher I could have asked for over the past three years. Your patience in answering all my questions, troubleshooting experiments, and reading draft after draft of TAC reports and thesis revisions is commendable – I could not have done it without you! The time that you put into supporting both my academic and personal endeavours is invaluable, and I am beyond grateful for the great mentor and friend that you have become.

To Dr. Katey Rayner and Dr. Morgan Fullerton, thank you for being my TAC members. Thank you for offering me new and exciting ideas for experiments, and for creating a space where I felt comfortable discussing the shortcomings of my work. Your collaboration and expertise helped me to develop the full scope of my project.

Finally, I would like to thank all the members of the Mitochondrial Bioenergetics Laboratory for their guidance and friendship throughout the completion of this project. Special mentions go out to former lab members, Nina Hadžimustafić, Gaganvir Parmar, and Hussein Elkhatib, you have all uniquely contributed to my experience in the Harper Lab. To Hussein, thank you for your help pipetting all my BCAs and cell culture upkeep when I had hundreds of flasks.

To Gaganvir, thank you for your patience when I was so high energy and needed someone to talk to. And to Nina for her support, kindness, and friendship; thank you for being the first to welcome me to the Harper lab and for still putting up with me three years later. You all made the experience of completing a Master's project during a global pandemic more enjoyable!

Lastly, to thank my family and friends: my mum Tess, my brother Conor, my aunt Jane, my uncle Greg, my partner Alex, and my best friends Jade, Sarah, Lindsay, Sam, and Zoë for their love and support in every aspect of my life, but especially during the completion of this project. Absolute love and appreciation to my mum and Alex for getting me through the highest highs and the lowest lows over the past two years – thank you for helping me get to the end of this endeavour!

Current Lab Members

Principal Investigator

Mary-Ellen Harper, Ph.D.

Post-Doctoral Fellows

Chantal Pileggi, Ph.D.

Laboratory Technician

Jian Xuan

Ph.D. Students

Claire Fong-McMaster

Nidhi Kuksal

Michel Kanaan

Master's Students

Luke Kennedy

Table of Contents

List of Tables

List of Figures

List of Abbreviations

2DG	–	2-deoxy-D-glucose
ADP	–	Adenosine diphosphate
Akt (PKB)	–	Ak strain transforming (Protein kinase B)
AMA	–	Antimycin A
AMP	–	Adenosine monophosphate
AMPK	–	AMP-activated protein kinase
ANOVA	–	Analysis of variance
ANT	–	Adenine nucleotide translocase
APS	–	Ammonium persulfate
ATP	–	Adenosine triphosphate
B lymphocyte	–	Bone marrow lymphocyte
β-NGF	–	Beta-nerve growth factor
BCA	–	Bicinchoninic acid
BDNF	–	Brain-derived neurotrophic factor
BL	**–**	**Baseline**
BMI	–	Body mass index
BSA	–	Bovine serum albumin
cAMP	–	Cyclic adenosine monophosphate
CAT	–	Carboxyatractyloside
CI (NDUFB8)	–	Complex I (NADH dehydrogenase [ubiquinone] 1 beta subcomplex subunit 8)
CII (SDHB)	–	Complex II (Succinate dehydrogenase complex iron sulfur subunit B)
CIII (UQCRC2)	–	Complex III (Ubiquinol-cytochrome C reductase core protein 2)
CIV (COXII)	–	Complex IV (Cytochrome c oxidase subunit 2)
CoA	–	Coenzyme A
CoQ	–	Coenzyme Q (Ubiquinone)
CPT1	–	Carnitine palmitoyltransferase 1

CTACK	–	Cutaneous T cell-attracting chemokine (C-C motif chemokine ligand 27 [CCL27])
CS	–	Citrate synthase
CV (ATP5A)	–	Complex V (ATP synthase F1 complex, alpha subunit)
Cyt C	–	Cytochrome complex
DMEM	–	Dulbecco's modified Eagle's medium
DNA	–	Deoxyribonucleic acid
DR	**–**	**Diet-resistant**
Drp1	–	Dynamin-related protein 1
DS	**–**	**Diet-sensitive**
DTNB	–	5,5′-dithiobis-(2-nitrobenzoic acid) (Ellman's reagent)
DTT	–	Dithiothreitol
DEXA	–	Dual-energy X-ray absorptiometry
ECAR	–	Extracellular acidification rate
EDTA	–	Ethylenediaminetetraacetic acid
EPO	–	Erythropoietin
ER	–	Endoplasmic reticulum
ERK	–	Extracellular-signal-regulated kinase
ETC	–	Electron transport chain
FA	–	Fatty acid
$FADH_2$	–	Flavin adenine dinucleotide
FAO	–	Fatty acid oxidation
FCCP	–	Carbonyl cyanide-p-trifluoromethoxy-phenylhydrazone
FFM	–	Fat-free mass (Lean mass)
FGF-21	–	Fibroblast growth factor 21
FSH	–	Follicle-stimulating hormone
G-CSF	–	Granulocyte colony-stimulating factor
GAPDH	–	Glyceraldehyde 3-phosphate dehydrogenase
GLP-1	–	Glucagon-like peptide 1
GLUT4	–	Glucose transporter type 4

GPx	–	Glutathione peroxidase
GSH	–	Glutathione (γ-glutamyl-cysteinyl-glycine)
GSSG	–	Glutathione disulphide
GTP	–	Guanosine triphosphate
GTPase	–	Guanosine triphosphatase
GWAS	–	Genome-wide association studies
HbA1c	–	Glycated hemoglobin A1c
HEPES	–	Hydroxyethyl piperazineethanesulfonic acid
HIF1α	–	Hypoxia-inducible factor 1-alpha
HPLC	–	High-performance liquid chromatography
HRP	–	Horseradish peroxidase
IFN	–	Interferon
IGF-1	–	Insulin-like growth factor 1
IKK	–	IκB kinase
IL	–	Interleukin
IR	–	Insulin resistance
IκB	–	Inhibitor of NFκB
JAK	–	Janus kinase
JNK	–	c-Jun N-terminal kinase
Jun	–	Encoded by JUN proto-oncogene
kcal	–	Kilocalorie
KRH (KHB)	–	Krebs-Ringer HEPES buffer
LC3	–	Microtubule-associated light chain protein 3
LH	–	Luteinizing hormone
LPS	–	Lipopolysaccharide
MAPK	–	Mitogen-activated protein kinase
MAPKK	–	Mitogen-activated protein kinase kinase
MCP	–	Monocyte chemoattractant protein
METs	–	Metabolic equivalents

MFN1/2	–	Mitofusin 1/2
MIP	–	Macrophage inflammatory protein
MiR05	–	Mitochondrial respiration media
MPA	–	Meta-phosphoric acid
mRNA	–	Messenger ribonucleic acid
mTOR	–	Mammalian target of rapamycin
MuRF1	–	Muscle RING-finger protein 1
NADH	–	Nicotinamide adenine dinucleotide
NADPH	–	Nicotinamide adenine dinucleotide phosphate
NEAT	–	Non-exercise activity thermogenesis
NFκB	–	Nuclear factor kappa-light-chain-enhancer of activated B cells
NLR	–	NOD-like receptor
NNT	–	Nucleotide transhydrogenase
NOD	–	Nucleotide-binding oligomerization domain
Nrf2	–	Nuclear factor erythroid 2-related factor 2
O_2^-	–	Superoxide
OCR	–	Oxygen consumption rate
OH^-	–	Hydroxyl radical
OMM	–	Outer mitochondrial membrane
OPA1	–	Optic atrophy protein 1
OXPHOS	–	Oxidative phosphorylation
PBS	–	Phosphate-buffered saline
PCG1α	–	Peroxisome proliferator-activated receptor-gamma coactivator 1 alpha
PET	**–**	**Post-exercise training**
PFK	–	Phosphofructokinase
phospho (p)	–	Phosphorylated
P_i	–	Inorganic phosphate
PIC	–	Protease inhibitor cocktail
PINK1	–	PTEN-induced putative kinase 1

PKRN	–	Parkin
PMF	–	Protonmotive force
PTEN	–	Phosphatase and tensin homolog
PYY	–	Peptide tyrosine tyrosine
R-PLEX	–	Custom assay design
Redox	–	Reduction-oxidation
Rel	–	Encoded by REL proto-oncogene
RER	–	Respiratory exchange ratio
RIPA	–	Radioimmunoprecipitation assay
RNA	–	Ribonucleic acid
ROS	–	Reactive oxygen species
ROWL	**–**	**Rate of weight loss**
RQ	–	Respiratory quotient
SD	–	Standard deviation
SDF1α	–	Stromal cell-derived factor 1 alpha
SDS	–	Sodium dodecyl sulfate
SEM	–	Standard error of the mean
SHBG	–	Sex hormone-binding globulin
SLC7A11	–	Solute carrier family 7 member 11 (Cystine/glutamate antiporter [xCT])
SOD	–	Superoxide dismutase
STAT	–	Signal transducer and activator of transcription
T lymphocyte	–	Thymus lymphocyte
T2DM	–	Type II diabetes mellitus
TARC	–	Thymus- and activation-regulated chemokine (C-C motif chemokine ligand 17 [CCL17])
TBS-T	–	Tris-buffered saline with Tween 20
TCA	–	Tricarboxylic acid
TEMED	–	Tetramethylethylenediamine
TFA	–	Trifluoroacetic acid

TLR	–	Toll-like receptor
TNFα/β	–	Tumour necrosis factor alpha/beta
TOM20	–	Translocase of outer membrane receptor complex
U-PLEX	–	Custom multiplex of assays
UCP	–	Uncoupling protein
VCO_2	–	Rate of carbon dioxide elimination
VEGF	–	Vascular endothelial growth factor
VO_2	–	Rate of oxygen consumption

Introduction

1.1 Obesity

1.1.1 Obesity and weight loss

The worldwide prevalence of obesity, and obesity-related diseases, has risen dramatically in the past half-century. According to the World Health Organization, the majority of the world's population live in countries where being overweight or obese leads to the death of more people than being underweight, with over one-third of the global adult population currently classified as overweight[1]. Within Canada, 63.1% of the population was defined as overweight or obese in 2018, with 26.8% of Canadian adults classified as having obesity. The economic burden of obesity within Canada was estimated to be $7 billion in 2011, which was expected to increase to $9 billion by 2021[2]. Obesity is defined as having a body mass index (BMI) of 30 kg/m^2 or greater, where BMI is defined as a person's weight in kilograms divided by the square of the person's height in meters (kg/m^2)[1]. Obesity is associated with increased risks of developing many chronic diseases including, cardiovascular disease, type II diabetes mellitus (T2DM), musculoskeletal disorders and some cancers[1].

The fundamental etiology of obesity is an imbalance between energy intake and energy expenditure. Most frequently this is caused by an increase in caloric intake (*i.e.*, an energy-dense diet) and a decrease in physical activity. It is a complex, multifactorial disease involving the buildup of excess body fat and the expansion of adipose tissue which leads to increases in body mass and BMI. Although the excess body fat is predominantly stored in adipose tissues, it is also deposited ectopically in tissues such as liver and skeletal muscle. Another indicator of obesity is a modified profile of circulating plasma cytokine concentrations. Individuals with obesity tend to

have higher levels of pro-inflammatory cytokines (*e.g.*, TNFα, IL-6, leptin)[3,4] and lower levels of gut hormones associated with appetite control (*e.g.*, PYY, GLP-1, ghrelin)[3,5,6].

Treatments for obesity aim to induce negative energy balance, and options are currently limited to behaviour modifications (including diet and exercise), interdisciplinary behaviour interventions which frequently include cognitive behavioral therapy and dietary counselling, medications that suppress appetite or macronutrient absorption, and bariatric surgery. Lifestyle modification-based weight loss programs are the most commonly used methods, however, there is high interindividual variability in response to these treatments[7]. Behavioural programs often use very low-calorie total meal replacements in combination with behavioural counselling. Such programs can be successful at achieving and maintaining ~5-8% weight loss[8,9]. Genome-wide association studies (GWAS) have identified numerous genetic factors that contribute to individual responses to weight loss and weight gain[10–12]. In addition, differences in metabolic efficiency are an important contributor to weight loss response[7,13].

1.1.2 Obesity and skeletal muscle

Skeletal muscle accounts for about 40% of the average adult human body mass and contributes significantly to the determinant of whole-body energy expenditure. Even at rest, skeletal muscle accounts for approximately 20% of resting metabolic rate[14]. Skeletal muscle energy expenditure is also highly variable and changes dramatically from resting to maximal physical activity, during which muscle O_2 consumption can account for up to 90% of the whole-body oxygen uptake[14]. Skeletal muscle is strongly dependent on mitochondria for cellular energy transduction to produce ATP[15]. To successfully produce ATP, the muscle needs oxygen and a

source of carbon, predominantly fatty acids (FA), or postprandially, glucose, when it is abundant in the blood. Indeed, skeletal muscle accounts for 70-80% of postprandial glucose uptake[16].

The efficiency of skeletal muscle mitochondrial energy transduction is linked to adaptive thermogenesis, obesity susceptibility, and rate of weight loss in obesity[17]. Patients with obesity have lower proportions of oxidative type I fibres in skeletal muscle compared to proportions in the muscle tissue of lean controls[18–22]. Type I fibres are highly oxidative and dense in mitochondria, and the percentage of type I fibres inversely correlates with body fat percentage and insulin sensitivity[22–25]. Additionally, there is a positive association between type IIX (glycolytic) muscle fibres and BMI[26]. These findings support the conclusion that variation in skeletal muscle fibre size and composition are associated with weight loss variability and propensity for weight gain.

The metabolic consequences of obesity in skeletal muscle[27–36] include increased fatty acid uptake[37], increased oxidative stress[38], impaired insulin signaling[29], reduced and incomplete fatty acid oxidation[39,40], reduced mitochondrial content[41], and chronic activation of inflammatory pathways[42,43]. Together these metabolic consequences of obesity hinder skeletal muscle regenerative capacity[44]. Due to the effects of obesity on lipid metabolism, it results in elevated levels of lipid deposition in skeletal muscle and increased circulating lipid metabolites, which can reach toxic levels and have a negative impact on skeletal muscle repair and maintenance[45].

The balance between skeletal muscle hypertrophy and atrophy is dysregulated in obesity. It is hypothesized that this is largely due to decreased activity of Akt and mTOR signaling pathways. Several factors of obesity may be leading to these observed disruptions including lipid toxicity and low-grade systemic inflammation[45]. Such imbalances can lead to the functional limitations observed in individuals with obesity. Despite consistent observations that individuals

with obesity have greater absolute maximum muscle strength compared to lean counterparts, when normalized to body mass, individuals with obesity appear weaker[46].

1.2 Mitochondria

1.2.1 Oxidative phosphorylation

Mitochondria are intracellular organelles with a biologically critical function; they are an important site of cellular energy transduction for the formation of adenosine triphosphate (ATP). Mitochondria have two membranes, inner and outer, separated by an intermembrane space. They receive reducing equivalents from a series of oxidative processes including glycolysis, fatty acid oxidation, and the tricarboxylic acid (TCA) cycle, which feed into the electron transport chain (ETC) to produce a protonmotive force (PMF) across the inner membrane. The PMF is then used to drive ATP synthesis through a process referred to as oxidative phosphorylation (OXPHOS)[47].

The TCA cycle produces the reducing equivalents in the forms of nicotinamide adenine dinucleotide (NADH) and flavin adenine dinucleotide ($FADH_2$), which carry electrons to the ETC. The ETC is composed of four multiprotein complexes, that catalyze a series of redox reactions, which ultimately drive ATP production. Electrons are transferred through complexes I-IV, facilitated by electron carriers, coenzyme Q (CoQ), and cytochrome C (cyt C); protons are pumped by complexes I, III and IV from the matrix to the intermembrane space. The proton gradient that forms is used by ATP-synthase (complex V) to allow protons to leak back into the matrix and, in the process, synthesize ATP from inorganic phosphate (P_i) and adenosine diphosphate (ADP)[47].

The system is referred to as “coupled” when protons come back into the matrix almost exclusively through ATP-synthase to form ATP. However, protons also come in through the phosphate carrier and nicotinamide nucleotide transhydrogenase (NNT) during coupled OXPHOS.

Alternative pathways dissipate the proton gradient through the return of protons to the mitochondrial matrix, which does not result in ATP formation. These proton leak reactions are also referred to as "uncoupled" respiration[48]. The mechanisms of uncoupled respiration are not fully understood, although inner mitochondrial membrane proteins, including uncoupling proteins (UCPs)[49] and adenine nucleotide translocase (ANT)[50], have been shown to facilitate proton leak.

UCPs belong to the five-member mitochondrial anion carrier protein family[51]. UCP1 is widely studied in the context of cold-induced thermogenesis and is expressed exclusively in brown adipocytes. UCP3 is the only UCP expressed in skeletal muscle at the protein level and is also expressed in brown adipocytes and cardiac muscle cells[52]. ANT is responsible for the exchange of cytosolic ADP for mitochondrial ATP[50]. Up to 50% of proton leak that occurs in skeletal muscle is attributed to ANT, up to two-thirds of which is independent of its ADP/ATP exchange function[53]. After endurance exercise training, ANT protein expression in skeletal muscle increases, whereas UCP3 protein expression remains unchanged[54].

In tissues beyond brown adipose, proton leak is reciprocally related to ATP demand. It has been estimated that mitochondrial proton leak accounts for about 50% of the resting respiration rate in skeletal muscle of rats and approximately 20% of their standard metabolic rate[48]. There is considerable evidence to suggest that UCPs are activated in the presence of reactive oxygen species (ROS), presumably in a negative feedback mechanism to prevent further ROS production by the mitochondrial electron transport chain[55,56]. Overall UCP3 activity is thought to be significant, as research has demonstrated that in addition to increasing proton leak, it is associated with lower ROS production[57] and improved fatty acid oxidation[58,59].

1.2.2 Reactive oxygen species

ROS are a natural, but not proportional, by-product of mitochondrial respiration[60]. During the reduction of O_2 to H_2O, reactive intermediates, superoxide (O_2^-), hydrogen peroxide (H_2O_2), and hydroxyl radical (OH^-), are generated[61]. At low concentrations, ROS act as an important signaling molecule, but when they are being produced in larger quantities ROS contribute to cellular oxidative stress[62]. The gradual accumulation of oxidative damage leads to declines in cellular and tissue functions associated with aging[63]. Therefore, cells employ a variety of mechanisms to keep ROS within a tolerable range. Specifically, O_2^-, produced by the ETC, is rapidly dismutated into H_2O_2 by superoxide dismutase (SOD). H_2O_2 is substantially more stable than superoxide – it can traverse membranes and be further detoxified to H_2O with the help of catalase and glutathione peroxidases (GPx). GPxes performs a reduction reaction using glutathione (GSH) as an electron donor and producing GSSG (its oxidized form) as an end product[64]. Importantly, in addition to its role in maintaining redox homeostasis, glutathione is also thought to play a key role in the regulation of mitochondrial morphology[65]. The ratio of reduced to oxidized glutathione within cells is often used as a marker of cellular redox status[64]. In a resting cell, the GSH:GSSG ratio is approximately 100:1, however, in a state of oxidative stress, this ratio is often decreased to 10:1, or even 1:1[66]. Depletion of the GSH:GSSG ratio results in hyperfusion of the mitochondrial reticulum[65], which may contribute to altered mitochondrial function.

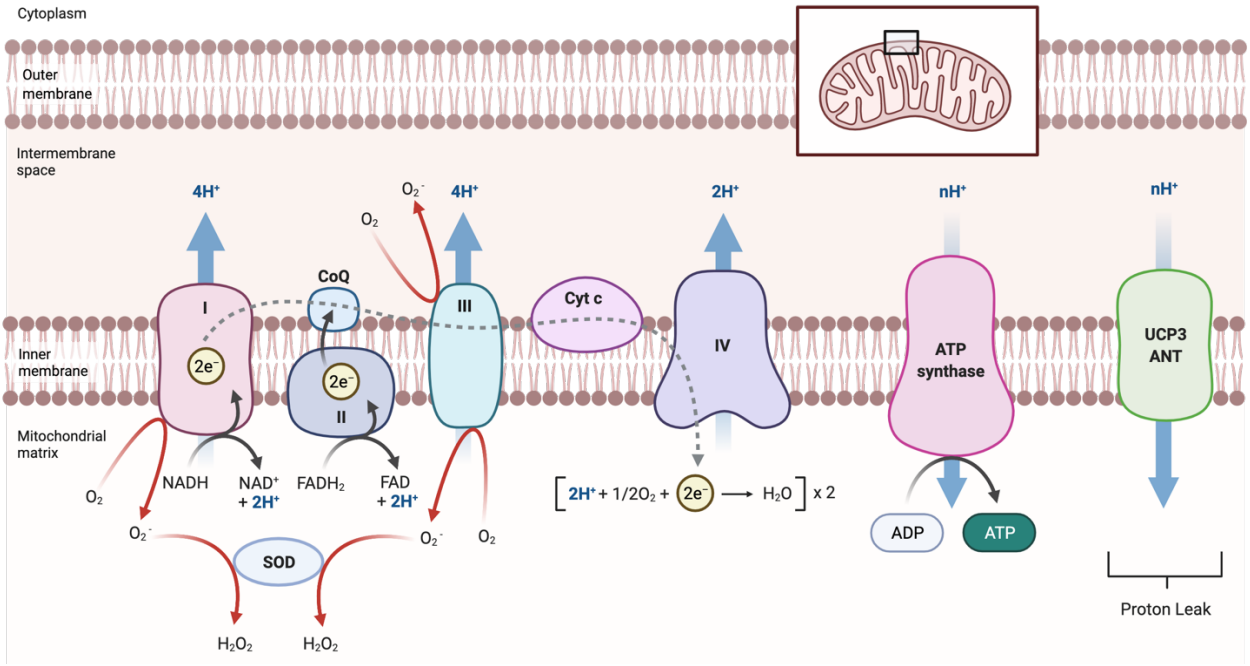

Figure 1. Mitochondrial oxidative phosphorylation, proton leak, and ROS production. Reducing equivalents enter the ETC at either CI or CII, and electrons systematically pass through the respiratory complexes (CIII and CIV) to the final electron acceptor, O_2. Protons are released into the intermembrane space as electrons move through CI, CIII and CIV, which establishes a PMF then used to drive ATP synthesis through CV (ATP synthetase). Mitochondrial proton leak is facilitated by proteins located on the inner mitochondrial membrane including UCPs and ANT. O_2 can be reduced to O_2^- by liberated electrons from CI and CIII. O_2^- can be rapidly dismutated into H_2O_2 by SOD. Direction of electron flow is indicated by the grey-dotted line. Proton extrusion or import is indicated by blue arrows. *Figure created with BioRender.com*.

1.2.3 Mitochondrial dynamics and mitophagy

Mitochondria are highly dynamic organelles that are continuously undergoing ultrastructural re-organization. In skeletal muscle, it is normal to see mitochondria form a branched reticulum network close to the endoplasmic reticulum (ER) and nucleus[67–69]. Mitochondrial fission, fusion, and mitophagy play critical roles in maintaining functional mitochondria when cells experience metabolic or environmental stressors. Fusion merges opposing mitochondrial membranes together, whereas fission disrupts a parent mitochondrion and allows fragments of the mitochondria to disassociate. Fusion uses a process of complementation

by mixing the contents of partially damaged mitochondria, which can be used to help mitigate stress[70]. Fission is needed to create new mitochondria, but it is also necessary to eliminate damaged mitochondria from the network during high levels of cellular stress[70].

Mitochondrial ultrastructure is governed by large guanosine triphosphatase (GTPase) proteins that control fusion and fission events. Outer mitochondrial membrane fusion is controlled by mitofusins 1 and 2 (MFN1/2) and inner mitochondrial membrane fusion is controlled by optic atrophy protein 1 (OPA1)[70]. MFN1 facilitates membrane docking and fusion by irreversibly tethering opposing outer membranes of adjacent mitochondria and inducing conformational changes mediated by GTP hydrolysis[71–73]. MFN2 also helps with outer membrane tethering, but additionally, plays an important role in connecting mitochondria to the endoplasmic reticulum to regulate Ca^{2+} uptake[74]. To complete the fusion process, OPA1 tethers the inner mitochondrial membranes[75].

Fission is promoted by the cytosolic GTPase protein, dynamin-related protein 1 (Drp1). This protein forms ring-like spiral structures that constrict around the budding membrane at sites of mitochondrial ER contact[76–78]. Fission terminates when the budding mitochondria are completely severed by the full constriction of the Drp1 ring. This occurs when GTPase domains connect, resulting in GTP hydrolysis and a conformational change that causes the constriction of Drp1[79].

Autophagy is a catabolic process to sequester and recycle damaged cellular components by lysosomal degradation. Autophagy of mitochondria, referred to as mitophagy, is a protective mechanism that clears the cell of damaged mitochondria to prevent cellular apoptosis[80]. PTEN-induced putative kinase 1 (PINK1) is a serine/threonine kinase, that accumulates on the outer mitochondrial membrane (OMM) of damaged mitochondria. The accumulation of PINK1 on the

OMM recruits and phosphorylates parkin (PRKN), an E3 ubiquitin ligase. Active PRKN mediates the ubiquitination of OMM proteins, including MFN1/2[81,82]. The accumulation of ubiquitinated proteins leads to the recruitment of autophagy machinery and the degradation of damaged mitochondria[83,84]. The contribution of the PINK1/PRKN pathway to mitophagy in skeletal muscle is not well understood. PINK1 has not been shown to accumulate during exercise-induced mitophagy, suggesting that mitophagy in skeletal muscle may be upregulated through a different pathway[85]. PRKN has been shown to alter mitophagic flux in skeletal muscle, but again it is unclear whether this occurs through the PINK1/PRKN pathway[86].

1.3 Immunity and Inflammation

1.3.1 The immune response

The immune response is broken down into innate immunity, which an organism is born with, and adaptive immunity, which an organism acquires following disease exposure. Innate immunity, also known as genetic or natural immunity, is encoded in the genes and offers lifelong protection. The innate immune response is fast-acting and non-specific, meaning that the response is the same no matter the specific virus or bacteria that it detects. It includes physical barriers, chemical barriers, and cellular defences[87].

Adaptive immunity is an organism's acquired immunity to a specific pathogen. Adaptive immunity is a slow-acting, specific response – through memory cells, it can last an organism's entire lifespan, but does not always. The adaptive immune response is characterised by the release of T and B lymphocytes, which leads to many copies of specific antibodies to neutralize or destroy their target antigen[88].

Inflammation is an essential response of innate immunity which can be induced by microbial infection or tissue damage. Inflammatory responses are elicited to provide broad-spectrum protection against infections and induce the adaptive immune response for long-term protection against specific pathogens[89]. However, chronic and uncontrolled inflammation can cause severe tissue damage resulting in major pathogenicity from an overactive immune system[42,43]. Because of this, there are many regulatory mechanisms in place to control the initiation, progression and resolution of inflammation induced by an immune response.

Nuclear factor κB (NFκB) is considered a master regulator of inflammation. NFκB comprises a family of five inducible transcription factors including NFκB1 (p50), NFκB2 (p52), RelA (p65), RelB, and c-Rel[90]. Activation of the canonical NFκB pathway is responsible for the transcriptional induction of proinflammatory cytokines, chemokines, and additional inflammatory mediators in different types of innate immune cells[90]. The canonical pathway is activated through surface receptors, TLRs, which then initiate an intracellular signaling cascade. When inflammation is not being activated, IκB proteins are bound to NFκB and inhibit translocation of NFκB into the nucleus. The cascade begins with activation of IκB kinase (IKK). Active IKK phosphorylates IκB which results in its degradation by the proteasome and the subsequent release of NFκB[91,92]. NFκB can now translocate into the nucleus and complete its function as a transcription factor. Preliminary evidence also suggests that NFκB activation stimulates mitochondrial fusion[93], promotes mitochondrial dysfunction[94] and the degradation of mitochondria by mitophagy[95].

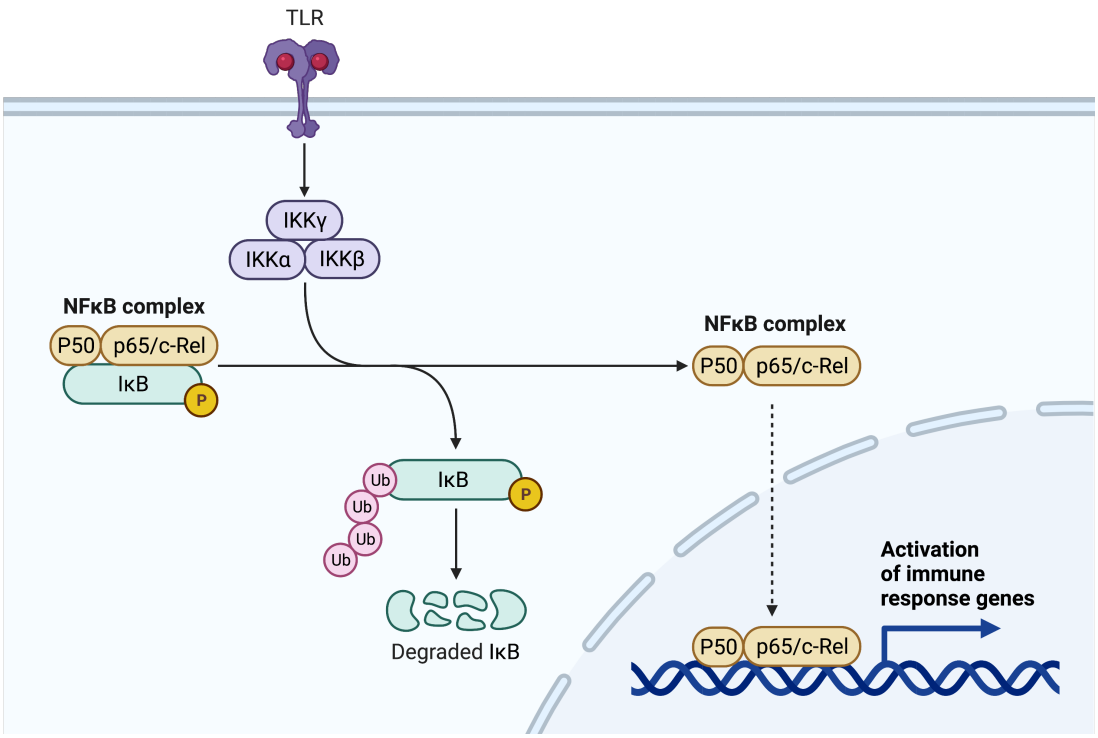

Figure 2. Canonical IKK-NFκB signaling pathway. IKK-NFκB signaling is activated through binding of a ligand to TLR surface receptors. This initiates an intracellular signaling cascade beginning with activation of the IκB kinase complex (IKK complex). Active IKK phosphorylates IκB which results in its degradation by the proteasome and the subsequent release of the NFκB complex. NFκB then translocates into the nucleus and initiates the transcription of several immune response genes. *Figure created with BioRender.com*.

The MAPK pathway is another commonly activated inflammatory response. MAPKs are a family of serine/threonine protein kinases and, in humans, include ERK1/2, JNK and p38 MAPK[96]. Their activation involves a series of at least three kinases, referred to simply as MAPK kinases (MAPKK), which in turn phosphorylate and activate the next kinase in the pathway until the terminal kinases are activated which phosphorylate and activate their respective transcription factors[97]. Like NFκB, the transcription factors translocate to the nucleus where they initiate transcription of genes to further promote the inflammatory response.

The final commonly activated pathway in an inflammatory response is the JAK/STAT pathway. JAKs are receptor-associated proteins that are activated by ligands and phosphorylate

one another. Their phosphorylation initiates the binding of STATs, which, once bound to JAKs are then also phosphorylated. STATs are cytoplasmic transcription factors that remain inactive until their phosphorylation and subsequent dimerization. Once in their active form, STATs also translocate to the nucleus and initiate inflammatory gene transcription[98].

1.3.2 Inflammatory nature of obesity

Obesity is associated with chronic low-grade inflammation in skeletal muscle and adipose tissue. There is evidence that chronic activation of pro-inflammatory signaling contributes to the development and progression of metabolic disorders such as insulin resistance, and T2DM. This inflammatory response is triggered by circulating pro-inflammatory cytokines such as interleukin-6 (IL-6), tumour necrosis factor-α (TNFα) and high concentrations of free fatty acids (FAs), such as palmitate[99,100]. All these proinflammatory cytokines go on to activate inflammatory signaling pathways which may lead to disturbances in mitochondrial morphology.

The metabolic consequences of obesity include increased fatty acid uptake[37], increased oxidative stress[38], and reduced or incomplete fatty acid oxidation[39,40]. As such, ferroptosis may also be induced in skeletal muscle tissue in individuals with obesity. Ferroptosis is a specific type of regulated cell death, which is iron- and ROS-dependent. The morphology of ferroptosis is distinct from other types of regulated cell death and can be characterised by the presence of smaller than normal mitochondria with condensed mitochondrial membrane densities, reduction or vanishing of mitochondria cristae, and outer mitochondrial membrane rupture[101–103]. Induction of ferroptosis can be recognized by the accumulation of lipid peroxidation products and lethal ROS[102,104]. Simply put, lipid peroxidation is the oxidative modification of lipids. Because of the pathways involved in the induction of ferroptosis, it can be inhibited by iron chelators, and lipid

peroxidation inhibitors, as well as, several other proteins that limit ROS production and reduce cellular iron uptake, including GPxes as previously discussed. On the other hand, ferroptosis can be induced through enzymes that promote ROS production, such as NADPH oxidase and p53.

1.3.3 Immunometabolism in skeletal muscle

Immunometabolism is an emerging field which investigates the interplay between the immune system and metabolism. Such investigations are especially important within the context of whole-body disorders, such as obesity. Nutrient overload and excess adipose tissue lead to increases in immune responses and overall inflammation. Moreover, tissues in the body, including adipose and skeletal muscle, are populated with immune cells, which can affect cellular metabolism within those tissues[42]. Additionally, skeletal muscle is recognized as a secretory organ which can release cytokines and myokines that communication with the immune system, or exert their effects within the muscle itself[105–107].

Within the context of mitochondria, chronic inflammatory conditions can alter a lot of important dynamic processes and promote mitochondrial dysfunction. In general, it leads to decreased biogenesis[108], decreased fusion, and increased fission events[94], as well as increased mitophagy, which correspond with a buildup of ROS and a reduction of PCG1α in the muscle cells[94,109]. However, the effects of inflammation on mitochondria are not unidirectional, as recent literature suggests that mitochondria also play a critical role as regulators of the inflammatory response.

Because of mitochondria's role in ROS production, they have been implicated in redox-sensitive inflammatory responses, including the activation of inflammasomes[110,111]. NOD-like receptors (NLR) are a family of cytosolic receptor proteins that, under certain conditions, are

capable of forming multiprotein complexes, termed inflammasomes[112]. Like other inflammatory signaling pathways, activation of inflammasomes leads to the processing and secretion of other proinflammatory cytokines, notably IL-1β. Inflammasomes can be activated through a number of mechanisms, not all of which are well understood, regardless, inflammasome activation is impaired by the inhibition of complex I or III of the mitochondrial respiratory chain[110,111]. In addition to their roles in inflammation, inflammasomes can regulate glucose and lipid metabolism, making them key players in the development of obesity, insulin resistance, and T2DM[112–114].

1.4 Molecular Basis of Diet-Resistant Obesity

1.4.1 Variability in weight loss

Researchers at the Ottawa Hospital Weight Management Program (OHWMP) observed a 10-fold variability in the rate of weight loss (ROWL) in the first 6 weeks of an intensively supervised 900 kcal/day meal replacement program in a cohort of 832 patients with obesity[115]. Once the data were corrected for factors known to affect weight loss (initial weight, age, sex, medical conditions including thyroid status and medications), a 2-fold variability remained, suggesting that there may be a biological basis for the observations (Figure 3)[57].

To further characterise factors potentially causing differences in weight loss response, otherwise healthy and highly compliant female participants of the OHWMP were grouped into quintiles based on rate of weight loss after 6 weeks on the Optifast (Nestlé) 900 kcal/day caloric-restricted diet. The women in the top 20% for rate of weight loss were classified as Diet-Sensitive (DS), and the women in the bottom 20% were classified as Diet-Resistant (DR) (Figure 3)[57]. Over the past 20 years, researchers have continued to identify key differences in skeletal muscle composition and metabolism between DS and DR individuals[12,57,116]. Importantly, ROWL in

response to caloric restriction is also predictive of weight loss success in patients who proceed with bariatric surgery[117], highlighting the importance of understanding the mechanisms that determine this response.

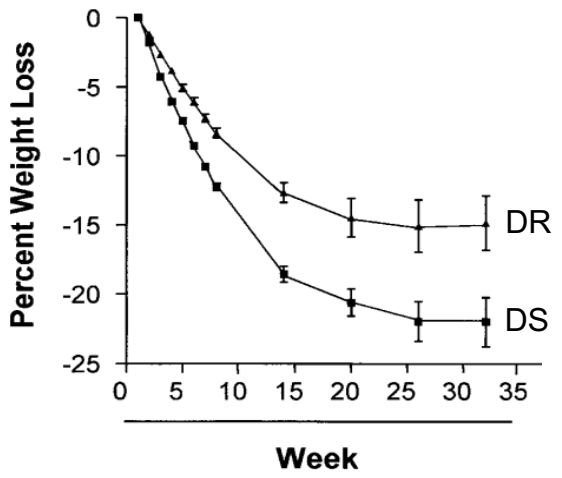

Figure 3. Weight loss in response to a 900 kcal/day diet varies by 2-fold in adherent patients matched for biological sex, age, and BMI. Women in the highest quintile for rate of weight loss [diet-sensitive (DS)] are compared with those in the lowest quintile for rate of weight loss [diet-resistant (DR)]. Data are corrected for factors known to affect weight loss (initial weight, age, sex, medical conditions including thyroid status and medications). *Figure modified from Harper et al*[57].

Differences in energy expenditure and resting metabolic rate (RMR) can also contribute to the risk for obesity development[13]. Energy expenditure is the sum of basal metabolic rate (~60% of total energy expenditure), the thermic effect of feeding (~10% of total energy expenditure), and non-resting energy expenditure (~30% of energy expenditure). Non-resting energy expenditure can be further divided into energy expenditure from voluntary physical activity (*i.e.*, exercise) and non-exercise activity thermogenesis (NEAT) which encompasses non-volitional movements, such as fidgeting[118,119]. As such, non-resting energy expenditure is the most affected by changes in body weight, and therefore also the most variable and controllable component of total energy

expenditure[120,121]. Energy expenditure from physical activity is important in defining both skeletal muscle mass and metabolism. Specifically, physical activity activates ATP hydrolysis for muscle contraction and increases energy expenditure.

Energy expenditure demonstrates high interindividual variation[122], which evidence suggests has a strong genetic component – highly similar RMRs have been observed between monozygotic versus dizygotic twins[123], and siblings within the same family[13]. Moreover, one's own energy expenditure is ever-changing and will naturally fluctuate throughout one's lifetime. Low 24-hour energy expenditure has been associated with weight gain over the course of two years[13]. Additionally, low RMR in late childhood has been associated with greater weight gain in adolescence[124]. Increases in body weight are generally accompanied by increases in fat-free mass (FFM) [125]. As such, when obesity develops, there can be increases in both total energy expenditure and RMR[125–128].

1.4.2 Mitochondrial dysfunction in diet-resistant obesity

Over the past 20 years, the Harper Laboratory has extensively studied the contribution of mitochondrial metabolism and energy transduction efficiency in the context of the diet-resistant phenotype. Specifically, they found that mitochondrial proton leak and mRNA expression of UCP3 are decreased in mitochondria isolated from skeletal muscle of DR versus DS individuals[57]. Further studies on primary myotubes isolated from DS and DR muscle biopsies demonstrate an almost 50% increase in leak respiration in DS women compared with DR, similar to the results from isolated mitochondria. However, the primary myotubes from these individuals have no apparent differences in protein expression of UCP3, ANT, or mitochondrial content[129]. Regardless, other studies have shown when the human form of UCP3 is overexpressed in mouse skeletal

muscle, mice are protected from diet-induced obesity, have higher energy expenditure, and display metabolic characteristics of enhanced fatty acid oxidation[58,130–132]. These data support the conclusion that differences in mitochondrial uncoupling in muscle impact the propensity for obesity and weight loss.

Declines in skeletal muscle mitochondrial content have repeatedly been associated with obesity[41,133–136], which leads us to hypothesize that there may be a link between skeletal muscle mitochondrial content and DR obesity. Substantial evidence supports the conclusion that mitochondrial oxidative capacity may drive weight loss success. When examining skeletal muscle fibre architecture, researchers observe an increase in the highly oxidative type I muscle fibres in DS versus DR individuals; this occurs largely at the expense of the proportion of type IIA fibres[116]. Interestingly, expression of genes involved in glucose and fatty acid metabolism is increased in blood collected from DS individuals during caloric restriction[116,137]. Higher enrichment of mitochondrial ETC transcripts is also observed in circulation prior to weight loss, suggesting that oxidative capacity could predict weight loss success[137,138].

The differences in ETC transcripts between DS and DR individuals translate into functional differences in skeletal muscle, where maximal mitochondrial respiration and complex I and II activities are lower in muscle tissue from DR versus DS participants[139]. Moreover, when challenged with a high-fat meal (~35% of daily kcal requirements based on indirect calorimetry; >60% calories from fat), skeletal muscle fatty acid clearance and maximal oxidative phosphorylation are lower in DR individuals[139]. This supports additional observations where high resting RER (VCO_2/VO_2 [*i.e.*, carbohydrate vs fat oxidation]) has been linked to weight gain[140]. Moreover, women with a high rate of weight loss have been identified as having a low resting RER[141]. *Ex vivo* studies at the level of skeletal muscle have shown that fatty acid oxidation is lower

in DR muscle[139], which has been attributed to decreased fatty acid availability and reduced fatty acid mobilization from adipose tissue[142,143].

1.5 Research Aims

1.5.1 Rationale for using exercise to target diet-resistant obesity

Exercise training has repeatedly been shown to improve muscle strength, body composition, immunity, bone mineral density, specific physical functions, and general quality of life[144]. Strenuous physical exercise can increase ROS production causing various forms of oxidative stress in skeletal muscle[145] and increase release of proinflammatory myokines[146]. However, regular moderate exercise involves a greatly increased endurance capacity and results in significantly increased numbers of muscle mitochondria[147]. Moderate exercise training can also lead to an increase in the activities of the mitochondrial OXPHOS complexes, even in muscles at rest, which decreases oxidative damage parameters[148]. Regular exercise has also been shown to reduce overall release of proinflammatory myokines[149].

Although a single bout of acute exercise initiates the activation of several pro-inflammatory pathways, these are necessary responses to mitigate the exercise-induced stress response. Exercise induces the activation of MAPK-ERK and IKK-NFκB signaling pathways in skeletal muscle[150]. Several proteins, including IκB, MAPK, and ERK, work in conjunction with NFκB to control downstream inflammation and immune responses. Evidence suggests that activation of these inflammatory pathways may be necessary to see the positive hypertrophic effects of exercise[151]. Moreover, evidence shows that regular moderate exercise ultimately leads to a decrease in inflammatory markers[152]. Roberts *et al* showed decreases in all serum lipids in humans after 3 weeks of diet and daily aerobic exercise[153]. Sriwijitkamol *et al* showed a 50% increase in IκB

proteins, suggesting a decrease in IKK-NFκB pathway activity, after 8 weeks of aerobic exercise[154]. It should be noted, however, that results in individuals with obesity have been less consistent – Polak *et al* saw a decrease in only plasma leptin (whereas all other plasma cytokines remained unaltered) after 12 weeks of aerobic exercise[155] and Christiansen *et al* found that it was diet-induced weight loss more so than exercise that leads to a decrease in inflammatory markers[156].

One cytokine, in particular, may play an especially important role in obesity and exercise response: IL-6. IL-6 has effects both as a pro- and anti-inflammatory cytokine and is well documented as being increased after exercise[157,158]. It has been shown to enhance glucose transport[159] and lipid oxidation in muscle tissue[105,160]. It may also play a role in induction of mitochondrial fission[161], and stimulation of lipolysis[162]. Wedell-Neergaard *et al* showed specifically that exercise in the presence of an IL-6 blockade reversed the effect of reduced visceral adipose tissue mass in individuals with obesity[163]. Therefore, regular moderate exercise may mitigate many of the detrimental effects seen due to the pro-inflammatory nature of obesity.

In rodent models, acute exercise has been shown to increase UCP3 mRNA expression in skeletal muscle[164,165]. As previously discussed, UCP3 activation can lead to increased energy expenditure and decreased oxidative stress[58]. Li *et al* were able to show that transgenic mice expressing the mitochondrial UCP in skeletal muscle were able to resist many of the negative effects of obesity and T2DM[166]. These finds are consistent with previously published data from the Harper lab where we showed that overexpression of UCP3 in transgenic mice prevents the accumulation of triglyceride in both adipose tissue and skeletal muscle[130] and decreases levels of circulating acylcarnitines which can be used as markers of incomplete muscle FAO[58].

Exercise also plays an important role in the mitigation of insulin and glucose regulatory pathways. Glucose transport in skeletal muscle is largely facilitated by GLUT4. Through either

insulin stimulation or muscle contraction stimulation, GLUT4 translocates from intracellular storage vesicles to the muscle cell surface where it facilitates glucose uptake into the cell[167]. Insulin resistance linked to obesity impairs insulin-stimulated glucose uptake[168,169], but the pathway can still be activated through muscle contraction stimulation[170]. The development of insulin resistance in skeletal muscle also precedes and predicts the development of T2DM[171,172]. Additionally, exercise training confers numerous other benefits related to glucose homeostasis including increased GLUT4 expression[173,174], increased Akt[175,176], increased AMPK[177], and decreased HbA1c[178].

Within the context of obesity, physical exercise can be a challenge. Moreover, dietary restriction has been shown to lead to more weight loss than exclusively increasing energy expenditure through exercise. Exercise tends to have superior effects in reducing visceral adiposity than diet-induced weight loss[179,180], however, changes in visceral adiposity do not necessarily reflect total body weight loss[179]. Regardless, the combination of caloric restriction with aerobic and resistance exercise (rather than either alone) has been shown to enhance the capacity for maintained weight loss and can improve the functional status of adults with obesity. Exercise training can induce muscle fibre protein synthesis and hypertrophy, leading to increases in mitochondrial respiration[181] and muscle cross-sectional area, and therefore overall lean body mass. Moreover, aerobic exercise can induce the fibre type switching of glycolytic type IIX and IIB to oxidative type I[182,183], which would be particularly useful to diet-resistant patients with obesity due to the lower proportion of type I fibres observed in *vastus lateralis* muscle. Thus, when considering the previous findings in DR individuals of decreased muscle hypertrophy[116] and mitochondrial function[57,129], exercise training may induce beneficial molecular adaptions that increase mitochondrial bioenergetics and reduce inflammation of skeletal muscle in DR individuals.

1.5.2 Research questions

The proposed research is intended to answer the following questions:

- Are there differences in systemic and/or muscle inflammation between DR and DS individuals?
- Does exercise training improve inflammation and mitochondrial bioenergetics in women with obesity?
- Do primary myotubes isolated from DR and DS individuals exhibit differences in inflammation and/or bioenergetics in response to an inflammatory challenge?

1.5.3 Hypotheses

The overall aim of this study is to determine whether six weeks of exercise training improves skeletal muscle mitochondrial function and reduces inflammatory response in muscle tissue and primary myotubes obtained from women with obesity defined as diet-sensitive (DS) and diet-resistant (DR). Based on previous research, we hypothesize that exercise training will increase mitochondrial function and reduce inflammatory responses to a greater extent in DR versus DS women.

Preliminary mining of previously published DS and DR *rectus femoris* skeletal muscle transcriptomes (GEO accession no. GSE17371)[116] using *eVITTA*[184] suggests that DS and DR women exhibit several differences in mRNA expression levels within the IKK-NFκB signaling pathway (Figure 4). Specifically, TLR4 is higher in DS individuals, IL-1β is higher in DS individuals, IκBα is higher in DS individuals, IKKα/β are higher in DR individuals, and NFκB is higher in DR individuals. These findings lead us to hypothesize that IKK-NFκB signaling in DS individuals is more heavily regulated through the canonical pathway with TLR4.

The proposed mechanistic studies will allow the first-ever investigations into the role of inflammation in the control of muscle metabolism in individuals with obesity who have markedly different capacities for diet-induced weight loss. Conclusions from these studies may contribute to the development of personalized treatments, especially for those who have great difficulties losing weight and maintaining weight loss.

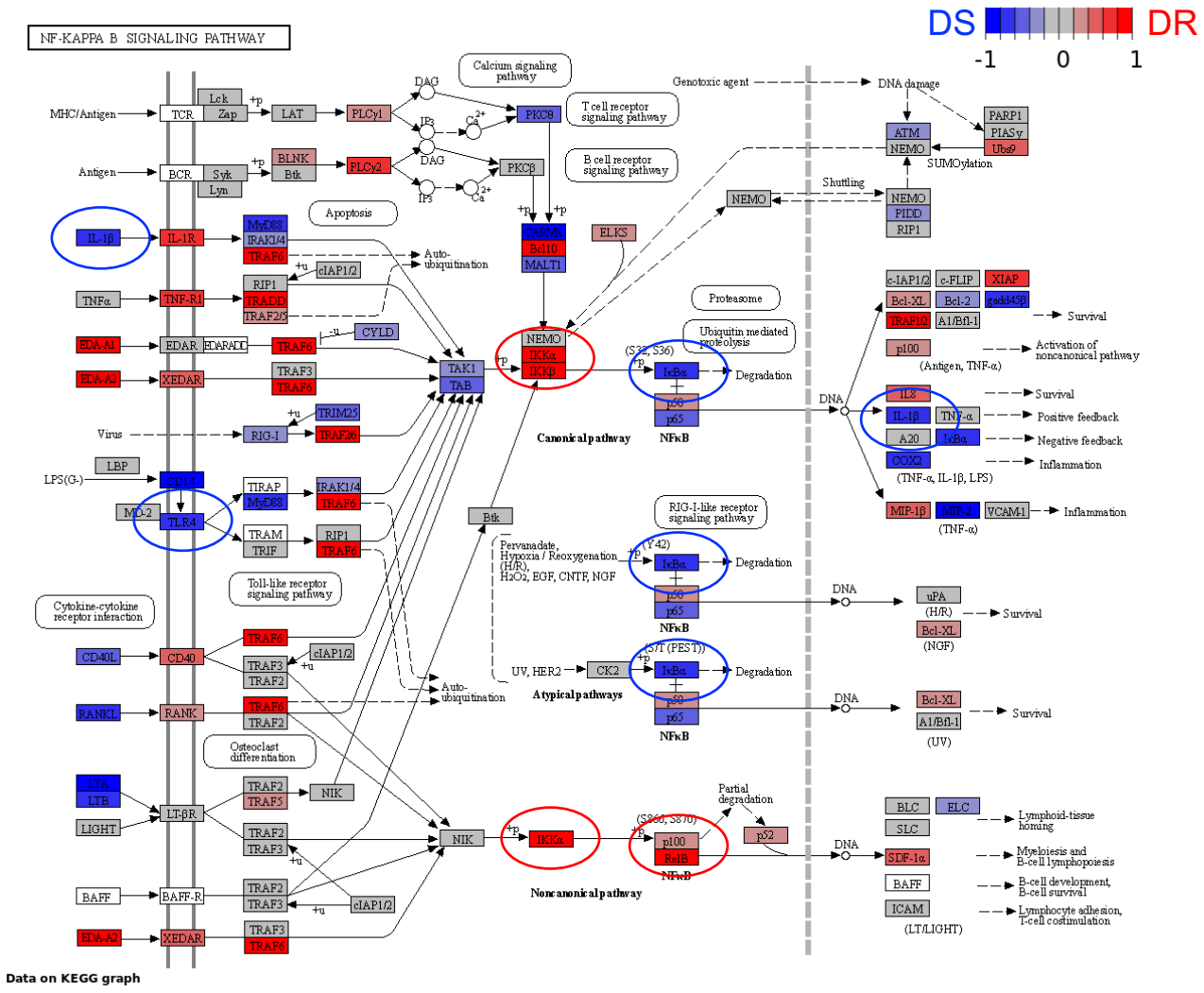

Figure 4. Differences in the NFκB signaling pathway from DS and DR transcriptomics data. The IKK-NFκB pathway with proteins and cytokines highlighted based on relative abundance in transcriptomics data from DS and DR individuals. The brighter the shade of blue, the higher the expression in DS individuals and the brighter the shade of red, the higher the expression in DR individuals. (Brighter colours do not necessarily indicate statistical significance). Of note, TLR4 appears higher in DS individuals, IL-1β appears higher in DS individuals, IκBα appears higher in DS individuals, IKKα/β appear higher in DR individuals, and NFκB appears higher in DR individuals. *Figure created with eVITTA*[184].

Materials and Methods

2.1 Participant selection and matching

All participants provided informed oral and written consent. This study was approved by the Ottawa Health Science Network Research Ethics Board (Protocol #2011658) and the University of Ottawa Council of Research Ethics Board (Protocol #H01-12-06).

Participants were previously classified into quintiles based on rate of weight loss (ROWL) during the first 6 weeks of a 26-week program, in which a 900 kcal/day meal replacement was consumed (Optifast 900; Nestlé Health Sciences). Comprehensive compliance to the Ottawa Hospital Weight Management Program (OHWMP) was determined as previously described[57,116], where only diet-adherent women who had previously completed the OHWMP were strictly classified into quintiles based on ROWL by computer software developed by the clinic[185]. Rate of weight loss calculations were corrected for age, initial body weight and BMI calculated based on serial measures in the first 6 weeks[115]. In brief, patients were excluded from quintile characterization in the OHWMP and further metabolic studies if: they did not meet the adherence criteria; they were absent for <2 visits during the initial 6 weeks on meal replacement; physician notes expressed reservations about self-reported compliance; and/or there was inadequate completion of the laboratory testing protocol. Compliant weight-stable women were invited to participate in the present study if they were in the top 20% in ROWL (DS) or bottom 20% in ROWL (DR).

Patients invited to participate were excluded from the present study if they had prior bariatric surgery or were taking any medications known to affect rate of weight loss including: medications that affect glucose homeostasis, appetite suppressants, steroids, and/or medications/supplements which may affect muscle biology. Moreover, participants were non-

smokers, free from metabolic conditions such as diabetes, cardiovascular disease, cancer, and musculoskeletal conditions that result in impaired movement. Diet-sensitive and diet-resistant women were matched for age (±5 years), initial body weight (±20 kg), and BMI (±3 kg/m^2) at the time of participation.

2.2 Experimental design

The study consisted of a 6-week graded exercise intervention, during which participants were instructed to maintain their normal lifestyle and eating habits. Before commencing the exercise training intervention, participants were provided with an electronic food diary and accelerometer (Fitbit Charge, San Francisco, CA) to track levels of activity.

Meeting 1. Muscle Biopsy

At baseline, participants reported to the University of Ottawa Heart Institute for blood sampling, a *vastus lateralis* muscle biopsy, and collection of anthropometric measures including waist circumference, blood pressure, weight, and body composition assessed by bioimpedance (Tanita Corporation, Arlington Heights, IL).

Meeting 2. Metabolic Testing

Participants reported to the University of Ottawa's Behavioural and Metabolic Research Unit and underwent a dual-energy X-ray absorptiometry (DEXA) scan (GE Lunar, Prodigy Model), muscle function testing, indirect resting calorimetry, and a $VO_{2submaximum}$ test.

Intervention (6 consecutive weeks)

The exercise intervention consisted of 18-supervised exercise sessions performed on non-consecutive days for six weeks. Each exercise session consisted of 30 minutes of treadmill walking, starting at six metabolic equivalents (METs) calculated using $VO_{2submaximum}$ and

increasing by 10% weekly. Following the treadmill walk, participants completed four sets of resistance-based exercises at 60%-80% of their predicted one repetition maximum.

Post-Intervention Meeting 1. Metabolic Testing

48-hours after the final exercise training session, participants reported to the University of Ottawa's Behavioural and Metabolic Research Unit again for a DEXA scan (GE Lunar, Prodigy Model), muscle function testing, indirect resting calorimetry, and a $VO_{2submaximum}$ test.

Post-Intervention Meeting 2. Muscle Biopsy

72 hours following the final metabolic testing visit, participants reported to the University of Ottawa Heart Institute for blood sampling, a second *vastus lateralis* muscle biopsy, and collection of anthropometric measures including waist circumference, blood pressure, weight, and body composition assessed by bioimpedance (Tanita Corporation, Arlington Heights, IL).

2.3 *Vastus lateralis* muscle sampling, tissue collection and preparation

Muscle biopsies were collected from participants after an overnight fast prior to the immobilization period (baseline [BL]) and following the six weeks of supervised exercise training (post-exercise training [PET]). Local anaesthetic (1% xylocaine) was injected subcutaneously overlying the *vastus lateralis* (VL), and a small incision was made into the skin and underlying fascia. A 5 mm Bergstrom needle, modified for manual suction, was used to extract ~100 mg of *vastus lateralis* muscle, which was immediately divided for different analyses. One aliquot was placed into ice-cold culture media for subsequent isolation of primary myoblasts. The remaining tissue was snap-frozen in liquid nitrogen and stored at -80°C for later analyses of protein expression and enzymatic activities.

2.4 Fasting plasma biochemical analysis

Fasted blood samples were analysed by the Ottawa Hospital Laboratory Services.

2.5 Cell culture

A 25 mg sample of muscle tissue was cultured, and satellite cells were grown to 80% confluency in growth media (Ham's F10 media with 12.5% BGS, 1% antibiotic-antimycotic, 826 nM dexamethasone, 8.3 ng/mL human epidermal growth factor, 25 pmol insulin, and 2.5 µL/mL gentamycin). Cells were lifted using trypsin digestion, and then satellite cells were isolated via immune-sorting using a magnetic column and anti-CD56 MicroBeads (Miltenyi Biotec). Labeled myoblasts were then eluted and grown in growth media. At ~80% confluence, primary myoblasts were differentiated into myotubes for 7±1 days in differentiation media (Dulbecco's modified Eagle's medium [DMEM] with 2% horse serum, 1% antibiotic-antimycotic, and 2.5 µg/mL gentamycin). Myotubes were lifted using trypsin digestion and then harvested and pelleted in cold 1X PBS. Pellets were stored at -80°C to be used for enzymatic assays, HPLC, and western blots.

2.6 Mitochondrial stress test on primary myotubes

Primary myoblasts were lifted using trypsin digestion, and cell counts were recorded using the Countess Automated Cell Counter (Invitrogen) according to manufacturer's instructions for myoblasts. 15,000 cells were plated in each well of a 96-well Seahorse plate. Upon reaching ~80% confluency (~24 hours after plating), the myoblasts were differentiated into myotubes for 7±1 days in differentiation media.

The day before the assay, the Agilent Seahorse XFe96 Sensor Cartridge was hydrated with 200 µL of sterile water in each well and incubated in a non-CO^2 incubator at 37°C overnight. On

the day of the assay, the water was replaced with non-CO_2 incubated Agilent Seahorse XF Calibrant and the cartridge was incubated for an additional hour (non-CO_2 incubator, 37°C). The Seahorse plate was washed three times with Seahorse media (pH 7.4) (HCO_3-free DMEM powder with 5.5 mM D-glucose, 1 mM sodium pyruvate, 4 mM L-glutamine), and subsequently incubated in a non-CO_2 incubator at 37°C for 30 minutes.

Oxygen consumption rate (OCR) was measured following consecutive additions of 2.5 μM oligomycin (resting state 4), 2 μM carbonyl cyanide-p-trifluoromethoxyphenylhydrazone (FCCP) (maximally uncoupled), 5 μM/10 μM antimycin-A/rotenone (non-mitochondrial), and 20 μM monensin (maximal glycolysis). Drugs were prepared in Seahorse media and loaded in ports A through D, respectively. After the assay, the cells were washed twice with 200 μL of 1X PBS and then placed in 40 μL of RIPA buffer. A bicinchoninic acid (BCA) assay (Bio-Rad) was performed to determine protein concentration in each well and Seahorse assay measurements were normalized to protein content.

2.7 Citrate synthase enzymatic assay of primary myotubes

Pellets set aside for enzymatic assays were resuspended in RIPA buffer with 0.1% protease inhibitor cocktail (PIC) (Sigma) and lysed with a 28-gauge needle. The homogenate was cleared by centrifugation at 14,000 g for 10 minutes at 4°C. The supernatant was extracted, and the pellet was disposed of. CS activity was determined by measuring absorbance at 412 nm in 50 mM Tris-HCl (pH 8.0) with 0.2 mM DTNB, 0.1 mM acetyl-coA and 0.25 mM oxaloacetate, using a 96-well microplate reading spectrophotometer (BioTek Synergy) at room temperature. Rate of absorbance change and path length of each well was determined using BioGen 5.0. The enzyme activities were calculated using the extinction factor 13.6 $mM^{-1}cm^{-1}$. A BCA assay (Bio-Rad) was performed to

determine protein concentration for each sample and enzymatic assay measurements were normalized to protein content.

2.8 Western blot analysis of skeletal muscle homogenate

Frozen muscle was homogenized using a bead mill homogeniser (Fisherbrand Bead Mill 24 Homogenizer) in ice-cold RIPA buffer (Millipore) supplemented with 0.5mM Na_3VO_4 and 0.1% PIC (Sigma). Samples were cleared by centrifugation at 14,000 g for 10 minutes at 4°C. A BCA assay (Bio-Rad) was performed to determine protein concentration. Samples were prepared with a final protein concentration of 2 µg/µL in 1X Laemmli buffer (0.2 M Tris-HCl [pH 6.8], 8% *w/v* sodium dodecyl sulfate [SDS], 40% *v/v* glycerol, 0.5 M dithiothreitol [DTT], 0.01% bromophenol blue), and boiled at 95°C for 5 minutes.

Acrylamide gels (30% acrylamide mix, 1.5 M Tris [pH 8.8], 10% SDS, 10% ammonium persulfate [APS], tetramethylethylenediamine [TEMED]) were cast with 5% stacking gels (30% acrylamide mix, 0.5 M Tris [pH 6.8], 10% SDS, 10% APS, TEMED). Proteins were separated by SDS-PAGE under reducing conditions at 150 V in running buffer (25 mM Tris base, 192 mM glycine, 0.1% SDS) for approximately 1 hour. Proteins were then transferred to PVDF membranes using TurboBlot (Bio-Rad) according to the manufacturer's protocol. Membranes were incubated with blocking buffer (5% BSA in Tris-buffered saline, 0.1% Tween 20 [TBS-T]) for 1 hour at room temperature. Membranes were then incubated overnight at 4°C with gentle rocking with primary antibodies against: Total Human OXPHOS antibody cocktail (Abcam #ab110411 1:1000), MFN1/2 (Abcam #ab57602, 1:1000), OPA1 (Abcam #ab42364, 1:1000), Drp1 (BD Biosciences #611113, 1:1000), MAPK (Cell Signaling #9212, 1:2000), p-MAPK (Cell Signaling #9211, 1:1000), ERK (Cell Signaling #9102, 1:2000), p-ERK (Cell Signaling #9106, 1:1000),

NFκB (Cell Signaling #8242, 1:1000), p-NFκB (Cell Signaling #3033, 1:1000), IκB (Cell Signaling #4814, 1:1000), p-IκB (Cell Signaling #2859, 1:1000), TLR4 (Abcam #ab13867, 1:1000), GAPDH (Santa Cruz #sc47724, 1:10,000) and vinculin (Abcam #ab129002, 1:5000). The next day, membranes were incubated with the appropriate secondary antibody in 5% skim milk in TBS-T for 1 hour with gentle rocking. Protein bands were visualized using the Immobilon ® Classico Western HRP substrate (Millipore). Signals were captured using a ChemiDoc™ MP Imaging System (Bio-Rad). Densitometry band analysis was performed using Image J software. Abundances of target proteins are presented normalized to vinculin or GAPDH, as indicated.

2.9 TOM20 staining of primary myoblasts and microscopy

Primary myoblasts were lifted using trypsin digestion, and then a cell count was taken using the Countess Automated Cell Counter (Invitrogen) according to manufacturer's instructions for myoblasts. 50,000 cells were plated on coverslips in each well of a 24-well plate. Upon reaching ~50% confluency (~24 hours after plating), the myoblasts were fixed with 4% paraformaldehyde. Mitochondrial length was determined by staining with TOM20 (Santa Cruz Biotechnology, sc11415) in 1X PBS buffer containing 0.1% Triton X-100 and 1% BSA. Oregon green 488 goat anti-rabbit (Life Technologies, O-6381; 1:100) was diluted in 1X PBS containing 1% BSA and 0.1% Hoechst counterstain. Images were obtained using a Zeiss Axiolimager Z1 fluorescent microscope. Blinded analysis was conducted by quantifying 50 mitochondrial lengths from 3-5 fields of view for each cell line.

2.10 High-performance liquid chromatography of primary myotubes

Pellets set aside for HPLC were resuspended in 1:1 buffer (1-part 0.25 M sucrose, 3 mM EDTA, 10 mM Tris buffer; 1-part mobile phase [90% ddH_2O, 10% HPLC-grade methanol, 0.1% trifluoroacetic acid (TFA) and 0.1% *w/v* meta-phosphoric acid (MPA)]). Samples were incubated on ice for 20 minutes and then pelleted by centrifugation at 14,000 g at 4°C for 20 minutes. The supernatant was used in the HPLC determination. 100 mM stocks of GSH and GSSH were diluted to 1 mM, 0.1 mM, 0.01 mM and 0.001 mM in 1:1 buffer and used to prepare a standard curve. Samples were loaded after the standards, and the area under the curve was measured for the peaks corresponding to the GSH and GSSG retention times. A BCA assay (Bio-Rad) was performed to determine protein concentration in each sample and GSH and GSSG measurements were normalized to protein content.

2.11 Radiolabeled glucose uptake analysis of primary myotubes

Primary myoblasts were lifted using trypsin digestion, and then a cell count was taken using the Countess Automated Cell Counter (Invitrogen) according to manufacturer's instructions for myoblasts. 180,000 cells were plated in each well of a collagen-coated 12-well plate. Upon reaching ~80% confluency (~24 hours after plating), the myoblasts were differentiated into myotubes for 7±1 days in differentiation media. Differentiated myotubes were serum-deprived for 3 hours before being incubated in KRH buffer (pH 7.4) (150 mM NaCl, 5 mM KCl, 1.2 mM $MgSO_4$, 1.2 mM NaH_2PO_4, 10 mM HEPES, 0.1% BSA) with or without 100 nM insulin for 1 hour at 37°C. 0.1 μCi/mL of radiolabeled [^{14}C] 2-deoxy-D-glucose ([^{14}C]2DG) and 10 μM D-glucose with or without 20 μM cytochalasin B was added to the cells and incubated for an additional 15 minutes at 37°C. Cells were washed twice with 1X PBS and then lysed in 0.1 M NaOH. Samples

were prepared in Ultima Gold™ MV scintillation fluid, and then read using the Tri-Carb 4910 TR Liquid Scintillation Analyzer (PerkinElmer). A BCA assay (Bio-Rad) was performed to determine protein concentration in each sample and glucose uptake data were normalized to protein content minus the protein content of collagen alone.

2.12 U-PLEX and R-PLEX assays of EDTA fasted plasma

U-PLEX Metabolic Group 1 (Human) assay was performed on EDTA fasted plasma according to the manufacturer's protocol (Meso Scale Discovery [MSD]). U-PLEX Biomarker Group 1 (Human) assay was performed on EDTA fasted plasma according to the manufacturer's protocol (MSD). U-PLEX Custom Metabolic Group 1 (Human) assay was performed on EDTA fasted plasma according to the manufacturer's protocol (MSD), with selections for FGF-21, Glucagon, PYY, BDNF, β-NGF, FSH, LH, C-peptide, and Ghrelin. U-PLEX Custom Biomarker (Human) assay was performed on EDTA fasted plasma according to the manufacturer's protocol (MSD), with selections for G-CSF, IFN-α2a, IL-1α, IL-15, IL-18, TNF-β, CTACK, SDF-1α, EPO, and MIP-5. R-PLEX Antibody Sets assay was performed on EDTA fasted plasma according to the manufacturer's protocol (MSD), with selections for Osteonectin, SHBG, and IGF-1.

2.13 Western blot analysis of treated primary myotubes

Myoblasts were differentiated as previously described. Differentiated myotubes were treated with 500 μM palmitate conjugated to 18 μM BSA, 18 μM BSA, or 100 pg/mL of LPS for 24 hours before being lifted using trypsin digestion and then pelleted in cold 1X PBS. Pellets were stored at -80°C until sample preparation for western blots.

Samples were prepared on ice. Pellets set aside for western blot were resuspended in lysis buffer (10 mM Tris-HCl [pH 7.4], 150 mM NaCl, 0.5% *v/v* Triton X-100, and 1 mM EDTA) with 0.1% PIC (Sigma) and 0.5mM Na_3VO_4 and lysed with a 28-gauge needle. Samples were cleared by centrifugation at 14,000 g for 10 minutes at 4°C. A BCA assay (Bio-Rad) was performed to determine protein concentration. Samples were prepared with a final protein concentration of 2 µg/µL in 1X Laemmli buffer (0.2 M Tris-HCl [pH 6.8], 8% *w/v* SDS, 40% *v/v* glycerol, 0.5 M DTT, 0.01% bromophenol blue), and boiled at 95°C for 5 minutes.

Proteins were separated by SDS-PAGE under reducing conditions as previously described and transferred to nitrocellulose membranes using wet transfer at 100 V in transfer buffer (25 mM Tris Base, 192 mM glycine, 20% methanol) for 1 hour. Membranes were blocked and then incubated overnight at 4°C with gentle rocking with primary antibodies against: NFκB (Cell Signaling #8242, 1:1000), p-NFκB (Cell Signaling #3033, 1:1000), IκB (Cell Signaling #4814, 1:1000), p-IκB (Cell Signaling #2859, 1:1000), TLR4 (Abcam #ab13867, 1:1000), PRKN (Santa Cruz #sc32282, 1:1000), LC3II//I (Cell Signaling #12741, 1:1000), GPx4 (Abcam # ab16800, 1:1000), Nrf2 (Abcam #ab31163, 1:1000), SLC7A11 (Abcam #ab175186, 1:1000), SOD1 (Santa Cruz #sc11407, 1:1000), SOD2 (Santa Cruz #sc30080, 1:1000), and HIF1α (Cell Signaling #3716, 1:1000). The next day, membranes were incubated with the appropriate secondary antibody in 5% skim milk in TBS-T for 1 hour with gentle rocking. Protein bands were visualized using the Immobilon ® Classico Western HRP substrate (Millipore). Signals were captured using a ChemiDoc™ MP Imaging System (Bio-Rad). Densitometry band analysis was performed using Image J software. To control for gel-to-gel variation, bands of interest were normalized by re-probing the membranes with loading control GAPDH (Santa Cruz #sc47724, 1:10,000).

2.14 High-resolution respirometry of treated permeabilized myotubes

High-resolution respirometry on digitonin-permeabilized LPS treated myotubes was conducted using an Oxygraph-2k system (OROBOROS Instruments, Innsbruck, Austria). Two sets of myoblasts were differentiated into myotubes for 7±1 days in differentiation media. 24 hours before the experiment 100 pg/mL of LPS was added to one of the sets of cells. Cells were lifted by trypsin digestion and pellets were resuspended in mitochondrial respiration media (MiR05) (pH 7.1, 37°C) (110 mM sucrose, 60 mM K-lactobionate, 20 mM HEPES, 20 mM taurine, 10 mM KH_2PO_4, 3 mM $MgCl_2$, 0.5 mM EGTA, and 1 mg/ml fraction V BSA). Experiments were performed in duplicate at 37°C in 2 mL of MiR05. Following the addition of cells to the chamber, they were permeabilized with 4.05 μM digitonin.

The standard assay protocol consisted of consecutive additions of: 2 mM malate, 5 mM pyruvate, 5 mM glutamate (CI substrates), 5 mM ADP with 5 mM $MgCl_2$ (CI OXPHOS), 10 mM succinate (CI+II OXPHOS), 1 μM carboxyatractyloside (CAT) (ANT-inhibited), 2.5 μM oligomycin (CI+II leak), 0.5 μM titrations of FCCP (maximal respiration, ETC) and 2.5 μM antimycin A.

The fatty acid oxidation assay protocol consisted of consecutive additions of: 2 mM malate, 125 μM palmitoylcarnitine, 5 mM ADP with 5 mM $MgCl_2$ (CI OXPHOS), 125 μM octanoylcarnitine (CPT1-independent respiration using lipid-based substrates), 5 mM pyruvate, 5 mM glutamate (CI substrates), 10 mM succinate (CI+II OXPHOS), 1 μM CAT (ANT-inhibited), 2.5 μM oligomycin (CI+II leak), 0.5 μM titrations of FCCP (maximal respiration, ETC) and 2.5 μM antimycin A. A BCA (Bio-Rad) assay was performed to determine protein concentration in each sample and high-resolution respirometry data was normalized to protein content.

2.15 Statistics

Statistical analysis was performed using Prism 9 for macOS (GraphPad Software Inc., La Jolla, CA). Statistical significance of DS versus DR was determined using a two-tailed paired Student's t-test. To assess the effect of the exercise intervention between DS and DR, a 2-way repeated-measures ANOVA was used with quintile and exercise as independent variables, followed by post hoc Holm-Šídák multiple comparison tests. To assess the effect of the inflammatory challenge and the exercise intervention between DS and DR, a 3-way repeated-measures ANOVA was used with quintile, exercise, and treatment as independent variables, followed by post hoc Holm-Šídák multiple comparison tests. Statistical differences were considered significant when the p-value was <0.05 (*$p<0.05$, **$p<0.01$, **$p<0.001$ DS vs DR; #$p<0.05$, ##$p<0.01$, ###$p<0.001$ BL vs PET). Prism software (GraphPad Software Inc.) was used to generate graphs. Data are presented as means±SD unless otherwise specified.

Results

3.1 Objective #1: Inflammation and mitochondrial function in muscle tissue and primary myotubes from diet-sensitive and diet-resistant women following exercise training.

Our recently published findings indicate that DR individuals have lower total body muscle mass and greater fat mass, as determined by DEXA, compared to DS individuals[186]. However, DS women have increased central adiposity, waist circumference, and higher fasting insulin levels. Together, these data suggest that DS women may be more predisposed to metabolic disease. Previous unpublished Somalogics plasma proteomics data revealed that DR women have elevated expression of inflammatory cytokines such as IL-12, erythropoietin, IL-23, MCP-1, and TARC[139], whereas there was a trend for higher TLR4 expression in DS women ($p=0.12$). Chronic low-grade inflammation is associated with obesity and loss of muscle mass through the activation of the ubiquitin proteome system and autophagy. Specifically, activation of the IKK-NFκB signaling pathway results in increased production of pro-inflammatory markers and the degradation of skeletal muscle proteins via increased MuRF1 expression. Preliminary evidence also suggests that NFκB activation stimulates mitochondrial fusion[93], promotes mitochondrial dysfunction[94], and promotes the degradation of mitochondria by mitophagy[95]. Therefore, this objective aims to determine molecular inflammatory signaling pathways that contribute to differences in body composition and mitochondrial function between DS and DR individuals before and after exercise training.

3.1.1 Body composition and blood biochemistry of DS and DR women

Ten women with obesity defined as DS and ten women with obesity defined as DR were matched based on age, weight, and BMI for our analysis. DEXA analysis revealed that aspects of

initial body composition differed between the DR and DS women. At BL, DR women had significantly less lean body mass than DS women (p=0.0003; Figure 5B), and although fat mass did not differ between groups, there is a strong trend for DR women to have higher percent body fat (p=0.057; Figure 5C). The exercise intervention did not change lean mass or body weight in either group but decreased percent body fat and fat mass preferentially in DR women compared to DS women (p=0.014 and p=0.015; Figure 6A, B). Additionally, as a first indication that there are differences in immune response, DR versus DS women had higher white blood cell count (WBC) at baseline (p=0.009; Table 1) and WBC was reduced post-exercise training only in DR women (p=0.037; Table 1).

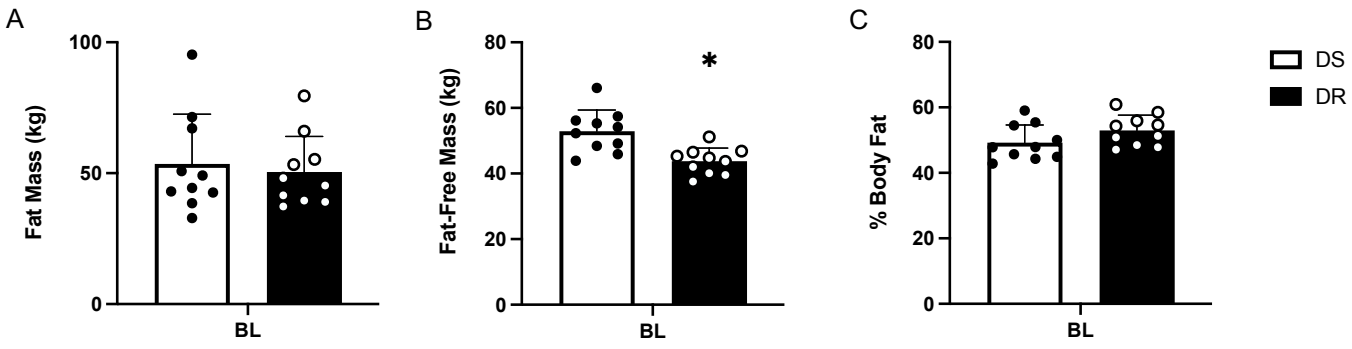

Figure 5. Body composition differs between DS and DR women. Participants underwent a Dual Energy X-ray Absorptiometry (DEXA) scan to measure their baseline total body composition. **(A)** Total body fat (kg). **(B)** Total lean body mass (kg). **(C)** Total body fat percentage. Data are expressed as mean±SD (n=10). *p<0.05 DS vs DR

Table 1. Baseline and post-exercise training anthropometric characteristics of DS and DR women. Anthropometric measurements were conducted on individuals at the time of pre- and post-intervention *vastus lateralis* muscle biopsies. *p<0.05 DS vs DR, #p<0.05 BL vs PET

	BL		***PET***	
Variable	***DS***	***DR***	***DS***	***DR***
n	10	10		
Age (years)	53.9 ± 7.7	53.2 ± 9.3	-	-
Height (cm)	165.85 ± 7.34	158.55 ± 4.99*	-	-
Bodyweight (kg)	110.67 ± 28.86	96.87 ± 17.55	111.07 ± 29.30	96.27 ±17.68
BMI (kg/m^2)	39.92 ± 8.00	38.66 ± 7.56	40.03 ± 8.20	38.38 ± 7.66
Waist circumference (cm)	124.11 ± 19.54	116.05±11.45	121.67±16.06	112.69±10.46
Body composition by DEXA				
Fat mass (kg)	53.53 ±18.98	50.49 ± 13.56*	53.56 ± 19.30	49.55 ± 14.11*$^{\#}$
Lean mass (kg)	52.88 ± 6.47	43.75 ± 4.04*	52.57 ± 6.47	44.20 ± 4.87*
% Body fat	49.23 ± 5.40	52.97 ± 4.66*	49.32 ± 5.57	52.00 ± 5.20*$^{\#}$
Fasting blood biochemistry				
Fasting glucose (mmol/L)	5.20 ± 0.49	5.02 ± 0.49	5.50 ± 0.72	5.24 ± 0.53
HbA1c (%)	5.79 ± 0.41	5.59 ± 0.28	5.63 ± 0.40$^{\#}$	5.49 ± 0.31
Fasting insulin (pmol/L)	91.20 ± 50.37	61.40 ± 24.31*	101.50 ± 58.52	60.4 ± 25.15*
HOMA-IR	3.06 ± 1.78	2.00 ± 0.89	3.65 ± 2.40	2.08 ± 1.01*
Fasting triglycerides (mmol/L)	1.38 ± 0.49	1.54 ± 0.52	1.25 ± 0.42	1.35 ± 0.58
Total cholesterol (mmol/L)	5.30 ± 0.87	5.09 ± 0.89	5.33 ± 0.83	5.26 ± 0.93
HDL cholesterol (mmol/L)	1.54 ± 0.26	1.47 ± 0.36	1.54 ± 0.09	1.50 ± 0.39
LDL cholesterol (mmol/L)	3.13 ± 0.78	2.95 ± 0.72	3.36 ± 0.74	3.22 ± 0.86
White blood cell count (x10^9/L)	6.14 ± 1.05	7.25 ± 1.32*	6.20 ± 1.38	6.44 ± 1.48$^{\#}$
Creatine kinase (U/L)	127.80 ± 81.13	68.67 ± 21.97*	110.5 ± 37.34	72.90 ± 30.68*

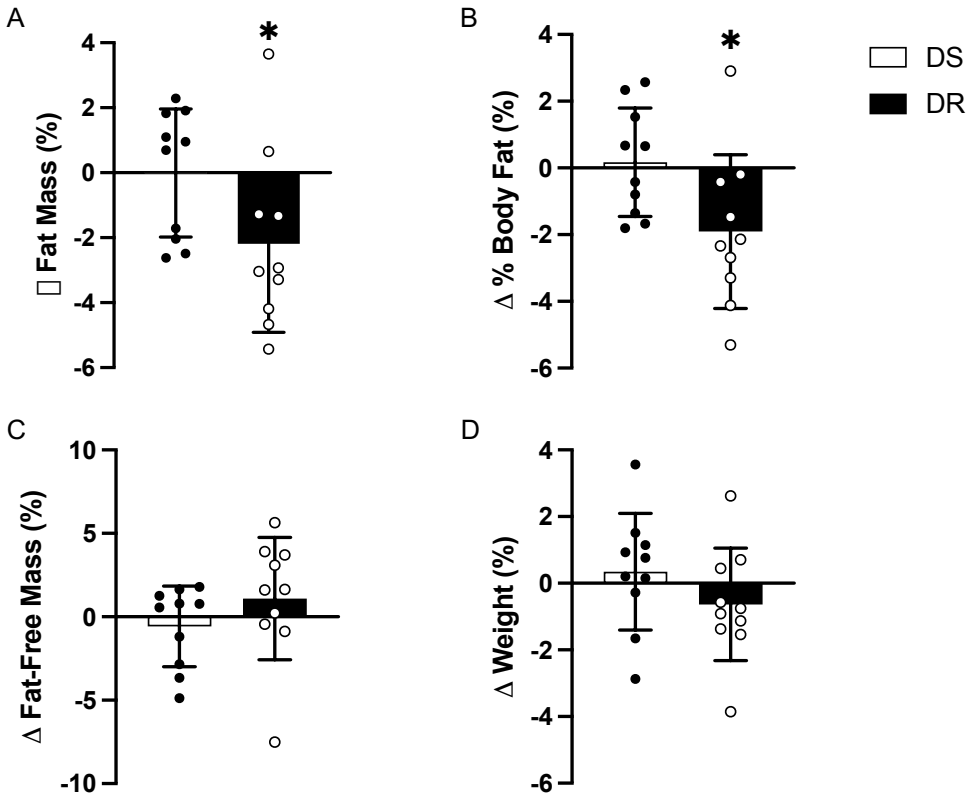

Figure 6. Exercise training preferentially lowers % body fat and fat mass in DR women. Participants underwent Dual Energy X-ray Absorptiometry (DEXA) scans pre- and post-exercise to measure changes in total body composition. **(A)** Change in percent body fat (%). **(B)** Change in total body fat mass (%). **(C)** Change in total lean body mass (%). **(D)** Change in total body weight (%). Data are expressed as mean±SD (n=10). Means were compared using a two-way paired Student's t-test. *p<0.05 DS vs DR

3.1.2 Myotube oxygen consumption and metabolic flexibility

Next, we determined the metabolic characteristics of the differentiated myotubes isolated from DS and DR women by quantifying oxygen consumption rate (OCR) using a modified approach to the Agilent Seahorse XF Cell Mitochondrial Stress Test assay[187,188]. At BL, basal respiration tended to be higher in primary myotubes from DS versus DR women (p=0.070). Interestingly, exercise training increased basal, maximal and non-mitochondrial respiration in DR myotubes only (p=0.002 [basal], p=0.007 [FCCP], p=0.004 [AMA/Rot]; Figure 7A). These results translate to the extrapolated data where basal (as defined as resting respiration minus non-

mitochondrial respiration), ATP-coupled, and maximal (as defined as maximal respiration minus non-mitochondrial respiration) respiration, as well as spare respiratory capacity, are all higher in DR women post-exercise training ($p=0.003$, $p=0.006$, $p=0.011$, $p=0.039$, respectively; Figure 7B, C, E, F).

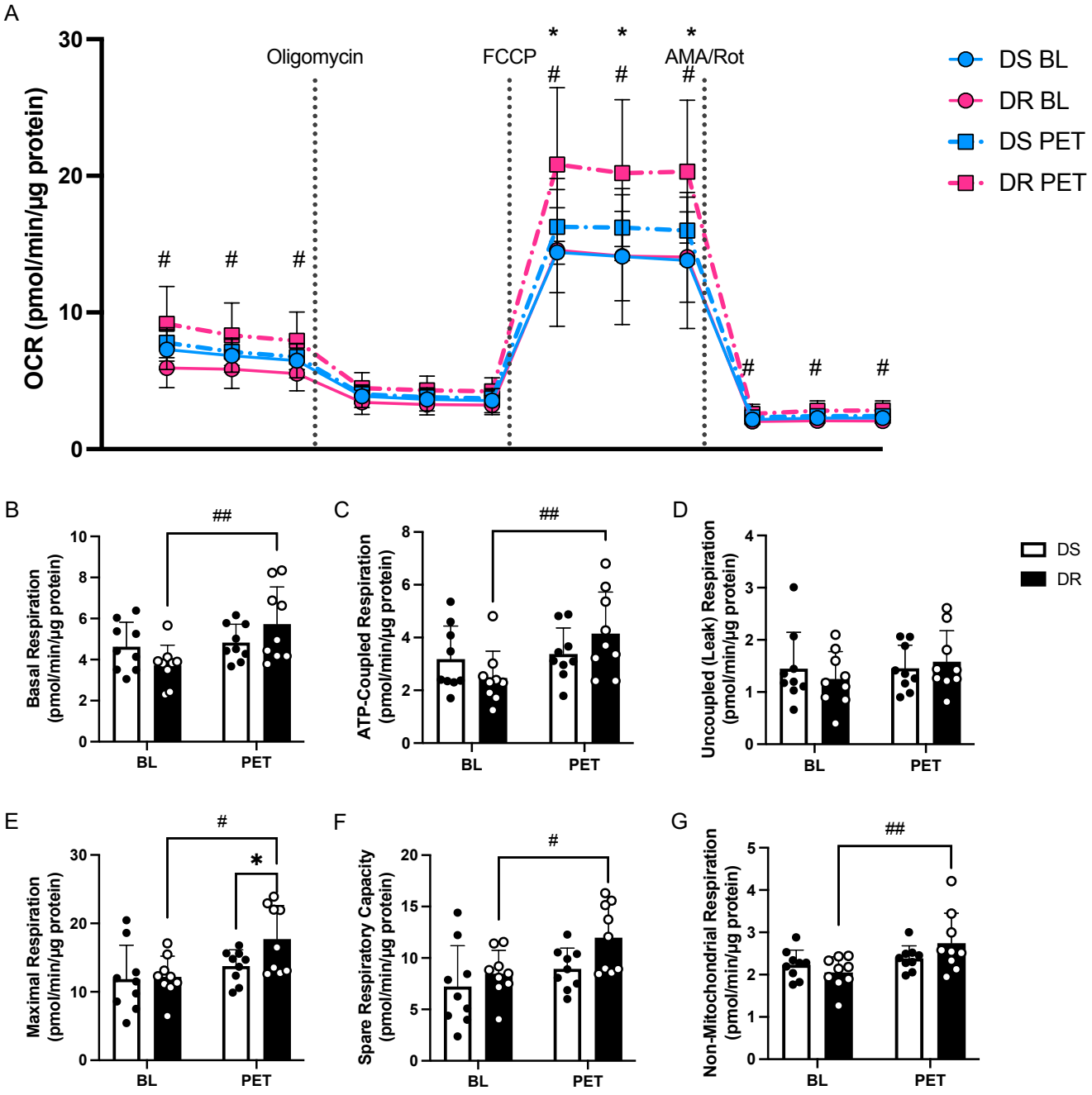

Figure 7. Exercise training preferentially increases respiration in DR primary myotubes. Differentiated primary myotubes underwent a modified mitochondrial stress test (Agilent Seahorse XFe96) to measure Oxygen Consumption Rate (OCR). **(A)** OCR trace, injections marked with dotted lines. **(B-G)** Quantification of **(B)** basal respiration, **(C)** ATP-coupled respiration, **(D)** uncoupled (leak) respiration, **(E)** maximal respiration, **(F)** spare respiratory capacity (defined as the difference between maximal and basal respiration) and **(G)** non-mitochondrial respiration. Data are expressed as mean±SD relative to µg of protein per well (n=9). Means were compared using a 2-way repeated-measures ANOVA. *p<0.05 DS vs DR, #p<0.05 BL vs PET

The Agilent Seahorse assay also measures extracellular acidification rate (ECAR), which quantifies changes in extracellular pH and is thus an indirect measurement of anaerobic glycolysis. A monensin injection was included to evaluate maximal ECAR. Basal glycolysis was higher in DS versus DR women (main effect quintile p=0.022; Figure 8A, B); and this continues as a trend with varying degrees after injections with oligo, FCCP, AMA/Rot and monensin (main effect quintile p=0.070, p=0.123, p=0.109, p=0.132; respectively). Inhibition of oxidative phosphorylation by oligomycin increased anaerobic glycolysis – this shift is known as compensatory glycolysis; a parameter which is indicative of cellular ability to manage energy demand under stress. Oligomycin-induced compensatory glycolysis has a strong trend towards increasing post-exercise training (main effect exercise p=0.053; Figure 8C), which, as indicated by post hoc tests, is seen to a greater degree in DR versus DS women (p=0.184 vs p=0.754, respectively).

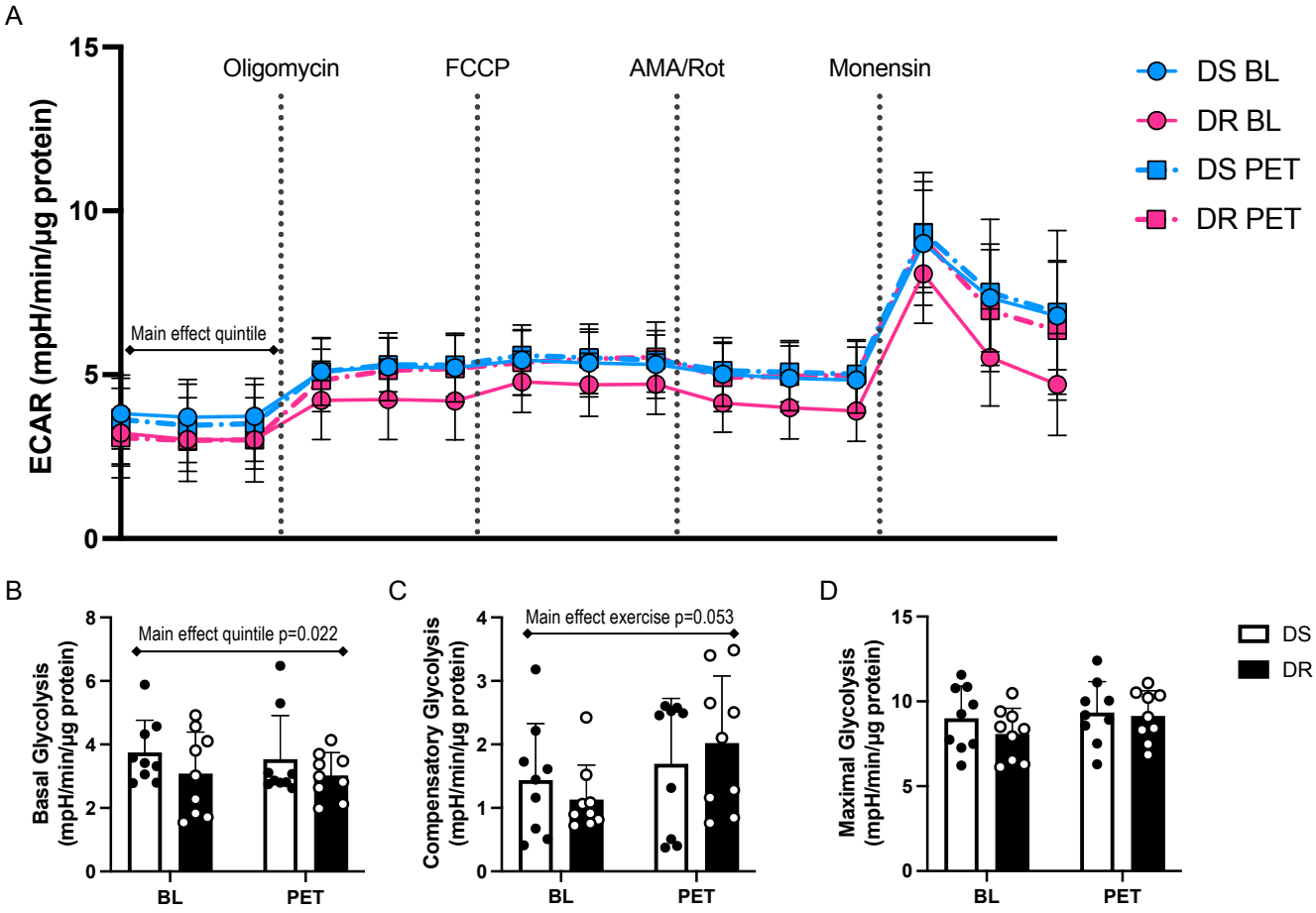

Figure 8. Glycolysis is higher in primary myotubes from DS vs DR women regardless of exercise training. Differentiated primary myotubes underwent a modified mitochondrial stress test (Agilent Seahorse XFe96) to measure Oxygen Consumption Rate (OCR) and Extracellular Acidification Rate (ECAR). **(A)** ECAR trace, injections marked with dotted lines. **(B-D)** Quantification of **(B)** basal glycolysis, **(C)** compensatory glycolysis, and **(D)** maximal glycolysis. Data are expressed as mean±SD relative to µg of protein per well (n=9). Means were compared using a 2-way repeated-measures ANOVA.

We next applied a publicly available algorithm[187,188] to evaluate ATP production by glycolysis and ATP production by oxidative phosphorylation. ATP production by OXPHOS was increased post-exercise in DR women during both basal and maximal respiration (p=0.006 and p=0.011, respectively; Figure 9B, C). Additionally, myotubes from DS women used more ATP production by glycolysis than their DR counterparts during basal respiration (main effect quintile p=0.022; Figure 9D).

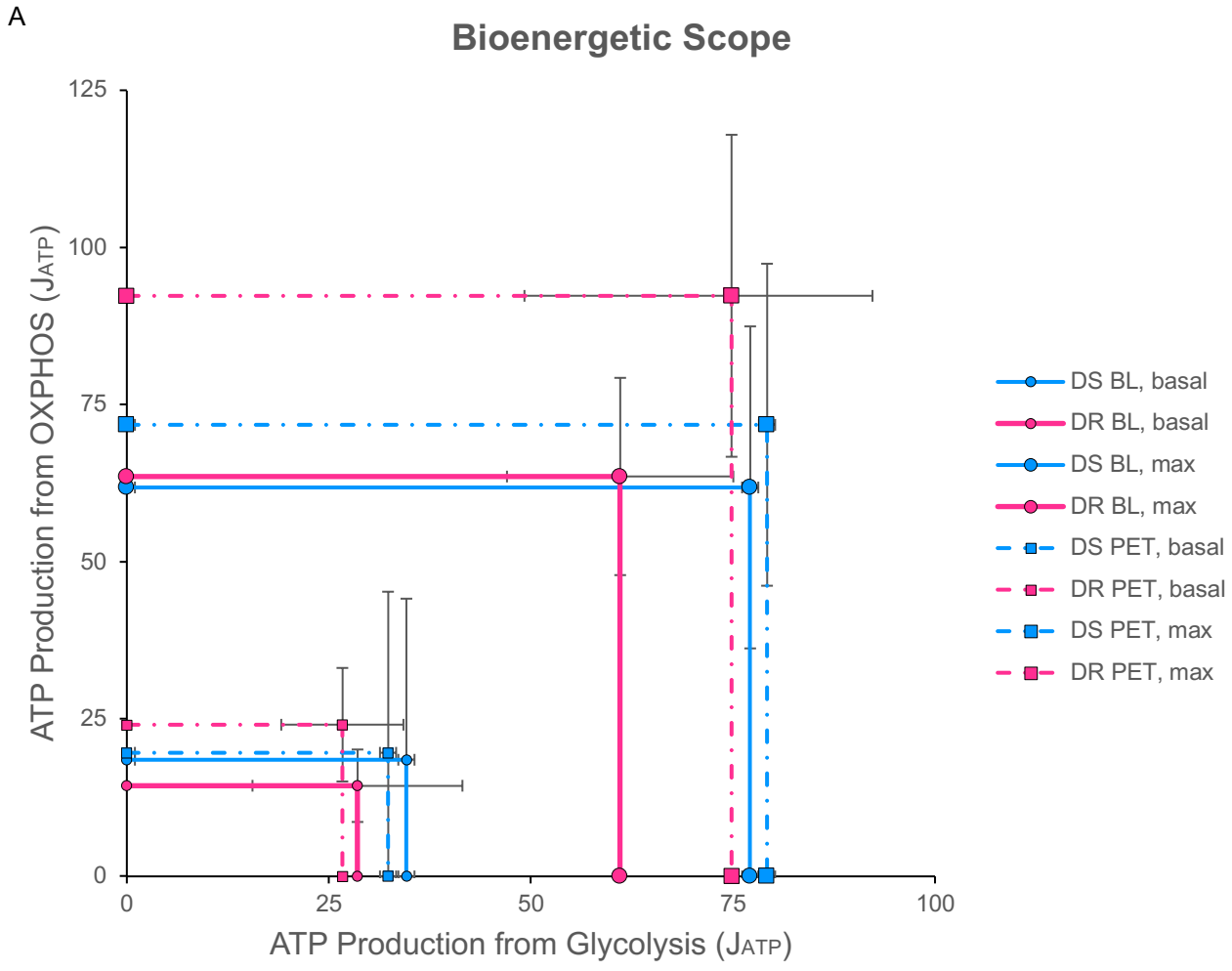

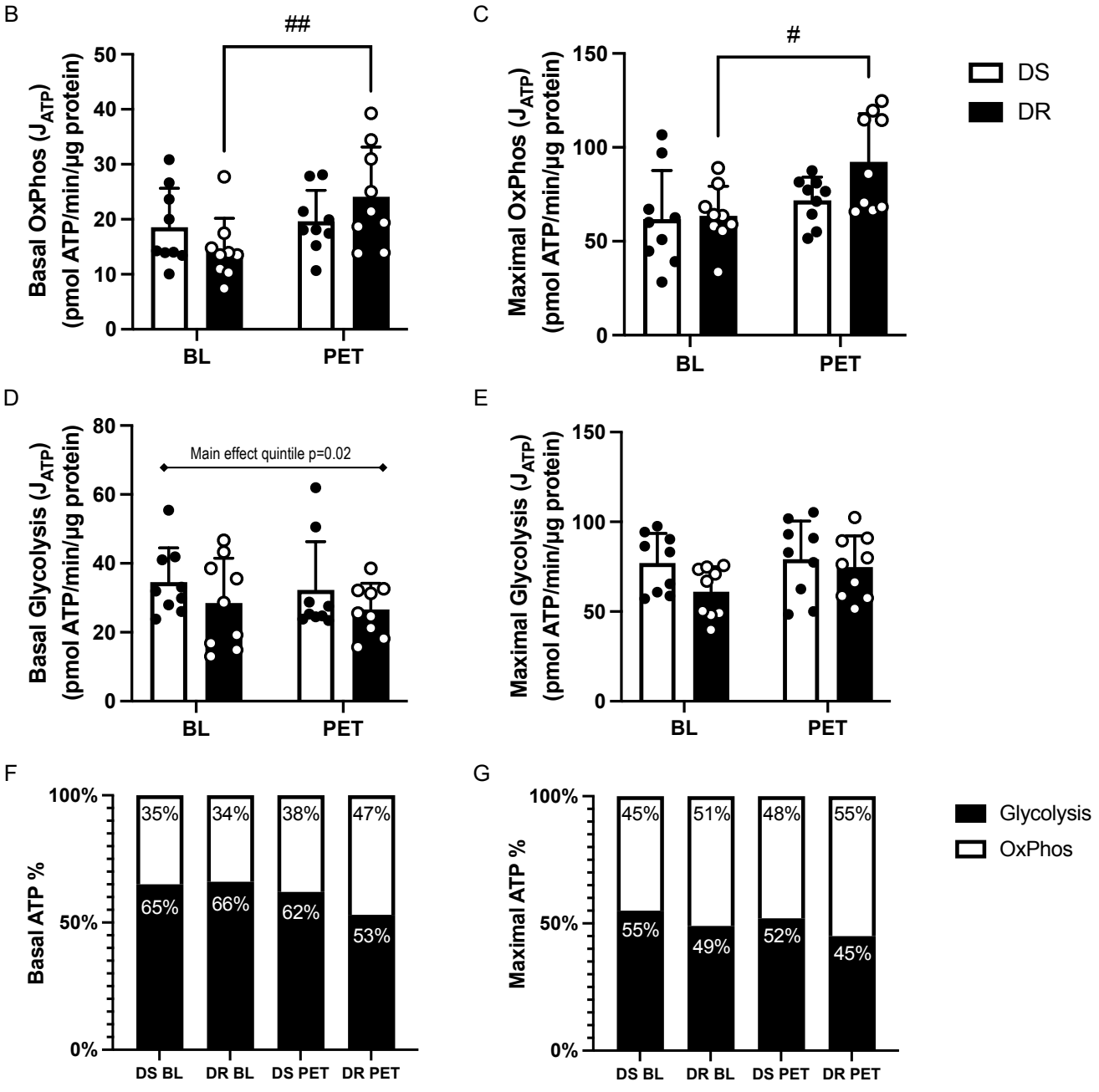

Figure 9. ATP production by OXPHOS is increased preferentially in DR myotubes post-exercise training. Differentiated primary myotubes underwent a modified mitochondrial stress test (Agilent Seahorse XFe96) and results were used to calculate ATP production by oxidative phosphorylation and glycolysis. **(A)** Bioenergetic scope. **(B-G)** Quantification of **(B)** ATP production by OXPHOS during basal respiration, **(C)** ATP production by OXPHOS during maximal respiration, **(D)** ATP production by glycolysis during basal respiration, **(E)** ATP production by glycolysis during maximal respiration, **(F)** bioenergetic capacity during basal respiration, and **(G)** bioenergetic capacity during maximal respiration. Data are expressed as mean±SD relative to µg of protein per well (n=9). Means were compared using a 2-way repeated-measures ANOVA. *$p<0.05$ DS vs DR, #$p<0.05$ BL vs PET

3.1.3 Myotube mitochondrial content

Next, we assessed citrate synthase activity, a marker of mitochondrial content[189] to confirm previous findings that regular moderate exercise increases mitochondrial content. Exercise-induced mitochondrial biogenesis has repeatedly been demonstrated in skeletal muscle[147,190], however, research on myotubes is limited and changes in CS activity have only been observed during *in vitro* experimentation (*i.e.*, electrical pulse stimulation)[191,192]. No significant differences in enzymatic activity were observed between any of the groups in primary myotubes (Figure 10).

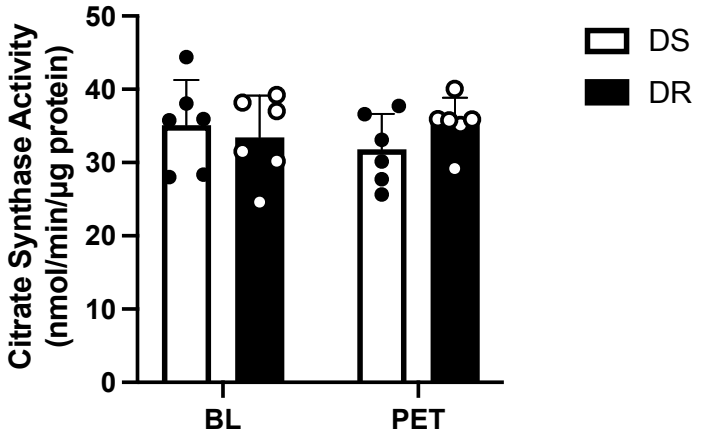

Figure 10. Total enzymatic activity of citrate synthase in myotube preparations does not differ between quintiles. Specific activities (nmol/min/µg protein) of citrate synthase (CS) were measured in differentiated primary myotubes. Data are expressed as mean±SD (n=6). Means were compared using a 2-way repeated-measures ANOVA.

3.1.4 Expression of mitochondrial OXPHOS complexes in muscle tissue

Western blotting was used to examine differences in the levels of expression of key subunits for each of the multiprotein complexes of the OXPHOS pathway. Exercise training increased the expression of complexes III, IV and V in homogenized skeletal muscle tissue from both DS and DR women (main effect exercise p=0.036, p=0.045, and p=0.046 respectively; Figure

11C, D, E). Similarly, there is a trend for increased CII expression post-exercise training (main effect exercise p=0.075 Figure 11B). Post hoc analyses revealed that exercise training increased CIV expression only in DS skeletal muscle (p=0.029; Figure 11D).

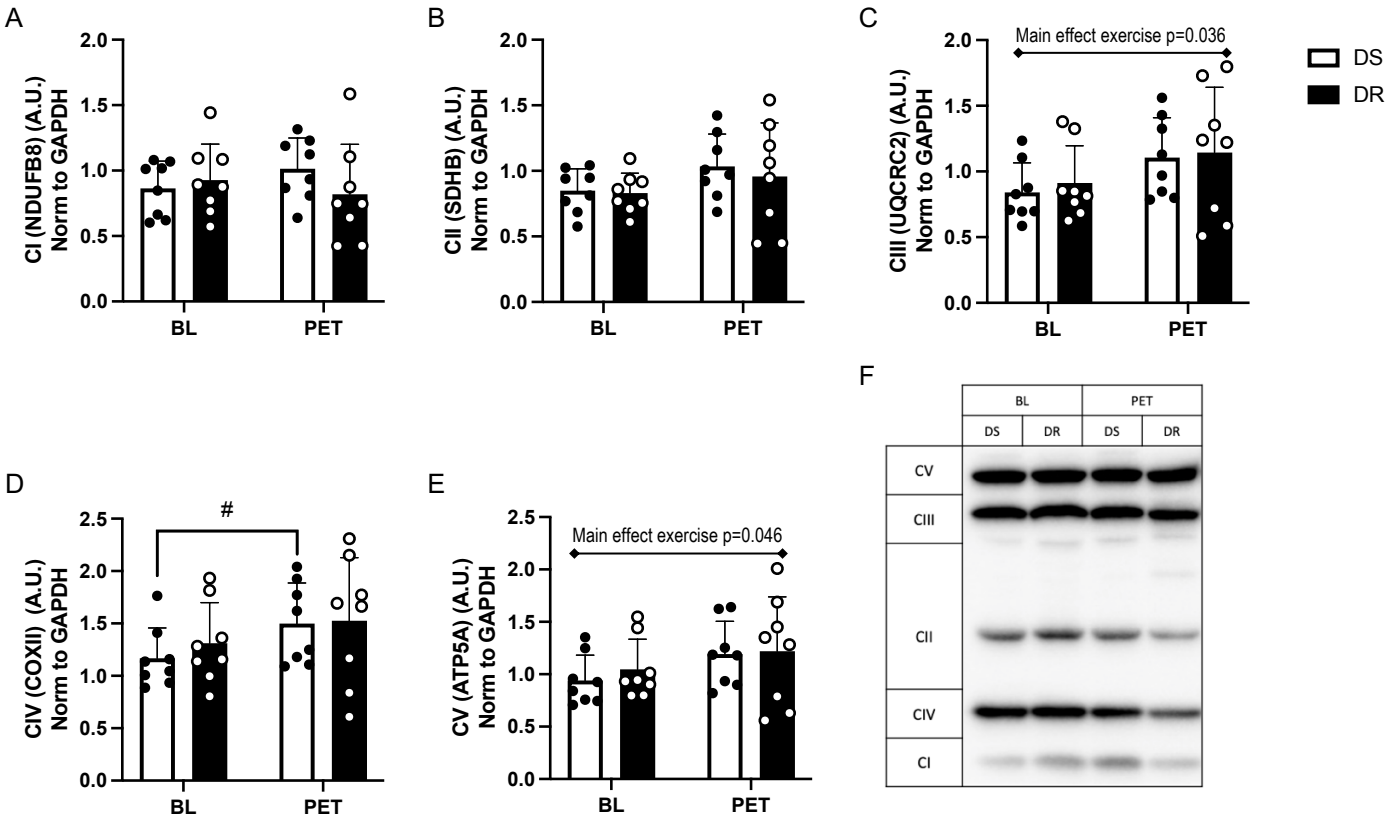

Figure 11. Exercise training increases expression of OXPHOS complexes in muscle tissue. Western blots were performed on muscle homogenate and used to quantify the protein expression of: **(A)** CI (NDUFB8), **(B)** CII (SDHB), **(C)** CIII (UQCRC2), **(D)** CIV (COXII), **(E)** CV (ATP5A). **(F)** Representative western blot of the indicated OXPHOS complexes. Data are expressed as mean±SD relative to GAPDH protein expression (n=6). Means were compared using a 2-way repeated-measures ANOVA. *p<0.05 DS vs DR, #p<0.05 BL vs PET

3.1.5 Mitochondrial dynamics and length

Exercise training promotes elongation of the mitochondrial network. To examine if enhanced mitochondrial fusion contributed to the observed increases in mitochondrial function, we quantified protein expression of key fusion and fission proteins.

There were no effects of ROWL quintile or exercise training on the expression of MFN1/2 or Drp1. However, exercise training tended to increase OPA1 expression in DS myotubes (quintile x exercise p=0.079; Figure 12A).

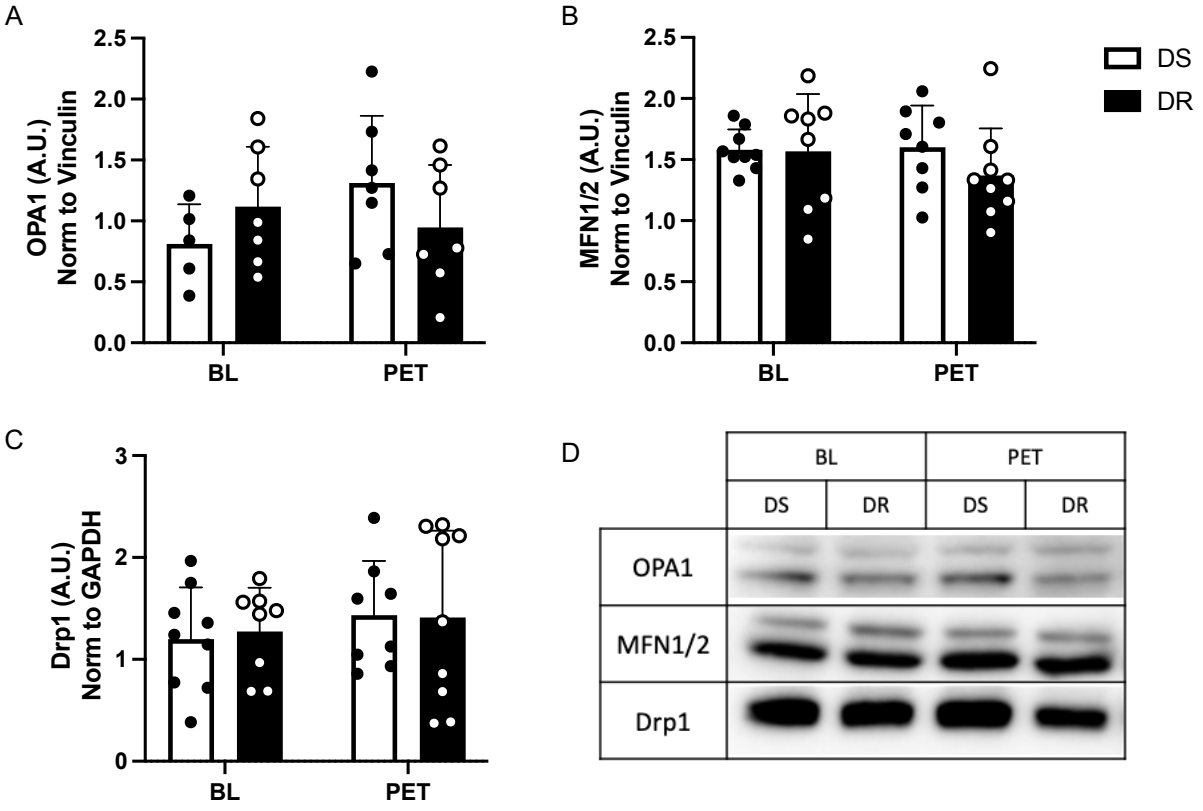

Figure 12. Markers of muscle mitochondrial dynamics remain unaltered between quintiles and pre- and post-exercise training. Western blots were performed on muscle homogenate and used to quantify protein levels of **(A)** OPA1, **(B)** MFN1/2, **(C)** Drp1. **(D)** Representative western blot of the indicated proteins. Data are expressed as Mean ±SD (n=9). Means were compared using a 2-way repeated-measures ANOVA. *p<0.05 DS vs DR, #p<0.05 BL vs PET

As the mitochondrial network is defined by the balance of dynamic fission and fusion processes, we next examined the effects of exercise training on mitochondrial length in primary myoblasts with quantitative morphometric analyses of TOM20-stained primary myoblasts. TOM20 is one of seven proteins that make up the translocase of the outer membrane of

mitochondria complex[193]. Exercise training resulted in a more fused mitochondrial reticulum, as indicated by an increase in mitochondrial length (main effect exercise p=0.0015). Post hoc analyses showed that this was driven by increased mitochondrial length in myoblasts isolated from DR women, (p=0.008; Figure 13A).

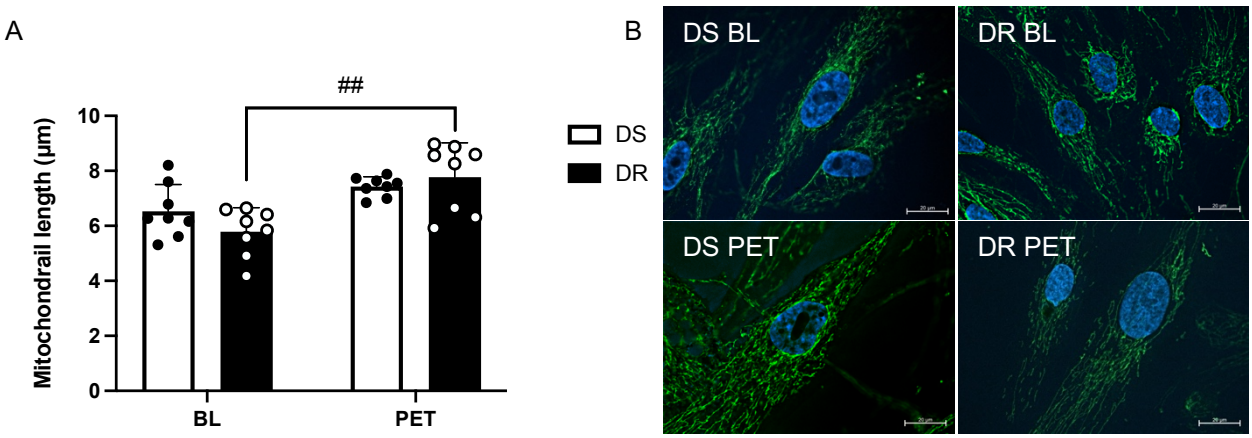

Figure 13. Mitochondrial length is preferentially increased in DR myoblasts post-exercise training. Primary myoblasts were stained with TOM20 and mitochondrial length was measured. **(A)** Mitochondrial lengths (µm). **(B)** Representative images with TOM20 (green) and DAPI (blue); scale bars: 20 µm. Data are expressed as mean±SD (n=8). Means were compared using a 2-way repeated-measures ANOVA. *p<0.05 DS vs DR, #p<0.05 BL vs PET

3.1.6 Glutathione redox and ROS emissions

We have previously observed differences in glutathione redox in DS versus DR cohorts of women. Additionally, because of the coupled nature of changes in OXPHOS and ROS emissions, we also wanted to examine possible differences in ROS production. In the presence of ROS, two GSH molecules are rapidly oxidized to GSSG. A decrease in the glutathione redox ratio (GSH:GSSG) is indicative of oxidative stress[64]. HPLC was used to determine whether there is any change in glutathione redox in primary myotubes pre- and post-exercise training.

In contrast to our previous findings, at BL there were no differences in glutathione redox between quintiles. However, exercise training increased total glutathione, GSH, and GSSG in primary myotubes from both DR and DS women (main effect p=0.0007 and p=0.047, respectively; Figure 14A, B). Post hoc analyses revealed that the post-exercise training increase in GSSG is primarily driven by DS women rather than DR women (exercise within DS p=0.062; exercise within DR p=0.886). These differences are also reflected in the amount of total glutathione and the GSH:GSSG ratio (p=0.020 and p=0.040, respectively; Figure 14C, D).

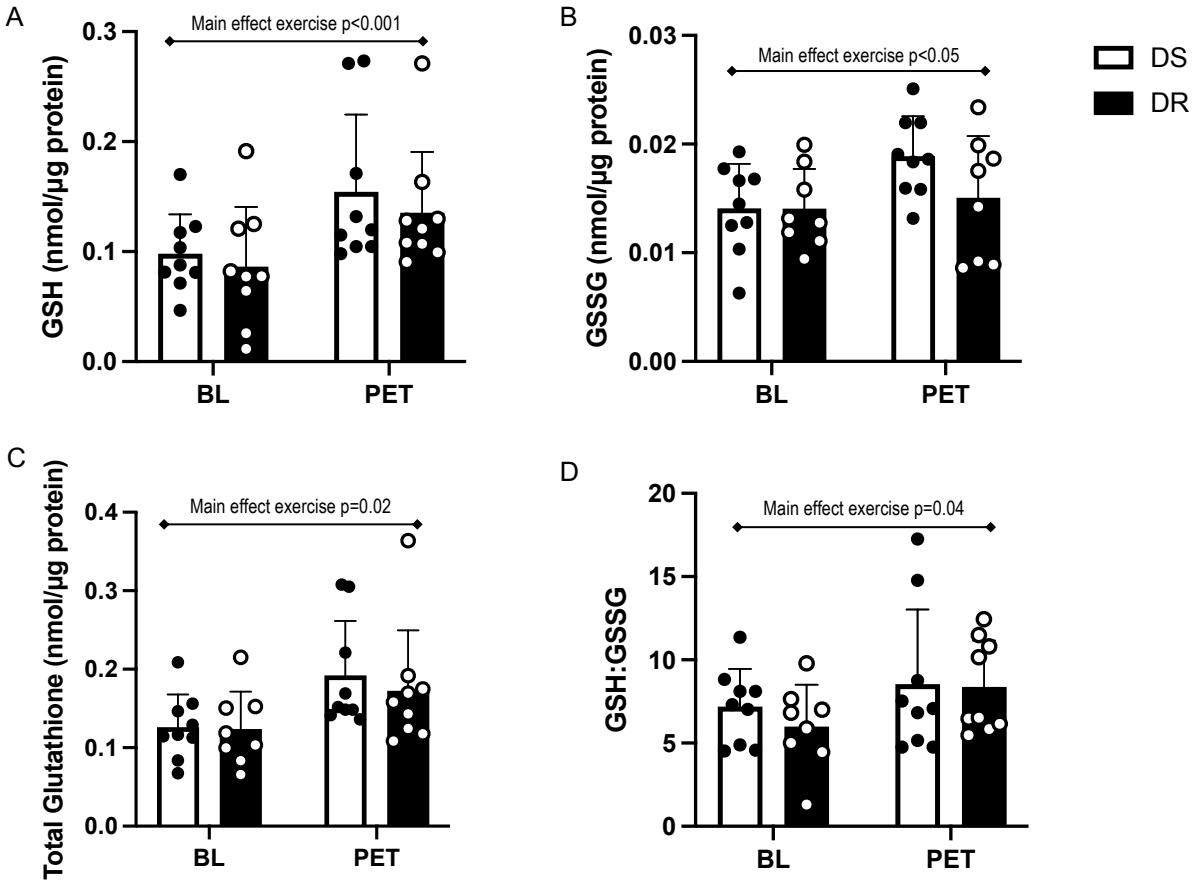

Figure 14. GSH:GSSG ratio is increased post-exercise training in both DS and DR primary myotubes. HPLC was performed on differentiated primary myotubes and used to quantify: **(A)** absolute concentration of GSH levels, **(B)** absolute concentration of GSSG levels, **(C)** total glutathione, and **(D)** GSH:GSSG ratio. Data are expressed as mean±SD relative to µg of protein per sample (n=9). Means were compared using a 2-way repeated-measures ANOVA.

3.1.7 Glucose uptake measurement and response to insulin stimulation

Skeletal muscle is strongly dependent on mitochondria for cellular energy transduction to produce ATP[15]. To successfully produce ATP, the muscle needs oxygen and a source of carbon, often fatty acids (FA) or glucose when it is abundant in the blood, as is the case after meals. Generally, muscle cells respond to insulin stimulation by increasing glucose uptake into the cells. However, exercise training enhances skeletal muscle glucose uptake through insulin-independent mechanisms and can begin to counteract the negative effects on glucose metabolism seen in insulin-resistant muscle[194].

Characterization of skeletal muscle glucose metabolism was performed by quantifying 14C-glucose uptake in primary myotubes from DS and DR women. There is a main effect of insulin stimulation ($p=0.001$; Figure 16A). This is primarily driven by significance between glucose uptake with and without insulin stimulation in the DS myotubes at baseline ($p=0.02$). This suggests that our primary myotubes isolated from individuals with obesity are insulin sensitive. Unspecific uptake was measured by adding cytochalasin B to the incubation mix; values are significantly lower in the presence of the glucose uptake inhibitor. There were no statistical differences between any of the groups for unspecific uptake.

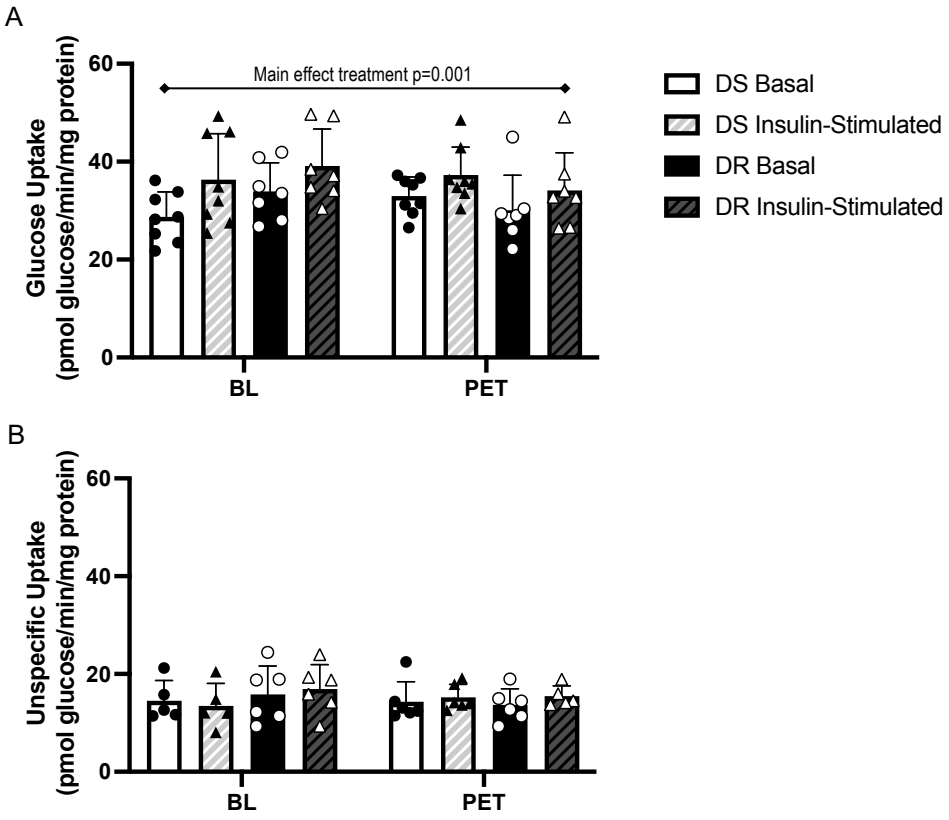

Figure 15. Primary myotubes are sensitive to insulin-stimulated glucose uptake. Differentiated myotubes were serum-deprived for 3 hours before being incubated in KRH buffer with or without 100 nM insulin for 1 hour. 0.1 µCi/mL of radiolabeled [14C]2DG and 10 µM D-glucose was added to the cells and incubated for an additional 15 minutes. Cells were lysed in 0.1 M NaOH and then scintillation reads were performed to measure: **(A)** Basal and insulin-stimulated glucose uptake. **(B)** Unspecific glucose uptake. Data are expressed as mean±SD relative to mg of protein per well (n=7). Means were compared using a 3-way repeated-measures ANOVA.

3.1.8 Plasma cytokine levels

Thirty cytokines were selected to examine the effects of exercise training on inflammation. The cytokines were analysed by U-PLEX assay (MSD; Rockville, MD) in fasted EDTA plasma samples from DS and DR women pre- and post-exercise. Specific cytokines were selected to confirm previous differences observed in unpublished Somalogics plasma proteomics data or because of their involvement in inflammatory pathways and pathways known to be affected by exercise.

At BL, DR women had higher concentrations of the chemokines CTACK and SDF1α, IL-18, total ghrelin, and the anorexigenic appetite hormone Peptide YY (PYY) ($p<0.0001$, $p=0.005$, $p=0.046$, $p=0.0003$, and $p=0.024$, respectively; Figure 17D, M, K, E, L). Post-exercise training, DR women continued to have higher concentrations of the chemokine CTACK, IL-18, and total ghrelin ($p=0.002$, $p=0.046$, and $p=0.0004$, respectively; Figure 17D, K, E), as well as now having higher concentrations of the neurotrophic factor BDNF ($p=0.019$; Figure 17A). Whereas DS women had higher plasma concentrations of C-peptide and IL-1α both at BL ($p=0.027$ and $p=0.002$, respectively) and PET ($p=0.039$ and $p=0.016$, respectively; Figure 17C, H). Additionally, DS women had higher concentrations of TARC and GLP1 (trending) regardless of exercise training (main effect quintile $p=0.041$ and $p=0.110$; Figure 17N, F), and a strong trend for having higher TNFα concentrations PET ($p=0.053$; Figure 17O). Exercise training increased plasma concentrations of β-NGF, IFNα2a, and GLP1 (trending) in both DS and DR women (main effect exercise $p<0.0001$, $p=0.004$, and $p=0.102$, respectively; Figure 17B, G, F). Moreover, exercise training increased CTACK, SDF1α and IL-15 to a greater extent in DS women ($p=0.015$, $p=0.004$, and $p=0.048$, respectively; Figure 17D, M, J). In contrast, exercise decreased plasma TNFα concentrations (main effect exercise $p=0.025$; Figure 17O). There were no differences between quintiles or with exercise training in inflammatory markers traditionally thought to be related to inflammation including those affected by exercise (Figure S1).

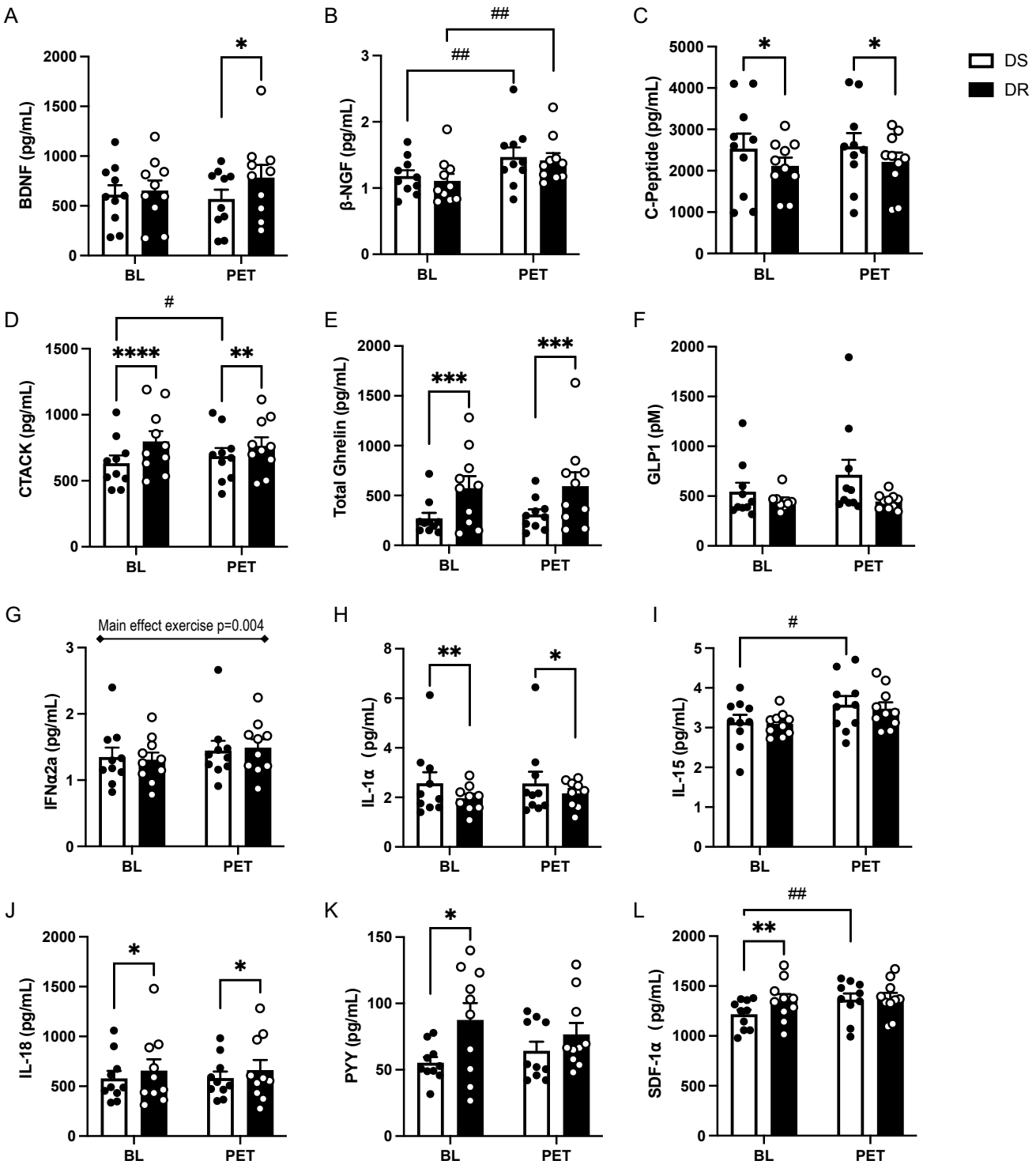
A
BDNF (pg/mL)
2000
1500
1000
500
0
*
BL
PET
B
β-NGF (pg/mL)
3
2
1
0
##
##
BL
PET
C
C-Peptide (pg/mL)
5000
4000
3000
2000
1000
0
*
*
BL
PET
DS
DR
D
CTACK (pg/mL)
1500
1000
500
0
#
****
**
BL
PET
E
Total Ghrelin (pg/mL)
2000
1500
1000
500
0
***
***
BL
PET
F
GLP1 (pM)
2000
1500
1000
500
0
BL
PET
G
Main effect exercise p=0.004
IFNα2a (pg/mL)
3
2
1
0
BL
PET
H
IL-1α (pg/mL)
8
6
4
2
0
**
*
BL
PET
I
IL-15 (pg/mL)
5
4
3
2
1
0
#
BL
PET
J
IL-18 (pg/mL)
2000
1500
1000
500
0
*
*
BL
PET
K
PYY (pg/mL)
150
100
50
0
*
BL
PET
L
SDF-1α (pg/mL)
2000
1500
1000
500
0
##
**
BL
PET

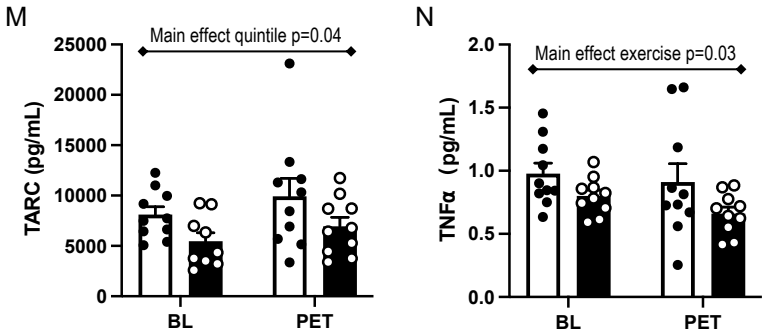

Figure 16. Effect of exercise training on the levels of various plasma cytokines. Expression of selected cytokines in fasted EDTA plasma samples from DS and DR women were analysed using U-PLEX assay including: **(A)** BDNF, **(B)** β-NGF, **(C)** C-peptide, **(D)** CTACK, **(E)** Total Ghrelin, **(F)** GLP1, **(G)** IFNα2a, **(H)** IL-1α, **(I)** IL-15, **(J)** IL-18, **(K)** PYY, **(L)** SDF1α, **(M)** TARC, **(N)** and TNFα. Data are expressed as mean±SEM (n=10). Means were compared using a 2-way repeated-measures ANOVA. *p<0.05 DS vs DR, #p<0.05 BL vs PET

3.1.9 Expression of inflammatory marker proteins in muscle tissue

Acute physical exercise initiates several beneficial effects in skeletal muscle, including improvements in glucose uptake[170], lipid metabolism[195], and insulin sensitivity[154]. However, exercise also induces the activation of MAPK-ERK and IKK-NFκB signaling pathways in skeletal muscle. Several proteins including IκB, MAPK, and ERK work in conjunction with NFκB to control downstream inflammation and immune responses. The magnitude of MAPK/ERK phosphorylation during exercise directly correlates with the intensity of the exercise being performed[196]. Despite the negative connotations with pro-inflammatory molecules, increases in MAPK and NFκB signaling are necessary responses to chronic and intermittent stressors[150]. Skeletal muscle myocytes release cytokines (termed myokines) during contractions which play important roles in regulating skeletal muscle repair and metabolism. As such, we next sought to determine the activation of key inflammatory signaling pathways by quantifying the expression of inflammatory mediators (NFκB, IκBα, MAPK, ERK, TLR4) in muscle homogenate from DS and DR women. The phosphorylated over total ratio of these key inflammatory proteins is used as an

index of inflammatory response since it is often the phosphorylation of proteins that induces downstream immune responses, although total protein expression may be altered as well.

Exercise training increased the expression of phospho-NFκB in both groups (main effect p=0.039); this was seen to a greater extent in DR versus DS women (p=0.0029 and p=0.11, respectively; Figure S2). The increase in phosphorylated NFκB was reflected by an increase in the phospho:total ratio post-exercise training in DR women only (exercise within DR p=0.0023, quintile within PET p=0.0069; Figure 18A). Additionally, post-exercise, DR versus DS women had higher expression of p-NFκB, which is reflected in the phospho:total ratio post-exercise (main effect quintile p=0.023 and p=0.0069, respectively; Figure S2, 18A).

Expression of total IκB was higher in DR versus DS women (main effect quintile p=0.029). Post hoc analyses revealed that total IκB was higher in DR women at baseline only (p=0.017; Figure S3). Exercise training decreased total IκB post-exercise in DR women (p=0.04; Figure S3). While there was no difference in the ratio of phosphorylated IκB to total IκB between any of the groups, exercise tended to decrease the expression of phosphorylated IκB post-exercise in DR women (p=0.121; Figure S3). Similarly, there is a trend for decreased expression of phosphorylated ERK in DR skeletal muscle following exercise training (p=0.052, Figure S5), but the ratio of phosphorylated to total ERK was not different between groups (Figure 18D). In contrast to the differences in NFκB signaling, no differences were observed in MAPK, or TLR4 expression (Figures 18C and 18E).

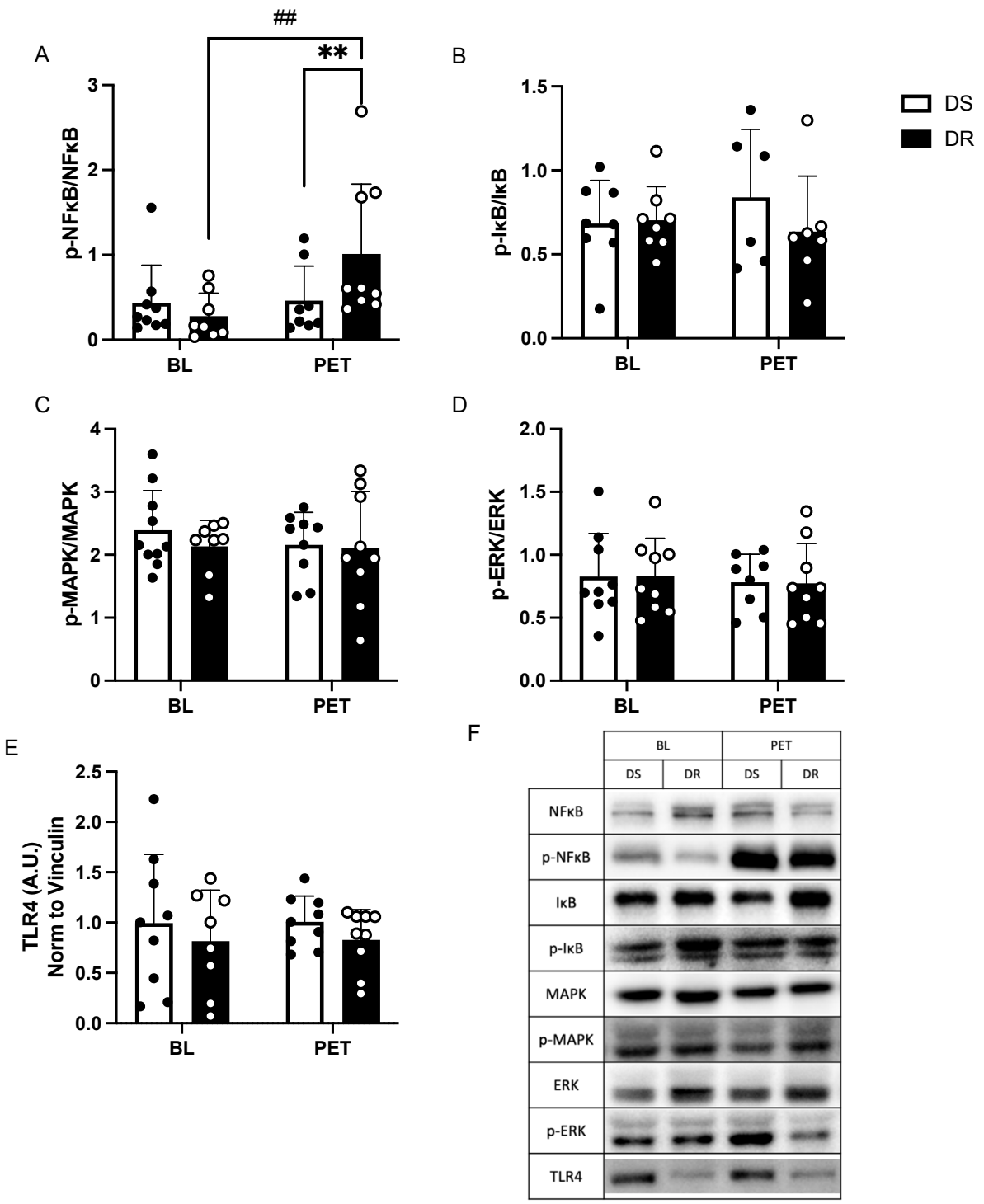

Figure 17. Phospho:total NFκB ratio is increased post-exercise training in DR muscle tissue. Western blots were performed on muscle homogenate and used to quantify: **(A)** the phospho:total NFκB ratio, **(B)** the phospho:total IκB ratio, **(C)** the phospho:total MAPK ratio, **(D)** the phospho:total ERK ratio, **(E)** the protein expression of TLR4 relative to vinculin. **(F)** Representative western blot of the indicated proteins. Data are expressed as mean±SD (n=9). Means were compared using a 2-way repeated-measures ANOVA. *p<0.05 DS vs DR, #p<0.05 BL vs PET

3.2 Objective #2: Immunometabolic response in primary myotubes derived from diet-sensitive and diet-resistant women following an *in vitro* inflammatory challenge.

Activation of inflammatory mediators by nutrient overload (*i.e.*, fatty acids) impairs mitochondrial homeostasis and contributes to insulin resistance[94]. Cultured primary myotubes retain many of the characteristics of skeletal muscle studied *in vivo*[197] and exposure of primary myotubes to inflammatory stimuli can help elucidate the molecular mechanisms that are altered in specific disease states. For example, myotubes isolated from individuals with T2D that are exposed to fatty acids or lipopolysaccharide (LPS) demonstrate impaired fatty acid oxidation[36,198] and altered myokine secretion[199] compared to myotubes isolated from non-diabetic controls.

Palmitate fatty acid treatment can be used as a nutrient overload challenge *in vitro*, and thus induce an inflammatory response. LPS is a component of the outer membrane of Gram-negative bacteria that induces an inflammatory response in skeletal muscle and is also considered to be a causative factor for the development of insulin resistance[200,201]. Emerging evidence suggests that high fat-containing diets can alter gut flora growth and intestinal wall permeability, elevating enterobacterial production and translocation of LPS into systemic circulation[202]. Therefore, to explore the differences in immunometabolic responses between the ROWL quintiles following exercise training, we employed palmitate and LPS as inflammatory challenges on primary myotubes isolated from DR and DS individuals.

3.2.1 Expression of inflammatory marker proteins in palmitate treated myotubes

Primary myoblasts isolated from DR and DS individuals were differentiated into myotubes and then treated with 500 μM palmitate to induce an inflammatory response. Western blot analysis was used to quantify the expression of inflammatory mediators (NFκB, IκBα, HIF1α, Nrf2, TLR4),

autophagic flux proteins (LC3II/I, PRKN), and proteins related to ROS, glutathione, and ferroptosis (GPx4, SLC7A11, SOD1, SOD2) in the treated primary myotubes[95,200,203].

Palmitate had little effect on inducing inflammatory protein expression, presumably because obesity is already a state of nutrient-load-induced chronic inflammation and the addition of 500 μM palmitate to the myotubes may not be enough to further induce an inflammatory response. Similar to the *ex vivo* skeletal muscle expression of NFκB, primary myotubes from DR women tended to have higher expression of p-NFκB than myotubes isolated from DS women regardless of treatment with palmitate (main effect quintile p=0.064; Figure S6). This observation was also reflected in the ratio, where DR myotubes tended to have a higher ratio of phosphorylated to total NFκB expression (main effect quintile p=0.055, respectively; Figure 19A). Consistent with the expression of IκB in skeletal muscle homogenate, the expression of phosphorylated and total IκB did not differ between groups after palmitate exposure (Figure 19B, S7).

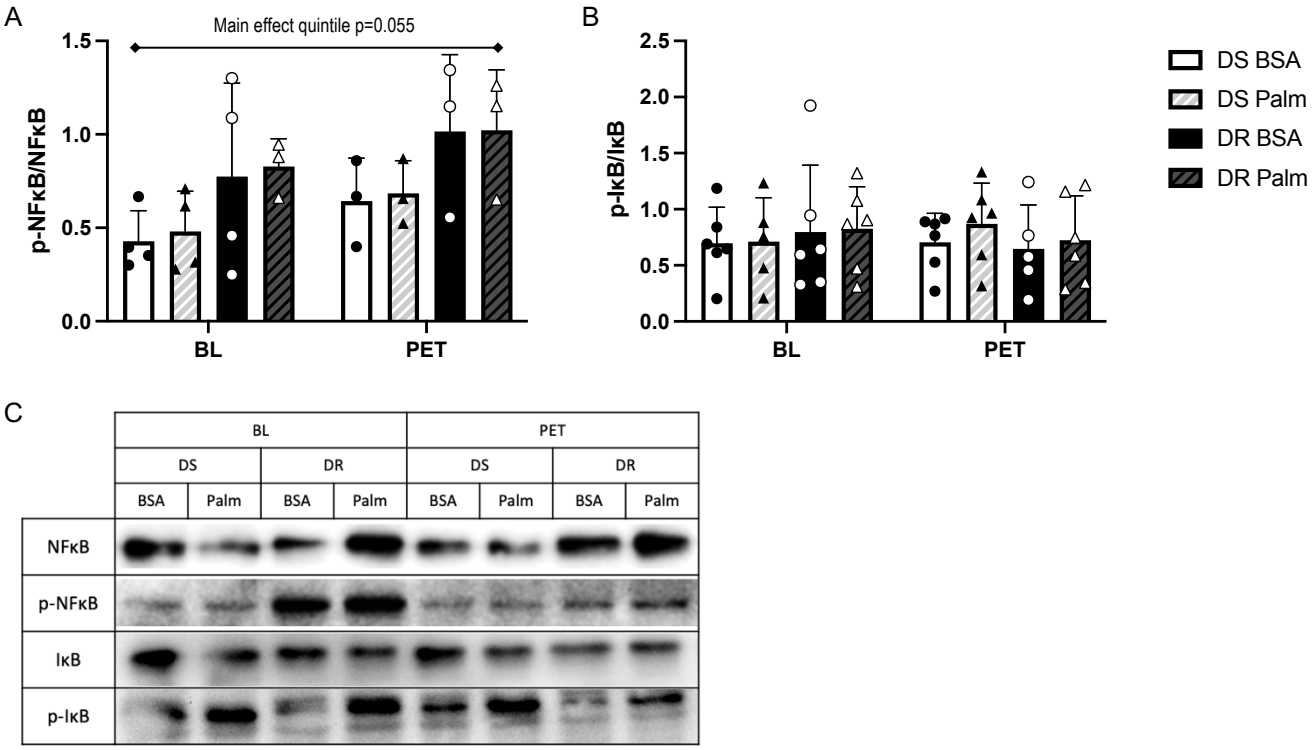

Figure 18. Phospho:total NFκB ratio is increased in DR vs DS primary myotubes. Differentiated myotubes were treated with 500 μM palmitate for 24 hours. Western blots were performed on treated cells and used to quantify: **(A)** the phospho:total NFκB ratio, **(B)** the phospho:total IκB ratio. **(C)** Representative western blot of the indicated proteins. Data are expressed as mean±SD relative to GAPDH protein expression (n=4 [NFκB], n=6 [IκB]). Means were compared using a 3-way repeated-measures ANOVA.

There is a strong trend for the LC3II/I ratio to increase post-exercise training regardless of quintile (p=0.063; Figure 20A). There is a strong trend for DR women to express increased quantities of PRKN (main effect quintile p=0.084; Figure 20C).

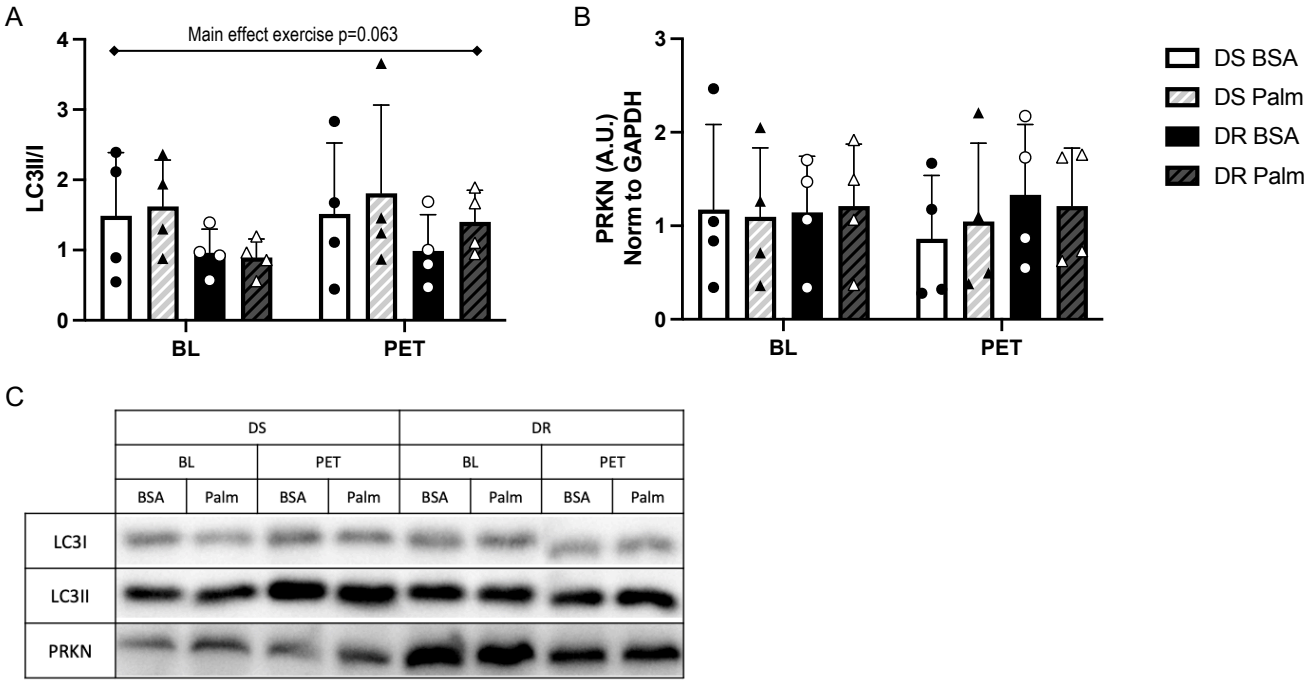

Figure 19. LC3II/I ratio is trending increased post-exercise training. Differentiated myotubes were treated with 500 μM palmitate for 24 hours. Western blots were performed on treated cells and used to quantify: **(A)** the LC3II/I ratio, **(B)** the protein expression of PRKN. **(C)** Representative western blot of the indicated proteins. Data are expressed as mean±SD relative to GAPDH protein expression (n=4). Means were compared using a 3-way repeated-measures ANOVA.

Markers of ferroptosis were not significantly altered in myotubes exposed to palmitate, apart from Nrf2, which increased following treatment with palmitate (main effect treatment $p=0.035$; Figure 21A). In addition, exercise training tended to enhance the expression of SLC7A11 in myotubes regardless of exposure to palmitate ($p=0.099$; Figure 21B).

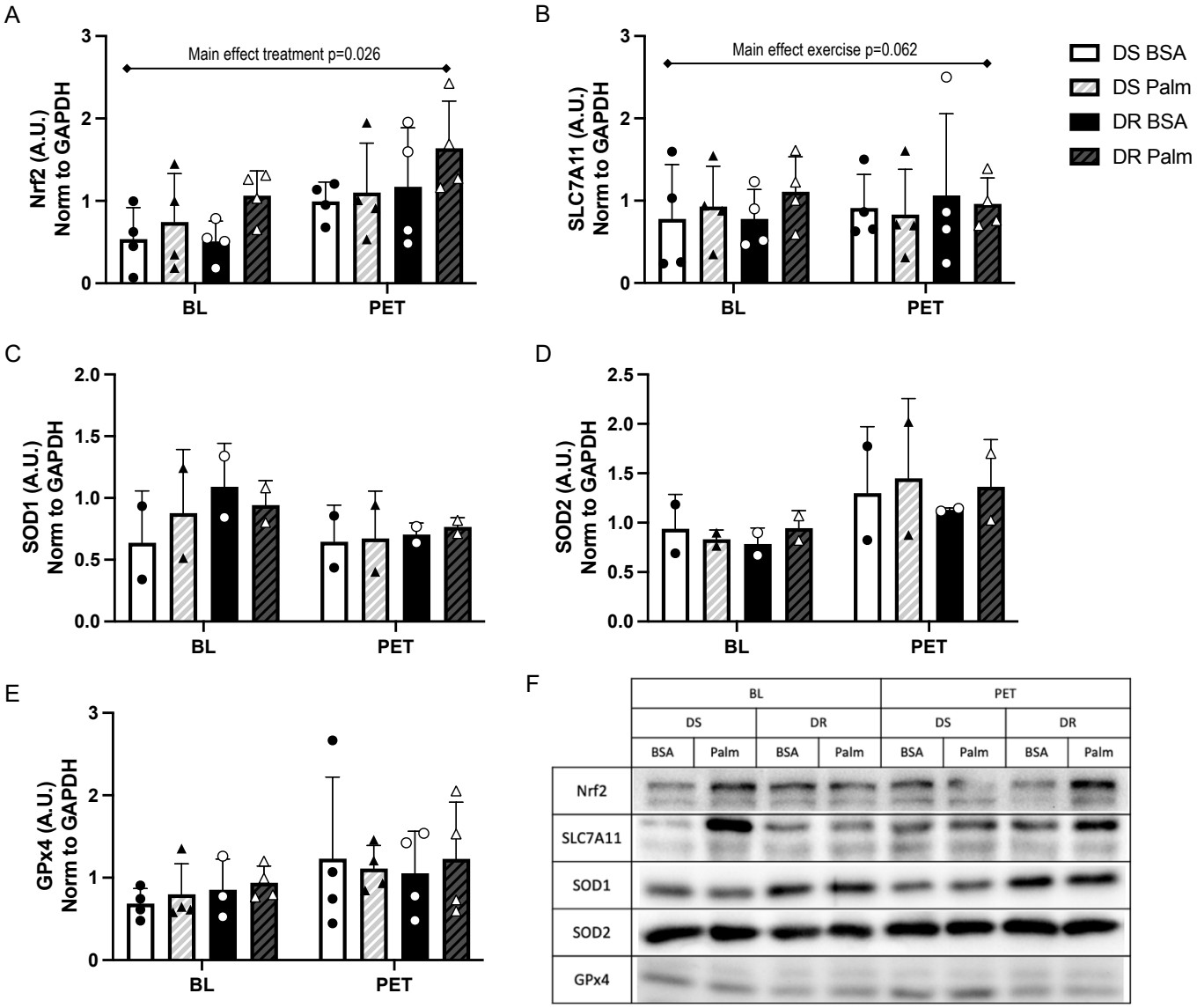

Figure 20. Expression of Nrf2 is increased after a palmitate inflammatory challenge. Differentiated myotubes were treated with 500 µM palmitate for 24 hours. Western blots were performed on treated cells and used to quantify: **(A)** the protein expression of Nrf2, **(B)** the protein expression of SLC7A11 (37kDa), **(C)** the protein expression of SOD1, **(D)** the protein expression of SOD2, **(E)** the protein expression of GPx4. **(F)** Representative western blot of the indicated proteins. Data are expressed as mean±SD relative to GAPDH protein expression (n=4 [Nrf2/SLC7A11/GPx4], n=2 [SOD1/2]). Means were compared using a 3-way repeated-measures ANOVA.

3.2.2 Expression of inflammatory marker proteins in LPS treated myotubes

As palmitate had little effect on inducing inflammatory responses, we next treated the primary myotubes with LPS to induce an inflammatory response. LPS activates inflammation through a canonical pathway using TLR4 surface receptors[201]. Primary myotubes were treated with 100 pg/mL LPS for 24 hours, and western blot analysis was used to quantify the expression of the key proteins involved in inflammatory responses.

Myotubes from DR women had higher expression of total NFκB regardless of LPS treatment (main effect quintile p=0.022; Figure S9). The LPS inflammatory challenge induced phosphorylation of NFκB (main effect treatment p=0.043; Figure S9), which was also reflected in the phospho:total ratio, where the ratio increased with treatment with LPS (p=0.039; Figure 22A). Similarly, exposure to LPS tended to increase the phosphorylation of IκB (main effect treatment p=0.067; Figure S10). Interestingly, myotubes isolated from both DR and DS women after exercise training exhibited an increase in the ratio of phosphorylated to total IκB (p=0.033), which also tended to be further amplified with LPS treatment (main effect treatment p=0.062; Figure 22B).

The increase in the ratio of phosphorylated to total IκB with exercise and LPS treatment could be due to the trend for decreased total IκB expression following both exercise and LPS treatment (p=0.146 and p=0.115, respectively; Figure S10). Consistent with the mechanism of action of LPS, TLR4 expression increased with LPS treatment (main effect p=0.041; Figure 22C). Moreover, myotubes isolated from DS women following exercise training exhibited increased TLR4 expression (quintile x exercise p=0.018).

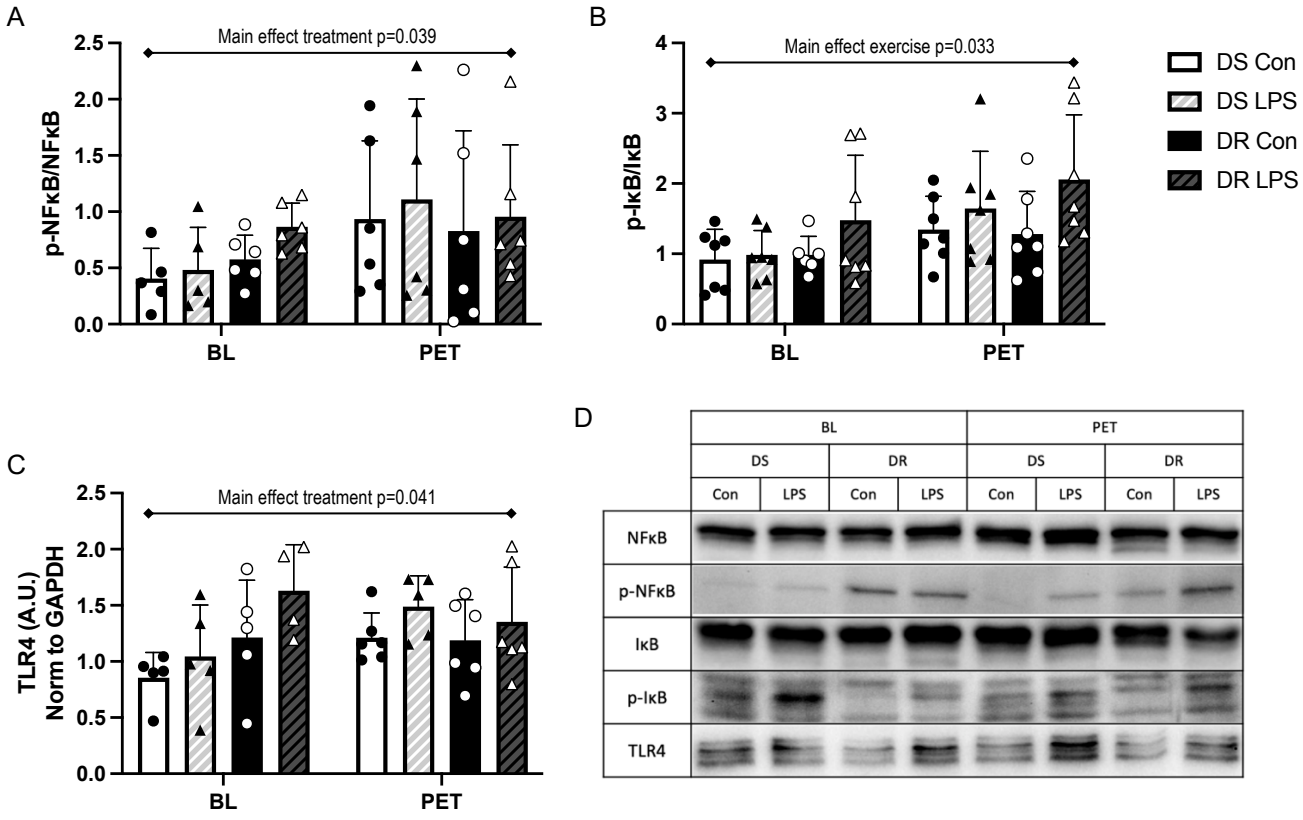

Figure 21. Inflammatory markers in primary myotubes are increased after an LPS inflammatory challenge. Differentiated myotubes were treated with 100 pg/mL LPS for 24 hours. Western blots were performed on treated cells and used to quantify: **(A)** the phospho:total NFκB ratio, **(B)** the phospho:total IκB ratio, **(C)** the protein expression of TLR4 relative to GAPDH. **(D)** Representative western blot of the indicated proteins. Data are expressed as mean±SD (n=6 [NFκB/TLR4], n=7 [IκB]). Means were compared using a 3-way repeated-measures ANOVA.

LC3I was preferentially expressed in DR versus DS women (main effect quintile p=0.046; Figure S11); however, there were no significant differences between any of the groups when examining the LC3II/I ratio. There is a trending interaction effect between exercise and quintile such that DS individuals tended to have an increased LC3II/I ratio post-exercise training and the reverse was seen in DR individuals (quintile x exercise p=0.082; Figure 23A). There is a trend for preferential expression of PRKN in DR versus DS myotubes (p=0.121; Figure 23B).

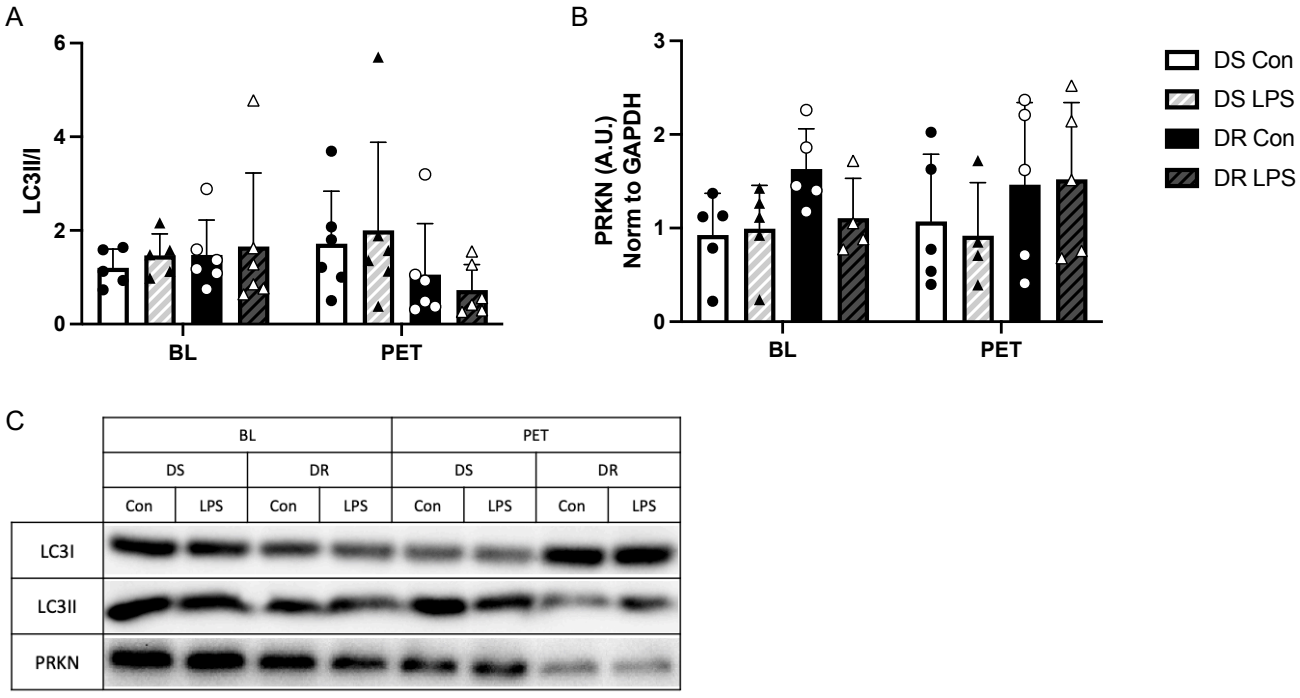

Figure 22. Marker of autophagic flux, LC3I, is preferentially expressed in DR vs DS women. Differentiated myotubes were treated with 100 pg/mL LPS for 24 hours. Western blots were performed on treated cells and used to quantify: **(A)** the LC3II/I ratio, **(B)** the protein expression of PRKN. **(C)** Representative western blot of the indicated proteins. Data are expressed as mean±SD relative to GAPDH protein expression (n=6 [LC3II/I], n=5 [PRKN]). Means were compared using a 3-way repeated-measures ANOVA.

Similar to the effects of palmitate, LPS did not alter the expression of key proteins involved in ferroptosis and the detoxification of ROS. However, exercise training tended to increase GPx4 expression in both DR and DS myotubes (main effect p=0.054; Figure 24C). Moreover, there is also a strong trend for DR myotubes to have higher expression of SLC7A11 than myotubes isolated from DS women (main effect p=0.055; Figure 24D).

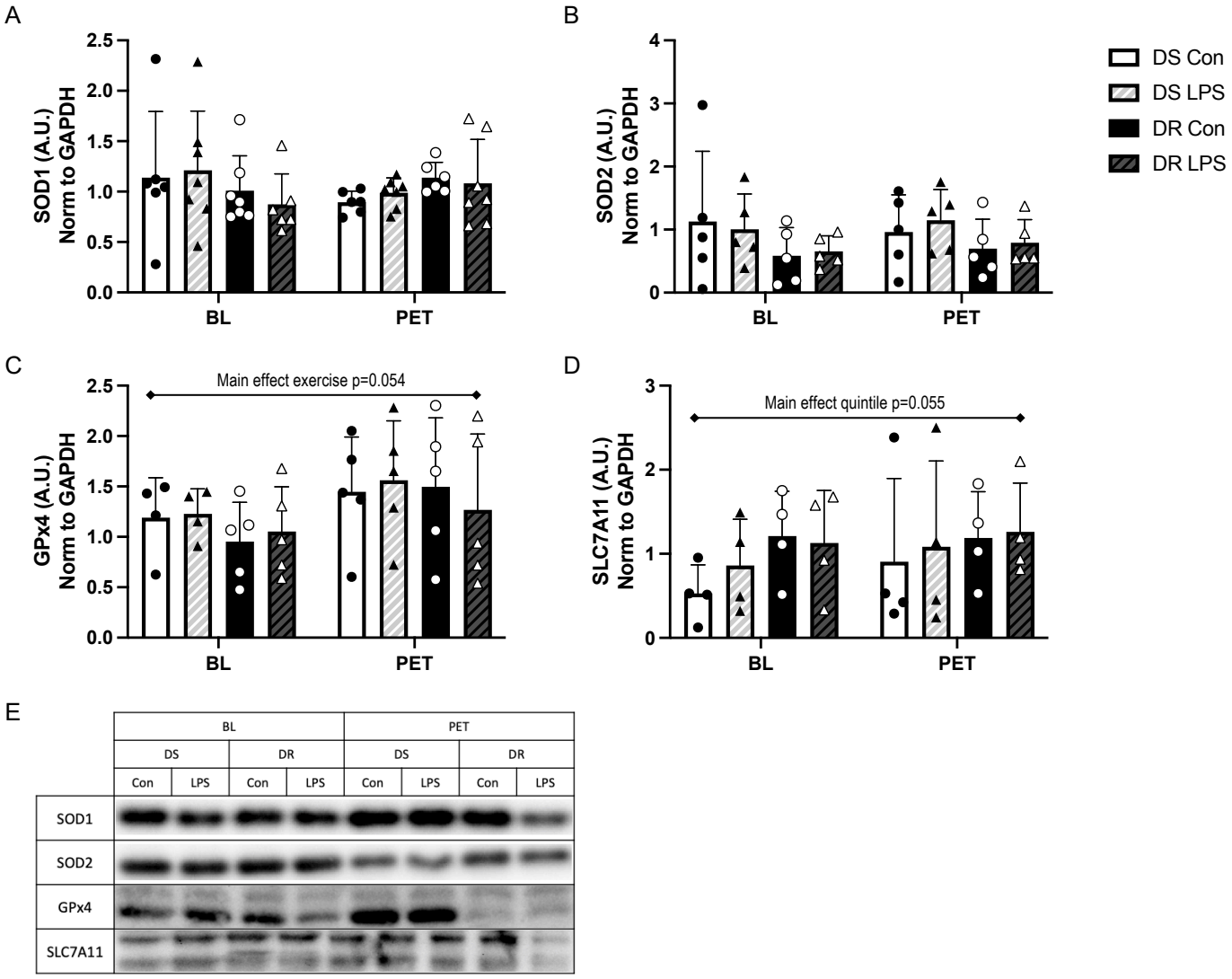

Figure 23. Exercise training increases the expression of GPx4. Differentiated myotubes were treated with 100 pg/mL LPS for 24 hours. Western blots were performed on treated cells and used to quantify: **(A)** the protein expression of SOD1, **(B)** the protein expression of SOD2, **(C)** the protein expression of GPx4, **(D)** the protein expression of SLC7A11. **(E)** Representative western blot of the indicated proteins. Data are expressed as mean±SD relative to GAPDH protein expression (n=7 [SOD1], n=5 [SOD2], n=5 [GPx4], n=4 [SLC7A11]). Means were compared using a 3-way repeated-measures ANOVA.

3.2.3 Mitochondrial bioenergetics in response to an inflammatory challenge

In DR and DS primary myotubes treated with 100 pg/mL LPS, mitochondrial respiration was quantified using high-resolution respirometry (Oroboros Oxygraph-2k). Various respiratory conditions were analysed with the addition of several different drugs including oligomycin-induced state 4, maximally uncoupled (FCCP induced), and ANT inhibited (CAT induced). Furthermore, non-mitochondrial respiration was measured following the addition of antimycin A.

Interestingly, respiratory capacity was enhanced in primary myotubes at BL when treated with LPS. Other studies hypothesize that the proinflammatory response induced by the IKK-NFκB signaling pathway may be critical for muscle regeneration post-exercise, and it has been demonstrated to increase the transcription of antioxidant genes[151,204]. We hypothesize that these pathways may be playing a role in the recovery of respiration post-LPS-induced inflammatory response.

Basal respiration tended to be higher in DS myotubes ($p=0.156$). Similarly, respiration from CI and CII OXPHOS (following the addition of ADP and succinate respectively) tended to be higher in DS versus DR myotubes ($p=0.141$ and $p=0.138$, respectively). ANT inhibited respiration (CAT induced) also tended to be higher post-exercise training (main effect $p=0.144$). Most notably, there is a strong trend for maximal respiration (FCCP-induced) to be increased post-LPS treatment ($p=0.096$; Figure 25).

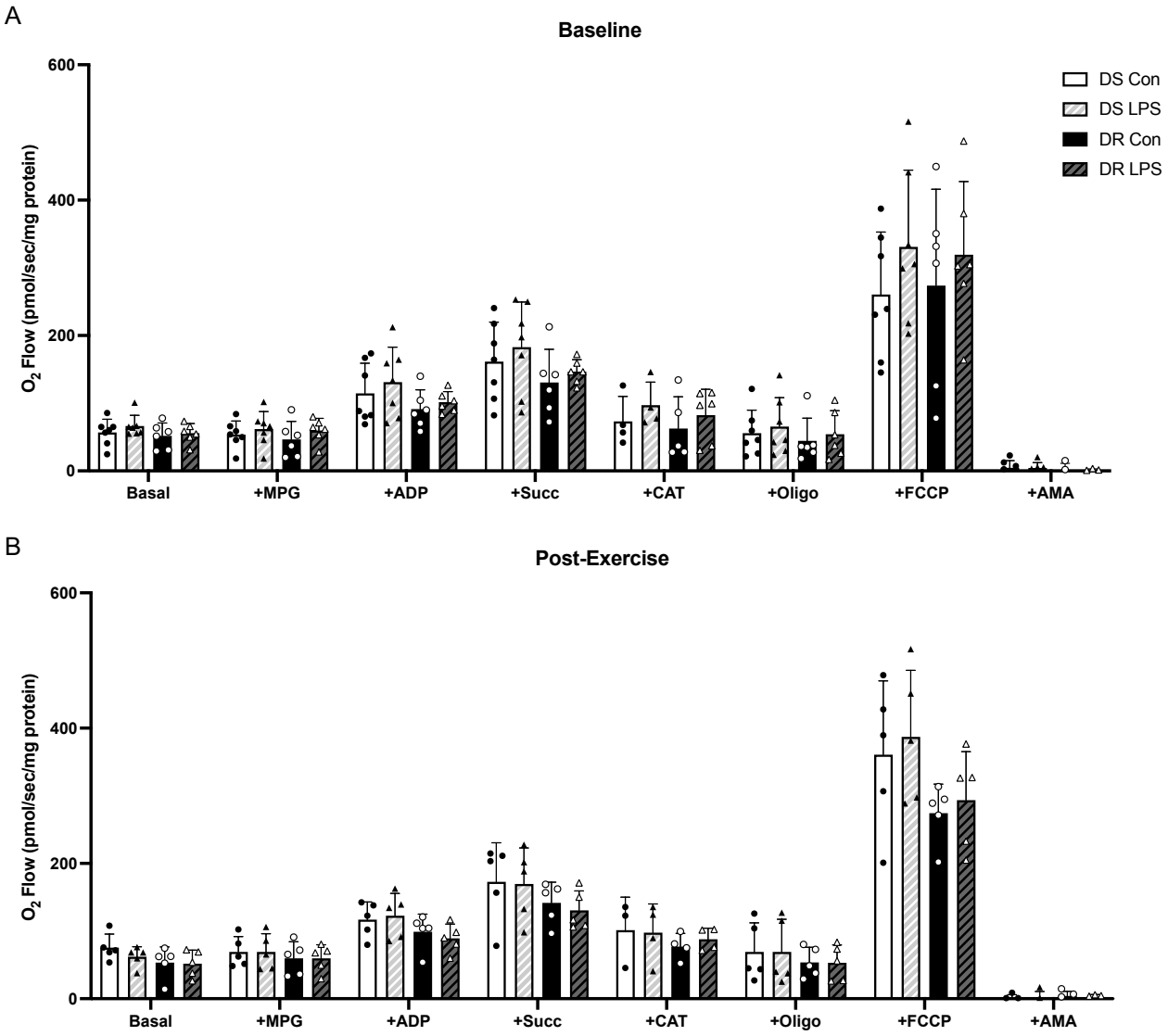

Figure 24. Maximal respiration of permeabilized myotubes is trending increased after an LPS inflammatory challenge. Differentiated myotubes were treated with 100 pg/mL LPS for 24 hours. High-resolution respirometry was performed using Oxygraph-2k to quantify: **(A)** mitochondrial respiration under various drug-induced conditions at baseline, **(B)** mitochondrial respiration under various drug-induced conditions post-exercise training. Data are expressed as mean±SD relative to protein per sample (mg) (n=7 [BL], n=5 [PET]). Means were compared using a 3-way repeated-measures ANOVA.

Mitochondrial respiration supported by fatty acid substrates was subsequently analysed to determine quintile differences in fatty acid oxidation in response to the LPS-induced inflammatory challenge. Both DR and DS myotubes demonstrated decreased CI OXPHOS + FAO respiration (following the addition of ADP) when treated with LPS (main effect treatment p=0.009; Figure 26). This is consistent with previously published findings that glycolysis is increased in skeletal muscle in an inflammatory state[205,206]. Exercise training tended to enhance fatty acid-supported respiration (main effect of exercise, ADP p=0.116, succinate p=0.144). Succinate also has a trending interaction effect where PET, myotubes tended to respond less to the LPS treatment (exercise x treatment p=0.123). Oligo has a significant interaction effect, whereby respiration of DS myotubes decreased after treatment with LPS (quintile x treatment p=0.049). Maximal respiration (FCCP-induced) is trending increased post-exercise (main effect p=0.181) and the recovery of respiratory capacity previously seen in the LPS treated cells in the standard protocol is no longer observed. Moreover, maximal respiration also has a significant interaction effect, where, once again, respiration of DS myotubes decreased after treatment with LPS (quintile x treatment (p=0.040).

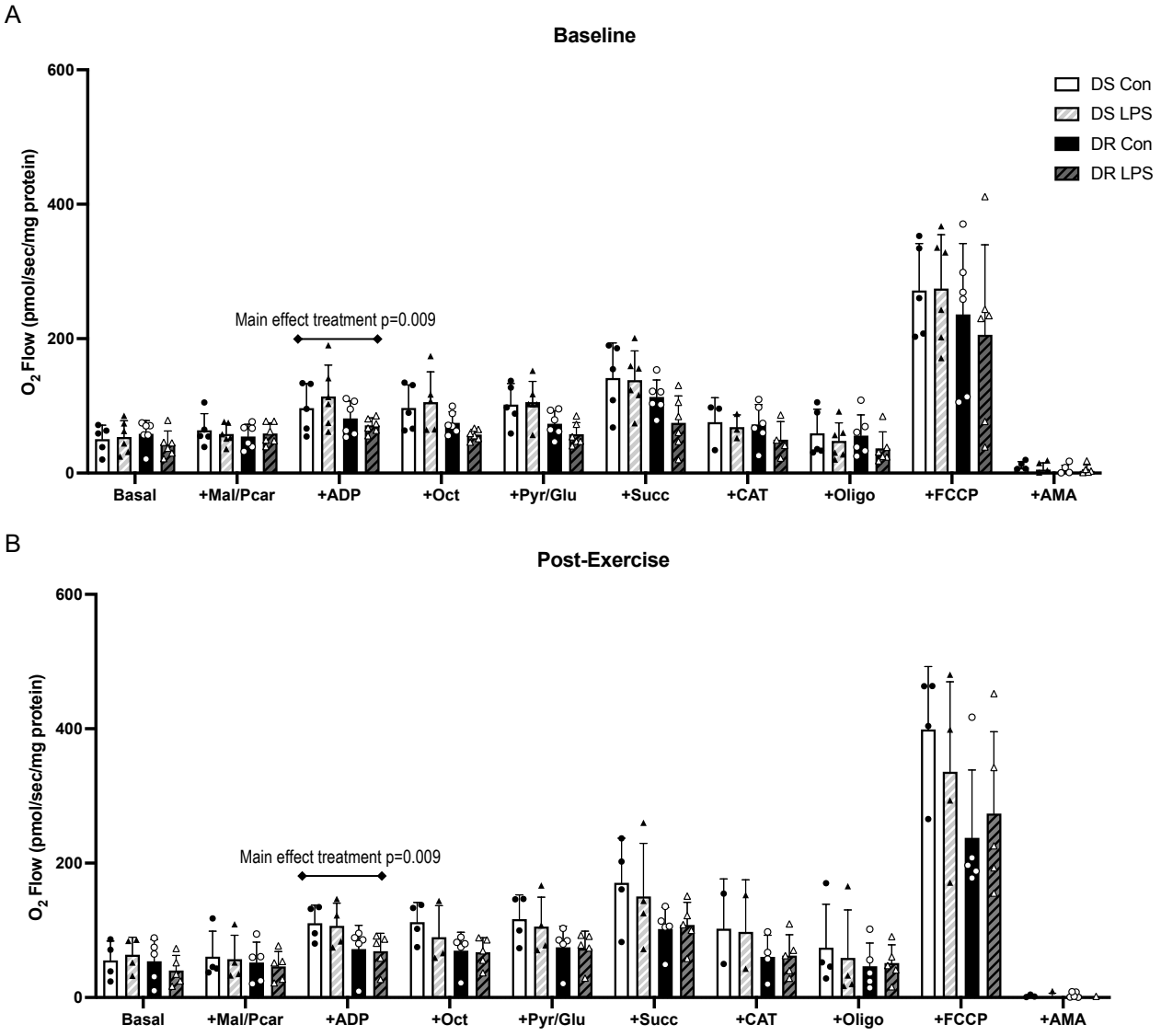

Figure 25. Fatty acid oxidation respiration is trending higher post-exercise training. Differentiated myotubes were treated with 100 pg/mL LPS for 24 hours. High-resolution respirometry was performed using Oxygraph-2k to quantify: **(A)** mitochondrial respiration under various drug-induced conditions at baseline, **(B)** mitochondrial respiration under various drug-induced conditions post-exercise training. Data are expressed as mean±SD relative to protein per sample (mg) (n=6 [BL], n=5 [PET]). Means were compared using a 3-way repeated-measures ANOVA.

Discussion

Research on this unique population of individuals with obesity in the highest (DS) and lowest (DR) quintiles for rate of weight loss has revealed that DS individuals have several skeletal muscle metabolic advantages, including increased mitochondrial proton leak[57], enhanced fatty acid metabolism[139], and a greater antioxidant capacity[129]. In these experiments, we have demonstrated the vast array of beneficial effects that regular physical exercise preferentially provides to DR women, including increased mitochondrial length and function. We also demonstrated that the IKK-NFκB pathway tends to be more active in DR women, despite lower concentrations of circulating plasma cytokines compared to DS women. Furthermore, exercise training enhanced the antioxidant capacity in both DS and DR women with obesity.

Obesity is associated with a high body fat percentage and increased visceral adipose tissue, which is a large risk factor in the development of metabolic disease[180]. Nevertheless, research has continuously demonstrated that regular physical exercise provides beneficial physiological effects and decreases the risk of cardiometabolic diseases[207]. Numerous studies have demonstrated that exercise training alone can improve body composition[180,208]. In the context of our population, at baseline, we observed altered body composition between DS and DR individuals, which was attributable to DR women having decreased lean body mass, suggesting they may be at greater risk of developing sarcopenia[209]. Interestingly, while exercise training did not significantly alter body weight in our populations, the exercise intervention improved body composition to a greater extent in DR women compared to DS. This suggests that exercise training is inducing beneficial metabolic adaptations that could enhance weight loss capacity in DR individuals. Indeed, the combination of caloric restriction with aerobic and resistance exercise has been shown to enhance

the capacity for maintained weight loss and can improve the functional status of adults with obesity[210].

The observation of exercise-induced improvements in body composition of DR individuals, along with previously characterized differences between DS and DR skeletal muscle, led us to hypothesize that cellular mitochondrial function would also be improved preferentially in DR women. Both skeletal muscle tissue and cultured primary myotubes were used to verify these hypotheses. Primary myotubes tend to retain the same metabolic characteristics as the donor tissue, including fat oxidation and metabolic flexibility[197,211,212]. Therefore, they are recognized as a good model for studying metabolic mechanisms of disease states such as diabetes and obesity.

In contrast to previous findings[129], we observed no difference in cellular leak respiration between DR and DS myotubes. The difference between our findings and those of Thrush *et al*[129] could be related to minor differences in the protocol followed, including different concentrations of oligomycin (which were independently optimized) and the Agilent Seahorse XF machine used (e24 vs e96). Regardless, we did observe an increase in myotube respiration in DR but not DS women post-exercise training, indicative of increased mitochondrial function, which supports our hypothesis that exercise would induce beneficial metabolic adaptions preferentially in DR individuals.

Research has shown that regular exercise can increase mitochondrial function[148] and induce mitochondrial biogenesis[147]. However, citrate synthase activity, a marker of mitochondrial density[189], was not increased following exercise training in primary myotubes from DR or DS individuals. While this is not consistent with previous observations of exercise-induced increases in mitochondrial content in skeletal muscle tissue, it may be because exercise trials that reported this effect were longer in duration and lasted several months[147]. Therefore, the increase in cellular

respiration in DR individuals could be reflective of enhanced mitochondrial function, rather than an increase in mitochondrial density. Additionally, despite evidence that primary myotube metabolic characteristics tend to mirror those *in vivo*, it is not without its limitations, including the lack of communication with surrounding cell types[197]. As such, gross mitochondrial content may be impacted if mitochondrial turnover is different between myotubes and muscle fibres. Because myotubes tend to be less differentiated than muscle cells, fusion events are less frequent but more stable in muscle fibers[213] – higher CS activity may be detected in muscle cells versus myotubes because of the promotion of healthier and more robust mitochondria[70,213]. Moreover, comparative profiling of *in vitro* skeletal muscle models has suggested that isolated primary muscle cells are more representative of type I oxidative fibres and may have lower mitochondrial content and/or dysfunctional mitochondria compared to *ex vivo* muscle[214]. Thus, citrate synthase may not be an appropriate marker of mitochondrial density *in vitro*.

Most cells can effectively switch between oxidative phosphorylation and glycolysis to meet energy demands. Moreover, cellular conditions can, not only push cells more towards one or the other for energy production, but can alter the overall bioenergetic capacity[215]. This flexibility in skeletal muscle metabolism is diminished in patients with obesity and T2DM[212,216]. In the present study, we evaluated metabolic flexibility using a publicly available analysis tool[187] and observed that DS women use more ATP production from glycolysis during basal respiration compared to DR women. Moreover, there is an observable increase in ATP production by OXPHOS in DR women post-exercise training, which suggests that exercise may be able to preferentially increase the cells' intrinsic ability to utilize the OXPHOS pathway in DR women. Consistent with our findings, myotubes isolated from healthy men following a 12-week exercise intervention showed improved glucose and lipid metabolism compared to myotubes isolated at baseline[217]. Taken

together, these findings suggest that exercise training may be able to reverse some of the detrimental effects that obesity has on the metabolic flexibility of myotubes.

Regular exercise training can lessen damage from reactive oxygen species[148], resulting from both decreased ROS production[218] and enhanced antioxidant capacity[219]. Improved cellular ability to detoxify ROS is often reflected in the GSH:GSSG ratio[64]. The Harper Lab has previously observed that glutathione redox was lower in primary myotubes isolated from DR individuals compared to DS individuals with obesity[129]. Therefore, GSH:GSSG ratio was measured to see if exercise training could lessen oxidative stress in primary myotubes from DR individuals. The ratio at baseline was found to be less than 10:1, which is indicative of a state of high oxidative stress. Exercise training increased the GSH:GSSG ratio in both DR and DS women, suggesting there may be enhanced capacity of glutathione-containing antioxidant enzymes (*i.e.*, GPx), and/or increased glutathione synthesis. Indeed, exercise training has been shown to enhance GPx activity in skeletal muscle, as well as γ-glutamyl-transpeptidase mediated uptake[220], and increased glutathione synthesis via γ-glutamyl-cysteine synthase[221,222].

The Harper Lab has previously demonstrated that expression of genes involved in glucose and fatty acid metabolism is increased in skeletal muscle tissue from DS versus DR individuals[116] and blood RNA transcriptomics prior to caloric restriction revealed upregulation of OXPHOS gene transcripts in DS individuals as well[138]. Thus, analysis of the mitochondrial OXPHOS subunits was performed to assess the impact of exercise training on protein expression in DS and DR muscle tissue. There was no difference in the expression of OXPHOS proteins between DS and DR individuals, which is consistent with our previous observations of protein expression in myotubes and skeletal muscle homogenate from separate cohorts of DR and DS patients[129,139]. Complementing our functional data, however, we observed an increase in the expression of

mitochondrial complexes II, III, IV and V in muscle homogenate from both DS and DR women post-exercise training, which is consistent with previously published research showing that exercise upregulates expression of genes and proteins involved in OXPHOS[148].

Exercise training resulted in a more fused mitochondrial reticulum in DR myotubes, as indicated by an increase in mitochondrial length. Since this same change was not observed in DS myotubes post-exercise training, and elongated mitochondria are more efficient at ATP production, we hypothesize the increase in bioenergetic capacity in DR myotubes following exercise training may be attributable to enhanced mitochondrial fusion. Although a balance of fission and fusion is necessary for healthy mitochondria, generally, a more fused mitochondrial reticulum is indicative of protected and more efficient mitochondria[27,223]. In contrast to our hypothesis, we did not observe any exercise-induced increases in mitochondrial fusion proteins (MFN1, MFN2, OPA-1), which may be due to transient changes in the expression of these proteins[224].

Obesity is associated with chronic low-grade inflammation which can contribute to the development of insulin resistance[225]. Observational studies have elucidated that exercise training may have anti-inflammatory effects by modulating circulating cytokine levels[226]. Based on our previous unpublished transcriptomic and plasma proteomic datasets, we hypothesized that patients with DR obesity may have higher systemic inflammation than individuals with DS obesity, which may contribute to the loss of muscle mass through the activation of the ubiquitin proteome system. In contrast to our hypothesis, very few inflammatory markers differed between DS and DR women at baseline. Notably, however, PYY and total ghrelin were increased in DS women at baseline. These are two hormones that have been implicated in appetite control and weight regulation[3,5,6], which is consistent with the increased ROWL seen in DS individuals. Exercise training did alter

the concentration of several plasma cytokines, including increasing β-NGF and IFNα2a, and decreasing TNFα. CTACK and SDF-1α were also increased PET in DS women only. CTACK and SDF-1α are chemokines with protective functions during an inflammatory response[227,228]. SDF-1α, in particular, has previous been shown to increase with physical exercise and be inversely correlated with blood glucose and insulin resistance[229,230].

Upon examination of expression of inflammatory markers in muscle homogenate, it can be concluded that the IKK-NFκB pathway tends to be more active in DR individuals. However, there were no differences in the MAPK-ERK pathway regardless of quintile or exercise status, despite previous observations that activation of the MAPK-ERK pathway tends to be induced by exercise[150]. However, changes in the expression of MAPK-ERK proteins tend to require longer exercise interventions[231,232] and are often less consistent in individuals with obesity[156].

In general, our data from both skeletal muscle homogenate and primary myotubes are consistent with an increase in inflammatory markers post-exercise training. In lean individuals, it has been shown many times that regular moderate exercise reduces inflammation[152–154]. However, as previously discussed, studies on individuals with obesity have been less consistent. Even after 12 weeks of regular endurance exercise, studies have shown only moderate decreases in a limited number of inflammatory markers[155]. In general, it is hypothesized that the beneficial effects of reduced inflammation as seen in lean individuals, may eventually be seen in individuals with obesity but only after weight loss and a longer period of regular exercise training. Additionally, a single bout of exercise does induce inflammation both during and immediately post-exercise, regardless of chronic exercise status. This increase in inflammation is important for many of the beneficial effects of exercise (*e.g.*, induction of antioxidants, muscle hypertrophy, et cetera)[151]. We hypothesize that the combination of increased inflammation following acute exercise and the

reduced cytokine clearance capacity of individuals with obesity may lead to the increase in expression of inflammatory markers that we observed.

To elucidate differences in skeletal muscle inflammation between DS and DR obesity, primary myotubes were treated with palmitate to induce an inflammatory response. However, we observed few differences following this inflammatory challenge. We hypothesize that because obesity is already a state of nutrient-load chronic inflammation, the addition of palmitate was not sufficient to induce any further inflammation. In healthy L6 myotubes, the threshold concentration at which palmitate induced a significant change in IκB and IL-6 gene expression was 400 μM[94]. The concentration of plasma-free fatty acids in obesity has been shown to be as high as 800 μM[233,234], suggesting that the threshold may have already been surpassed in the untreated myotubes. Moreover, gene expression evidence suggests that inflammatory responses to stress can be adaptive – demonstrating a strong initial response but habituating to repeated, similar stress[235]. As such, it is likely that in individuals with obesity, their muscle cells would have already begun to habituate to the chronic induction of stress. Together these findings are consistent with evidence that obesity induces a chronic state of inflammation[42,236].

When treated with LPS to induce inflammation, we observed an increase in NFκB and TLR4, suggesting that our aim to induce an inflammatory response in the primary myotubes was successful. LPS is a well-documented mediator of the IKK-NFκB pathway through canonical signaling using TLR4 surface receptors[201]. Activation of the IKK-NFκB pathway in response to LPS treatment did not differ between DS and DR myotubes. Additional experiments are needed to validate our hypothesis that DS individuals may regulate inflammation through the canonical pathway, using TLR4, more so than their DR counterparts.

High-resolution respirometry demonstrated that an LPS inflammatory challenge induced a recovery of OXPHOS respiratory capacity. We hypothesize that the activation of the IKK-NFκB pathway is inducing an acute protective mechanism which includes upregulating mitochondrial biogenesis, mitophagy, and the transcription of antioxidants[237]. This is consistent with previous findings that inflammation is a necessary mechanism to aid in the clearance of ROS as well as dead and dying cells[150,238]. NFκB increases the transcription of antioxidant genes, including MnSOD, NOX, and γ-GCS[204]. Several studies hypothesize that the proinflammatory response induced by the IKK-NFκB signaling pathway may be critical for muscle regeneration post-exercise[151], however chronic activation of the NFκB pathway still has many deleterious effects[239]. Moreover, primary myotubes isolated from DS individuals tend to exhibit higher respiratory rates than their DR counterparts, consistent with the observed trends in OCR measurements in our seahorse assays, where DS women also tended to exhibit greater OCR at baseline.

In high-resolution respirometry experiments, when myotubes were provided with FAs as an alternative fuel source, the aforementioned increase in respiration due to inflammation is no longer seen. This suggests that the combined stress of both LPS and FAs hinders cellular respiration. However, exercise training tended to increase maximal respiration in both DS and DR myotubes. This is consistent with the literature that exercise can promote FA clearance and FAO[58,240].

In conclusion, we demonstrate that six weeks of exercise training can improve skeletal muscle mitochondrial function, improve cellular glutathione redox, and increase certain inflammatory markers in individuals with obesity. Specifically, we demonstrate that exercise training lowers percent body fat and fat mass in DR women and enhances cellular maximal respiration in primary myotubes isolated from DR women. We also show that exercise training

enhances IKK-NFκB signaling in skeletal muscle; and that this was increased to a greater extent in DR versus DS women. Finally, there appears to be a recovery of respiratory capacity in myotubes treated with LPS which we hypothesize is due to activation of protective mechanisms.

Limitations and Alternatives

We acknowledge that there are limitations to the study that are worth noting. First, the small sample size and relatively short duration of the exercise intervention are limitations. Small sample sizes are a common limitation among human studies and no real alternative exists beyond complementing our results with additional experiments in animal models. Longer exercise interventions can elicit myofiber hypertrophy[181,241]; despite our observations in relation to muscle bioenergetics, our exercise intervention did not induce hypertrophy as per measurements of muscle fibre cross-sectional area[186].

Secondly, isolated primary myoblasts may not be completely reflective of *in vivo* metabolism. When examining isolated cell populations, there is a lack of communication with surrounding cell types[197], which may affect cellular protein composition and function. Comparative transcriptome profiling of human tissue and isolated myotubes suggests that the isolated cells may be more representative of type I oxidative fibres and thus may not reflect the heterogeneity in metabolism of human skeletal muscle[214]. Additionally, the isolation and culturing of primary cells may be selective for the healthiest and most robust myoblasts, and thus experiments performed on these cells may have been skewed towards representing healthier muscle. We also observed differences in growth rates between myoblasts isolated from different individuals. Although efforts were made to ensure experiments were conducted pairwise to limit variability, certain experiments were more susceptible to the differences in growth rates – notably the glucose uptake assays. Alternatives to *in vitro* glucose uptake assays include *in vivo* glucose tolerance testing and other blood chemistry markers, including HbA1c and HOMA-IR, which were recorded for our participants. Where possible, we also performed complementary experiments on

ex vivo muscle tissue as an alternative to account for the limitations in using primary myoblasts/tubes.

Furthermore, there are limitations with all experimental approaches; for example, cardiolipin may be a more appropriate marker for mitochondrial content rather than citrate synthase activity[189]. Lastly, several cytokines of interest were below the limit of detection for U-PLEX assays. It would be of value to repeat these experiments, as well as complement them with analysis of cytokine transcript levels from skeletal muscle biopsies.

Further experimentation is needed to validate some of our hypotheses. For example, protein markers of ferroptosis as measured by western blotting did not differ between groups, however, future experiments could analyse lipid peroxidation or iron metabolism. Additionally, our conclusions regarding differences in inflammation between quintiles tended to be variable; as a next step, I propose functional experiments, such as measuring NFκB translocation to the nucleus or knock in/down/out experiments, such as inhibiting TLR4 to examine mechanistic differences in inflammation between quintiles.

Conclusions and Future Directions

Research on individuals with obesity in the highest (DS) and lowest (DR) quintiles for rate of weight loss has revealed that DS individuals have several skeletal muscle metabolic advantages, including increased proportions of type I oxidative fibres, increased mitochondrial proton leak, enhanced fatty acid metabolism, and a greater antioxidant capacity. The findings from this thesis support using exercise to improve skeletal muscle mitochondrial metabolism in diet-resistant obesity. Our conclusions regarding inflammatory responses were more variable. Although, we were able to demonstrate that the IKK-NFκB pathway tends to be more active in DR individuals, further elucidation of mechanistic differences between DS and DR cohorts is needed.

To further characterize the inflammatory profiles of DS and DR individuals, cytokine transcript levels could be examined from skeletal muscle biopsies. A special focus on levels MuRF1 and Atrogin-1, as well as markers of protein synthesis, could be used to examine if the ubiquitin-proteasome pathway is contributing to the observed differences in lean body mass between DS and DR individuals with obesity. The proposed mechanistic studies will improve the understanding of how inflammation modulates changes in metabolism in these individuals and may identify novel pathways that can be targeted as viable options for treatments of obesity.

The focus of my study was skeletal muscle tissue. However, to have a more comprehensive picture of immunometabolism within DS and DR obesity, future analysis should include immune cells. Already some of our measurements of systemic inflammation indicate that there would be differences between quintiles, as well as changes induced by exercise. Such experimentation would provide novel insights into mechanisms of crosstalk between the immune system and skeletal muscle tissue.

In conclusion, exercise is often overlooked as a primary treatment for obesity, despite continuous evidence of the vast array of advantages that regular physical exercise provide to metabolic health, including increased mitochondrial density and function in skeletal muscle. Here, we have demonstrated that exercise training improves body composition, enhances cellular maximal respiration, and increases mitochondrial length preferentially in DR women. Taken together, these data highlight the importance of including exercise in the treatment of obesity, especially for those who have great difficulties losing weight, and maintaining weight loss.

References

1. Obesity and overweight. World Health Organization. Published 2020. https://www.who.int/news-room/fact-sheets/detail/obesity-and-overweight
2. Obesity in Canada. Obesity Canada. Published 2020. https://obesitycanada.ca/obesity-in-canada/
3. Vendrell J, Montserrat B, Vilarrasa N, et al. Resistin, adiponectin, ghrelin, leptin, and proinflammatory cytokines : relationships in obesity. *Obes Res*. 2004;12(6):962-971.
4. Coppack SW. Pro-inflammatory cytokines and adipose tissue. *Proc Nutr Soc*. 2001;60(3):349-356.
5. Vincent RP, Ashrafian H, le Roux CW. Mechanisms of disease: The role of gastrointestinal hormones in appetite and obesity. *Nat Clin Pract Gastroenterol Hepatol*. 2008;5(5):268-277.
6. De Silva A, Bloom SR. Gut hormones and appetite control: A focus on PYY and GLP-1 as therapeutic targets in obesity. *Gut Liver*. 2012;6(1):10-20.
7. Dent R, McPherson R, Harper ME. Factors affecting weight loss variability in obesity. *Metabolism*. 2020;113:154388.
8. Ard JD, Lewis KH, Rothberg A, et al. Effectiveness of a Total Meal Replacement Program (OPTIFAST Program) on weight loss: results from the OPTIWIN Study. *Obesity*. 2019;27(1):22-29.
9. American College of Cardiology *, American Heart Association Task Force on Practice Guideline *, Obesity Expect Panel *. Expert panel report: Guidelines (2013) for the management of overweight and obesity in adults. *Obesity*. 2014;22(S2):S41-S410.
10. Feero WG, Guttmacher AE, Collins FS. Genomic medicine — An updated primer. *N Engl J Med*. 2010;362:2001-2011.
11. Frayling TM, Timpson NJ, Weedon MN, et al. A common variant in the FTO gene is associated with body mass index and predisposes to childhood and adult obesity. *Science (80-)*. 2007;316(May):889-894.
12. Nikpay M, Lau P, Soubeyrand S, et al. SGCG rs679482 associates with weight loss success in response to an intensively supervised outpatient program. *Diabetes*. 2020;69(9):2017-2026.
13. Ravussin E, Lillioja S, Knowler WC, et al. Reduced rate of energy expenditure as a risk factor for body-weight gain. *N Engl J Med*. 1988;318(8):467-472.
14. Zurlo F, Larson K, Bogardus C, Ravussin E. Skeletal muscle metabolism is a major determinant of resting energy expenditure. *J Clin Invest*. 1990;86(5):1423-1427.
15. Gnaiger E. Capacity of oxidative phosphorylation in human skeletal muscle. New perspectives of mitochondrial physiology. *Int J Biochem Cell Biol*. 2009;41(10):1837-1845.
16. Baron AD, Brechtel G, Wallace P, Edelman SV. Rates and tissue sites of non-insulin- and insulin-mediated glucose uptake in diabetic rats. *Am J Physiol - Endocrinol Metab*. 1988;255(18):E769-E774.
17. Harper ME, Green K, Brand MD. The efficiency of cellular energy transduction and its implications for obesity. *Annu Rev Nutr*. 2008;28:13-33.
18. Kristensen D, Prats C, Larsen S, Ara I, Dela F, Helge JW. Ceramide content is higher in

type I compared to type II fibers in obesity and type 2 diabetes mellitus.
19. Stuart CA, South MA, Lee ML, et al. Insulin responsiveness in metabolic syndrome after eight weeks of cycle training. *Med Sci Sports Exerc*. 2013;45(11):2021.
20. Tanner CJ, Barakat HA, Dohm GL, et al. Muscle fiber type is associated with obesity and weight loss. *Am J Physiol Metab*. 2002;282(6):E1191-E1196.
21. Hickey MS, Carey JO, Azevedo JL, et al. Skeletal muscle fiber composition is related to adiposity and in vitro glucose transport rate in humans. *Am J Physiol Metab*. 1995;268(3):E453-E457.
22. Wade AJ, Marbut MM, Round JM. Muscle fibre type and aetiology of obesity. *Lancet*. 1990;335(8693):805-808.
23. Helge JW, Fraser AM, Kriketos AD, et al. Interrelationships between muscle fibre type, substrate oxidation and body fat. *Int J Obes 1999 239*. 1999;23(9):986-991.
24. Lillioja S, Young AA, Culter CL, et al. Skeletal muscle capillary density and fiber type are possible determinants of in vivo insulin resistance in man. *J Clin Invest*. 1987;80(2):415-424.
25. Scott W, Stevens J, Binder-Macleod SA. Human skeletal muscle fiber type classifications. *Phys Ther*. 2001;81(11):1810-1816.
26. Damer A, El Meniawy S, McPherson R, Wells G, Harper ME, Dent R. Association of muscle fiber type with measures of obesity: A systematic review. *Obes Rev*. Published online 2022.
27. Pileggi CA, Parmar G, Harper M. The lifecycle of skeletal muscle mitochondria in obesity. *Obes Rev*. 2021;22(5):e13164.
28. Coen PM, Hames KC, Leachman EM, et al. Reduced skeletal muscle oxidative capacity and elevated ceramide but not diacylglycerol content in severe obesity. *Obesity*. 2013;21(11):2362-2371.
29. Anderson EJ, Lustig ME, Boyle KE, et al. Mitochondrial H2O2 emission and cellular redox state link excess fat intake to insulin resistance in both rodents and humans. *J Clin Invest*. 2009;119(3):573-581.
30. Aguer C, McCoin CS, Knotts TA, et al. Acylcarnitines: potential implications for skeletal muscle insulin resistance. *FASEB J*. 2015;29(1):336-345.
31. Kelley DE, Goodpaster B, Wing RR, Simoneau JA. Skeletal muscle fatty acid metabolism in association with insulin resistance, obesity, and weight loss. *Am J Physiol*. 1999;277(6 Pt 1):E1130-41.
32. Kim JY, Hickner RC, Cortright RL, Dohm GL, Houmard JA. Lipid oxidation is reduced in obese human skeletal muscle. *Am J Physiol Metab*. 2000;279(5):E1039-44.
33. Simoneau JA, Colberg SR, Thaete FL, Kelley DE. Skeletal muscle glycolytic and oxidative enzyme capacities are determinants of insulin sensitivity and muscle composition in obese women. *FASEB J*. 1995;9(2):273-278.
34. Colberg S, Simoneau JA, Thaete FL, Kelley DE. Impaired FFA utilization by skeletal muscle in women with visceral obesity. *J Clin Invest*. 1995;95:1846-1853.
35. Goodpaster BH, He J, Watkins S, Kelley DE. Skeletal muscle lipid content and insulin resistance: evidence for a paradox in endurance-trained athletes. *J Clin Endocrinol Metab*. 2001;86(12):5755-5761.

36. Koves TR, Ussher JR, Noland RC, et al. Mitochondrial overload and incomplete fatty acid oxidation contribute to skeletal muscle insulin resistance. 2008;7(1):45-56.
37. Bonen A, Parolin ML, Steinberg GR, et al. Triacylglycerol accumulation in human obesity and type 2 diabetes is associated with increased rates of skeletal muscle fatty acid transport and increased sarcolemmal FAT/CD36. *FASEB J*. 2004;18(10):1144-1146.
38. Furukawa S, Fujita T, Shimabukuro M, et al. Increased oxidative stress in obesity and its impact on metabolic syndrome. *J Clin Invest*. 2004;114(12):1752-1761.
39. Kim JY, Hickner RC, Cortright RL, Dohm GL, Houmard JA. Lipid oxidation is reduced in obese human skeletal muscle. *Am J Physiol - Endocrinol Metab*. 2000;279(5 42-5):1039-1044.
40. Bell JA, Reed MA, Consitt LA, et al. Lipid partitioning, incomplete fatty acid oxidation, and insulin signal transduction in primary human muscle cells: Effects of severe obesity, fatty acid incubation, and fatty acid translocase/CD36 overexpression. *J Clin Endocrinol Metab*. 2010;95(7):3400-3410.
41. Ritov VB, Menshikova E V., He J, Ferrell RE, Goodpaster BH, Kelley DE. Deficiency of subsarcolemmal mitochondria in obesity and type 2 diabetes. *Diabetes*. 2005;54(1):8-14.
42. Ray I, Mahata SK, De RK. Obesity: An Immunometabolic Perspective. *Front Endocrinol (Lausanne)*. 2016;7(DEC):1-9.
43. Flock MR, Rogers CJ, Prabhu KS, Kris-Etherton PM. Immunometabolic role of long-chain omega-3 fatty acids in obesity-induced inflammation. *Diabetes Metab Res Rev*. 2013;29(6):431-445.
44. O'Leary MF, Wallace GR, Davis ET, et al. Obese subcutaneous adipose tissue impairs human myogenesis, particularly in old skeletal muscle, via resistin-mediated activation of NFκB. *Sci Rep*. 2018;8(1):1-13.
45. Akhmedov D, Berdeaux R. The effects of obesity on skeletal muscle regeneration. *Front Physiol*. 2013;4 DEC:371.
46. Tomlinson DJ, Erskine RM, Morse CI, Winwood K, Onambélé-Pearson G. The impact of obesity on skeletal muscle strength and structure through adolescence to old age. *Biogerontology*. 2016;17(3):467-483.
47. Voet D, Voet JG, Pratt CW. *Fundamentals of Biochemistry: Life at the Molecular Level*. 5th ed. Wiley; 2016.
48. Rolfe DFS, Brand MD. Contribution of mitochondrial proton leak to skeletal muscle respiration and to standard metabolic rate. *Am J Physiol - Cell Physiol*. 1996;271(4 40-4).
49. Echtay KS, Roussel D, St-Pierre J, et al. Superoxide activates mitochondrial uncoupling proteins. *Nature*. 2002;415(January):96-99.
50. Cadenas S, Buckingham JA, St-Pierre J, Dickinson K, Jones RB, Brand MD. AMP decreases the efficiency of skeletal-muscle mitochondria. *Biochem J*. 2000;351(2):307.
51. Argyropoulos G, Harper ME. Uncoupling proteins and thermoregulation. *J Appl Physiol*. 2002;92:2187-2198.
52. Krauss S, Zhang CY, Lowell BB. The mitochondrial uncoupling-protein homologues. *Nat Rev Mol Cell Biol*. 2005;6(3):248-261.
53. Brand MD, Pakay JL, Ocloo A, et al. The basal proton conductance of mitochondria depends on adenine nucleotide translocase content. *Biochem J*. 2005;392(2):353-362.

54. Fernström M, Tonkonogi M, Sahlin K. Effects of acute and chronic endurance exercise on mitochondrial uncoupling in human skeletal muscle. *J Physiol*. 2004;554(3):755-763.
55. Mailloux RJ, Harper ME. Mitochondrial proticity and ROS signaling: Lessons from the uncoupling proteins. *Trends Endocrinol Metab*. 2012;23(9):451-458.
56. Mailloux RJ, Seifert EL, Bouillaud F, Aguer C, Collins S, Harper ME. Glutathionylation acts as a control switch for uncoupling proteins UCP2 and UCP3. *J Biol Chem*. 2011;286(24):21865-21875.
57. Harper ME, Dent R, Monemdjou S, et al. Decreased mitochondrial proton leak and reduced expression of uncoupling protein 3 in skeletal muscle of obese diet-resistant women. *Diabetes*. 2002;51(8):2459-2466.
58. Aguer C, Fiehn O, Seifert EL, et al. Muscle uncoupling protein 3 overexpression mimics endurance training and reduces circulating biomarkers of incomplete β-oxidation. *FASEB J*. 2013;27(10):4213-4225.
59. Seifert EL, Bézaire V, Estey C, Harper ME. Essential role for uncoupling protein-3 in mitochondrial adaptation to fasting but not in fatty acid oxidation or fatty acid anion export. *J Biol Chem*. 2008;283(37):25124-25131.
60. Turrens JF. Superoxide production by the mitochondrial respiratory chain. *Biosci Rep*. 1997;17(1):3-8.
61. Murphy MP. How mitochondria produce reactive oxygen species. *Biochem J*. 2009;417(1):1-13.
62. Hamanaka RB, Chandel NS. Mitochondrial reactive oxygen species regulate cellular signaling and dictate biological outcomes. *Trends Biochem Sci*. 2010;35(9):505-513.
63. Berlett BS, Stadtman ER. Protein oxidation in aging, disease, and oxidative stress. *J Biol Chem*. 1997;272(33):20313-20316.
64. Townsend DM, Tew KD, Tapiero H. The importance of glutathione in human disease. *Biomed Pharmacother*. 2003;57(3):145-155.
65. Shutt T, Geoffrion M, Milne R, McBride HM. The intracellular redox state is a core determinant of mitochondrial fusion. *EMBO Rep*. 2012;13(10):909-915.
66. Chai YC, Ashraf SS, Rokutan K, Johnston Jr. RB, Thomas JA. S-thiolation of individual human neutrophil proteins including actin by stimulation of the respiratory burst: Evidence against a role for glutathione disulfide. *Arch Biochem Biophys*. 1994;310(1):273-281.
67. Kirkwood SP, Munn EA, Brooks GA. Mitochondrial reticulum in limb skeletal muscle. *Am J Physiol - Cell Physiol*. 1986;251(3 (20/3)).
68. Ogata T, Yamasaki Y. Ultra-high-resolution scanning electron microscopy of mitochondria and sarcoplasmic reticulum arrangement in human red, white, and intermediate muscle fibers. *Anat Rec*. 1997;248(2):214-223.
69. Szabadkai G, Simoni AM, Rizzuto R. Mitochondrial Ca2+ uptake requires sustained Ca2+ release from the endoplasmic reticulum. *J Biol Chem*. 2003;278(17):15153-15161.
70. Youle RJ, van der Bliek AM. Mitochondrial fission, fusion, and stress. *Science (80-)*. 2012;337(August):1062-1066.
71. Koshiba T, Detmer SA, Kaiser JT, Chen H, McCaffery JM, Chan DC. Structural basis of mitochondrial tethering by mitofusin complexes. *Science (80-)*. 2004;305(5685):858-862.
72. Chen H, Detmer SA, Ewald AJ, Griffin EE, Fraser SE, Chan DC. Mitofusins Mfn1 and

Mfn2 coordinately regulate mitochondrial fusion and are essential for embryonic development. *J Cell Biol*. 2003;160(2):189-200.

73. Brandt T, Cavellini L, Kühlbrandt W, Cohen MM. A mitofusin-dependent docking ring complex triggers mitochondrial fusion in vitro. *Elife*. 2016;5:e14618.
74. de Brito OM, Scorrano L. Mitofusin 2 tethers endoplasmic reticulum to mitochondria. *Nature*. 2008;456(7222):605-610.
75. Meeusen S, DeVay R, Block J, et al. Mitochondrial inner-membrane fusion and crista maintenance requires the dynamin-related GTPase Mgm1. *Cell*. 2006;127(2):383-395.
76. Hailey DW, Rambold AS, Satpute-Krishnan P, et al. Mitochondria supply membranes for autophagosome biogenesis during starvation. *Cell*. 2010;141(4):656-667.
77. Ingerman E, Perkins EM, Marino M, et al. Dnm1 forms spirals that are structurally tailored to fit mitochondria. *J Cell Biol*. 2005;170(7):1021-1027.
78. Smirnova E, Griparic L, Shurland DL, van der Bliek AM. Dynamin-related protein Drp1 is required for mitochondrial division in mammalian cells. *Mol Biol Cell*. 2001;12(8):2245-2256.
79. Kamerkar SC, Kraus F, Sharpe AJ, Pucadyil TJ, Ryan MT. Dynamin-related protein 1 has membrane constricting and severing abilities sufficient for mitochondrial and peroxisomal fission. *Nat Commun*. 2018;9(1):1-15.
80. Lewis MR, Lewis WH. Mitochondria in tissue culture. *Science (80-)*. 1914;39(1000):330-333.
81. Gegg ME, Cooper JM, Chau KY, Rojo M, Schapira AHV, Taanman JW. Mitofusin 1 and mitofusin 2 are ubiquitinated in a PINK1/parkin-dependent manner upon induction of mitophagy. *Hum Mol Genet*. 2010;19(24):4861-4870.
82. McLelland GL, Goiran T, Yi W, et al. Mfn2 ubiquitination by PINK1/parkin gates the p97-dependent release of ER from mitochondria to drive mitophagy. *Elife*. 2018;7:1-35.
83. Pickrell AM, Youle RJ. The roles of PINK1, Parkin, and mitochondrial fidelity in parkinson's disease. *Neuron*. 2015;85(2):257-273.
84. Yamano K, Matsuda N, Tanaka K. The ubiquitin signal and autophagy: an orchestrated dance leading to mitochondrial degradation. *EMBO Rep*. 2016;17(3):300-316.
85. Drake JC, Laker RC, Wilson RJ, Zhang M, Yan Z. Exercise-induced mitophagy in skeletal muscle occurs in the absence of stabilization of Pink1 on mitochondria. *Cell Cycle*. 2019;18(1):1-6.
86. Gouspillou G, Godin R, Piquereau J, et al. Protective role of Parkin in skeletal muscle contractile and mitochondrial function. *J Physiol*. 2018;596(13):2565-2579.
87. Akira S, Uematsu S, Takeuchi O. Pathogen recognition and innate immunity. *Cell*. 2006;124(4):783-801.
88. Bonilla FA, Oettgen HC. Adaptive immunity. *J Allergy Clin Immunol*. 2010;125(2 SUPPL. 2):S33-S40.
89. Hoebe K, Janssen E, Beutler B. The interface between innate and adaptive immunity. *Nat Rev Immunol*. 2004;5(10):971-974.
90. Liu T, Zhang L, Joo D, Sun SC. NF-κB signaling in inflammation. *Signal Transduct Target Ther*. 2017;2(April).
91. Gilmore TD. Introduction to NF-κB: players, pathways, perspectives. *Oncogene 2006 2551*.

2006;25(51):6680-6684.
92. Delhalle S, Blasius R, Dicato M, Diederich M. A beginner's guide to NF-kappaB signaling pathways. *Ann N Y Acad Sci*. 2004;1030:1-13.
93. Nan J, Hu H, Sun Y, et al. TNFR2 stimulation promotes mitochondrial fusion via Stat3- and NF-kB-dependent activation of OPA1 expression. *Circ Res*. 2017;121(4):392-410.
94. Nisr RB, Shah DS, Ganley IG, Hundal HS. Proinflammatory NFkB signalling promotes mitochondrial dysfunction in skeletal muscle in response to cellular fuel overloading. *Cell Mol Life Sci*. 2019;76(24):4887-4904.
95. Zhong Z, Umemura A, Sanchez-Lopez E, et al. NF-κB restricts inflammasome activation via elimination of damaged mitochondria. *Cell*. 2016;164(5):896-910.
96. Cowan KJ, Storey KB. Mitogen-activated protein kinases: new signaling pathways functioning in cellular responses to environmental stress. *J Exp Biol*. 2003;206(7):1107-1115.
97. Seger R, Krebs EG. The MAPK signaling cascade. *FASEB J*. 1995;9(9):726-735.
98. Rawlings JS, Rosler KM, Harrison DA. The JAK/STAT signaling pathway. *J Cell Sci*. 2004;117(8):1281-1283.
99. Fève B, Bastard JP. The role of interleukins in insulin resistance and type 2 diabetes mellitus. *Nat Rev Endocrinol*. 2009;5(6):305-311.
100. Funaki M. Saturated fatty acids and insulin resistance. *J Med Investig*. 2009;56(3-4):88-92.
101. Stockwell BR, Angeli JPF, Bayir H, et al. Ferroptosis: A regulated cell death nexus linking metabolism, redox biology, and disease. *Cell*. 2017;171(2):273-285.
102. Gao M, Yi J, Zhu J, et al. Role of mitochondria in ferroptosis. *Mol Cell*. 2019;73(2):354-363.
103. Cao JY, Dixon SJ. Mechanisms of ferroptosis. *Cell Mol Life Sci*. 2016;73(11-12):2195-2209.
104. Wang H, Liu C, Zhao Y, Gao G. Mitochondria regulation in ferroptosis. *Eur J Cell Biol*. 2020;99(1):151058.
105. Pedersen BK, Febbraio MA. Muscles, exercise and obesity: Skeletal muscle as a secretory organ. *Nat Rev Endocrinol*. 2012;8(8):457-465.
106. Leal LG, Lopes MA, Batista ML. Physical exercise-induced myokines and muscle-adipose tissue crosstalk: A review of current knowledge and the implications for health and metabolic diseases. *Front Physiol*. 2018;9(SEP):1-17.
107. Wu H, Ballantyne CM. Skeletal muscle inflammation and insulin resistance in obesity. *J Clin Invest*. 2017;127(1):43-54.
108. Valerio A, Cardile A, Cozzi V, et al. TNF-α downregulates eNOS expression and mitochondrial biogenesis in fat and muscle of obese rodents. *J Clin Invest*. 2006;116(10):2791-2798.
109. Gkikas I, Palikaras K, Tavernarakis N. The role of mitophagy in innate immunity. *Front Immunol*. 2018;9(JUN):1-15.
110. Missiroli S, Genovese I, Perrone M, Vezzani B, Vitto VAM, Giorgi C. The role of mitochondria in inflammation: From cancer to neurodegenerative disorders. *J Clin Med*. 2020;9(3).
111. Tschopp J. Mitochondria: Sovereign of inflammation? *Eur J Immunol*. 2011;41(5):1196-

1202.
112. Henao-Mejia J, Elinav E, Thaiss CA, Flavell RA. Inflammasomes and metabolic disease. *Annu Rev Physiol*. 2014;76:57-78.
113. Martins AR, Nachbar RT, Gorjao R, et al. Mechanisms underlying skeletal muscle insulin resistance induced by fatty acids: Importance of the mitochondrial function. *Lipids Health Dis*. 2012;11:1-11.
114. Dabravolski SA, Orekhova VA, Baig MS, et al. The role of mitochondrial mutations and chronic inflammation in diabetes. *Int J Mol Sci*. 2021;22(13).
115. Dent R, McPherson R, Harper ME. Variability in weight loss in highly compliant women on a controlled dietary regimen. *Obes Res*. 1999;7(S1):98S.
116. Gerrits MF, Ghosh S, Kavaslar N, et al. Distinct skeletal muscle fiber characteristics and gene expression in diet-sensitive versus diet-resistant obesity. *J Lipid Res*. 2010;51(8):2394-2404.
117. Azar M, Nikpay M, Harper ME, McPherson R, Dent R. Can response to dietary restriction predict weight loss after Roux-en-Y gastroplasty? *Obesity*. 2016;24(4):805-811.
118. Levine JA. Measurement of energy expenditure. *Public Health Nutr*. 2005;8(7a):1123-1132.
119. Levine JA, Schleusner SJ, Jensen MD. Energy expenditure of nonexercise activity. *Am J Clin Nutr*. 2000;72(6):1451-1454.
120. Ravussin E, Bogardus C. Relationship of genetics, age, and physical fitness to daily energy expenditure and fuel utilization. *Am J Clin Nutr*. 1989;49:968-975.
121. Leibel RL, Rosenbaum M, Hirsch J. Changes in energy expenditure resulting from altered body weight. *N Engl J Med*. 1995;332(10):621-628.
122. Pontzer H, Yamada Y, Sagayama H, et al. Daily energy expenditure through the human life course. *Science (80-)*. 2021;373(6556):808-812.
123. Fontaine E, Savard R, Tremblay A, Despres JP, Poehlman E, Bouchard C. Resting metabolic rate in monozygotic and dizygotic twins. *Acta Genet medicae Gemellol twin Res*. 1985;34(1-2):41-47.
124. Hohenadel MG, Hollstein T, Thearle M, et al. A low resting metabolic rate in late childhood is associated with weight gain in adolescence. *Metabolism*. 2019;93:68-74.
125. Ravussin E, Burnand B, Schutz Y, Jequier E. Twenty-four-hour energy expenditure and resting metabolic rate in obese, moderately obese, and control subjects. *Am J Clin Nutr*. 1982;35(3):566-573.
126. James WPT, Bailes J, Davies HL, Dauncey MJ. Elevated metabolic rates in obesity. *Lancet*. 1978;311(8074):1122-1125.
127. Prentice AM, Black AE, Coward WA, et al. High levels of energy expenditure in obese women. *Br Med J (Clin Res Ed)*. 1986;292(6526):983-987.
128. Prentice AM, Black AE, Coward WA, Cole TJ. Energy expenditure in overweight and obese adults in affluent societies: an analysis of 319 doubly-labelled water measurements. *Eur J Clin Nutr*. 1996;50(2):93-97.
129. Thrush AB, Zhang R, Chen W, et al. Lower mitochondrial proton leak and decreased glutathione redox in primary muscle cells of obese diet-resistant versus diet-sensitive humans. *J Clin Endocrinol Metab*. 2014;99(11):4223-4230.

130. Costford SR, Chaudhry SN, Salkhordeh M, Harper ME. Effects of the presence, absence, and overexpression of uncoupling protein-3 on adiposity and fuel metabolism in congenic mice. *Am J Physiol Metab*. 2006;290(6):E1304-E1312.
131. Bezaire V, Spriet LL, Campbell S, et al. Constitutive UCP3 overexpression at physiological levels increases mouse skeletal muscle capacity for fatty acid transport and oxidation. *FASEB J*. 2005;19(8):977-979.
132. Wang S, Subramaniam A, Cawthorne MA, Clapham JC. Increased fatty acid oxidation in transgenic mice overexpressing UCP3 in skeletal muscle. *Diabetes, Obes Metab*. 2003;5(5):295-301.
133. Kelley DE, He J, Menshikova E V., Ritov VB. Dysfunction of mitochondria in human skeletal muscle in type 2 diabetes. *Diabetes*. 2002;51(10):2944-2950.
134. Chomentowski P, Coen PM, Radikova Z, Goodpaster BH, Toledo FGS. Skeletal muscle mitochondria in insulin resistance: differences in intermyofibrillar versus subsarcolemmal subpopulations and relationship to metabolic flexibility. *J Clin Endocrinol Metab*. 2011;96(2):494-503.
135. Holloway GP, Thrush AB, Heigenhauser GJ, et al. Skeletal muscle mitochondrial FAT/CD36 content and palmitate oxidation are not decreased in obese women. *Am J Physiol Metab*. 2007;292(6):E1782-9.
136. Simoneau J, Veerkamp JH, Turcotte LP, Kelley DE. Markers of capacity to utilize fatty acids in human skeletal muscle: relation to insulin resistance and obesity and effects of weight loss. *FASEB J*. 1999;13(14):2051-2060.
137. Ghosh S, Dent R, Harper ME, Stuart J, McPherson R. Blood gene expression reveal pathway differences between diet-sensitive and resistant obese subjects prior to caloric restriction. *Obesity*. 2011;19(2):457-463.
138. Ghosh S, Dent R, Harper ME, Stuart J, McPherson R. Blood gene expression profiling prior to caloric restriction demonstrates upregulation of oxidative phosphorylation in obese, diet-sensitive subjects. In: *Obesity*. Vol 18. Nature Publishing Group; 2010:S219-S219.
139. Thrush AB, Antoun G, Nikpay M, et al. Diet-resistant obesity is characterized by a distinct plasma proteomic signature and impaired muscle fiber metabolism. *Int J Obes*. 2018;42(3):353-362.
140. Zurlo F, Lillioja S, Esposito-Del Puente A, et al. Low ratio of fat to carbohydrate oxidation as predictor of weight gain: study of 24-h RQ. *Am J Physiol Metab*. 1990;259(5):E650-E657.
141. Piccolo BD, Keim NL, Fiehn O, Adams SH, Van Loan MD, Newman JW. Habitual physical activity and plasma metabolomic patterns distinguish individuals with low vs. high weight loss during controlled energy restriction. *J Nutr*. 2015;145(4):681-690.
142. Kelley DE, Mandarino LJ. Fuel selection in human skeletal muscle in insulin resistance: a reexamination. *Diabetes*. 2000;49(5):677-683.
143. Randle PJ, Garland PB, Hales CN, Newsholme EA. The glucose fatty-acid cycle its role in insulin sensitivity and the metabolic disturbances of diabetes mellitus. *Lancet*. 1963;281(7285):785-789.
144. Villareal DT, Aguirre L, Gurney AB, et al. Aerobic or resistance exercise, or both, in dieting obese older adults. *N Engl J Med*. 2017;376(20):1943-1955.
145. Pinho RA, Andrades ME, Oliveira MR, et al. Imbalance in SOD/CAT activities in rat

skeletal muscles submitted to treadmill training exercise. *Cell Biol Int*. 2006;30(10):848-853.

146. Garneau L, Parsons SA, Smith SR, Mulvihill EE, Sparks LM, Aguer C. Plasma myokine concentrations after acute exercise in non-obese and obese sedentary women. *Front Physiol*. 2020;11(February):1-8.
147. Davies KJA, Packer L, Brooks GA. Biochemical adaptation of mitochondria, muscle, and whole-animal respiration to endurance training. *Arch Biochem Biophys*. 1981;209(2):539-554.
148. Silva LA, Pinho CA, Scarabelot KS, et al. Physical exercise increases mitochondrial function and reduces oxidative damage in skeletal muscle. *Eur J Appl Physiol*. 2009;105(6):861-867.
149. Coen PM, Flynn MG. Chronic Exercise and Immunity. In: *Lifestyle Medicine*. 2nd ed. CRC Press; 2013:605-614.
150. Kramer HF, Goodyear LJ. Exercise, MAPK, and NF-κB signaling in skeletal muscle. *J Appl Physiol*. 2007;103(1):388-395.
151. Evans WJ, Cannon JG. The metabolic effects of exercise-induced muscle damage. *Exerc Sport Sci Rev*. 1991;19(1):99-125.
152. Petersen AMW, Pedersen BK. The anti-inflammatory effect of exercise. *J Appl Physiol*. 2005;98(4):1154-1162.
153. Roberts CK, Won D, Pruthi S, Lin SS, Barnard RJ. Effect of a diet and exercise intervention on oxidative stress, inflammation and monocyte adhesion in diabetic men. *Diabetes Res Clin Pract*. 2006;73(3):249-259.
154. Sriwijitkamol A, Christ-Roberts C, Berria R, et al. Reduced skeletal muscle inhibitor of κBβ content is associated with insulin resistance in subjects with type 2 diabetes: Reversal by exercise training. *Diabetes*. 2006;55(3):760-767.
155. Polak J, Klimcakova E, Moro C, et al. Effect of aerobic training on plasma levels and subcutaneous abdominal adipose tissue gene expression of adiponectin, leptin, interleukin 6, and tumor necrosis factor alpha in obese women. *Metabolism*. 2006;55(10):1375-1381.
156. Christiansen T, Paulsen SK, Bruun JM, Pedersen SB, Richelsen B. Exercise training versus diet-induced weight-loss on metabolic risk factors and inflammatory markers in obese subjects: A 12-week randomized intervention study. *Am J Physiol - Endocrinol Metab*. 2010;298(4):824-831.
157. Ostrowski K, Rohde T, Zacho M, Asp S, Pedersen BK. Evidence that interleukin-6 is produced in human skeletal muscle during prolonged running. *J Physiol*. 1998;508 (Pt 3)(Pt 3):949-953.
158. Steensberg A, Van Hall G, Osada T, Sacchetti M, Saltin B, Pedersen BK. Production of interleukin-6 in contracting human skeletal muscles can account for the exercise-induced increase in plasma interleukin-6. *J Physiol*. 2000;529 Pt 1(Pt 1):237-242.
159. Pedersen BK, Febbraio MA, Mooney RA. Interleukin-6 does/does not have a beneficial role in insulin sensitivity and glucose homeostasis. *J Appl Physiol*. 2007;102(2):814-819.
160. Petersen EW, Carey AL, Sacchetti M, et al. Acute IL-6 treatment increases fatty acid turnover in elderly humans in vivo and in tissue culture in vitro. *Am J Physiol - Endocrinol Metab*. 2005;288(1 51-1):155-162.
161. Fix DK, VanderVeen BN, Counts BR, Carson JA. Regulation of skeletal muscle DRP-1 and

FIS-1 protein expression by IL-6 signaling. *Oxid Med Cell Longev*. 2019;2019:1-12.
162. Van Hall G, Steensberg A, Sacchetti M, et al. Interleukin-6 stimulates lipolysis and fat oxidation in humans. *J Clin Endocrinol Metab*. 2003;88(7):3005-3010.
163. Wedell-Neergaard AS, Lang Lehrskov L, Christensen RH, et al. Exercise-induced changes in visceral adipose tissue mass are regulated by IL-6 signaling: A randomized controlled trial. *Cell Metab*. 2019;29(4):844-855.e3.
164. Zhou M, Lin BZ, Coughlin S, Vallega G, Pilch PF. UCP-3 expression in skeletal muscle: Effects of exercise, hypoxia, and AMP-activated protein kinase. *Am J Physiol - Endocrinol Metab*. 2000;279(3 42-3):622-629.
165. Noland RC, Hickner RC, Jimenez-Linan M, et al. Acute endurance exercise increases skeletal muscle uncoupling protein-3 gene expression in untrained but not trained humans. *Metabolism*. 2003;52(2):152-158.
166. Li B, Nolte LA, Ju ES, et al. Skeletal muscle respiratory uncoupling prevents diet-induced obesity and insulin resistance in mice. *Nat Med 2000 610*. 2000;6(10):1115-1120.
167. Ploug T, Van Deurs B, Ai H, Cushman SW, Ralston E. Analysis of GLUT4 distribution in whole skeletal muscle fibers: identification of distinct storage compartments that are recruited by insulin and muscle contractions. *J Cell Biol*. 1998;142(6):1429-1446.
168. Ryder JW, Yang J, Galuska D, et al. Use of a novel impermeable biotinylated photolabeling reagent to assess insulin- and hypoxia-stimulated cell surface GLUT4 content in skeletal muscle from type 2 diabetic patients. *Diabetes*. 2000;49(4):647-654.
169. Garvey WT, Maianu L, Zhu JH, Brechtel-Hook G, Wallace P, Baron AD. Evidence for defects in the trafficking and translocation of GLUT4 glucose transporters in skeletal muscle as a cause of human insulin resistance. *J Clin Invest*. 1998;101(11):2377-2386.
170. Jessen N, Goodyear LJ. Contraction signaling to glucose transport in skeletal muscle. *J Appl Physiol*. 2005;99(1):330-337.
171. Batista TM, Haider N, Kahn CR. Defining the underlying defect in insulin action in type 2 diabetes. *Diabetologia*. 2021;64(5):994-1006.
172. Martin BC, Warram JH, Krolewski AS, et al. Role of glucose and insulin resistance in development of type 2 diabetes mellitus: results of a 25-year follow-up study. *Lancet*. 1992;340(8825):925-929.
173. Houmard JA, Shinebarger MH, Dolan PL, et al. Exercise training increases GLUT-4 protein concentration in previously sedentary middle-aged men. *Am J Physiol - Endocrinol Metab*. 1993;264(6 27-6).
174. Stuart CA, Howell MEA, Baker JD, et al. Cycle training increased glut4 and activation of mammalian target of rapamycin in fast twitch muscle fibers. *Med Sci Sports Exerc*. 2010;42(1):96-106.
175. Sakamoto K, Aschenbach WG, Hirshman MF, Goodyear LJ. Akt signaling in skeletal muscle: Regulation by exercise and passive stretch. *Am J Physiol - Endocrinol Metab*. 2003;285(5 48-5):1081-1088.
176. Jaiswal N, Gavin MG, Quinn WJ, et al. The role of skeletal muscle Akt in the regulation of muscle mass and glucose homeostasis. *Mol Metab*. 2019;28(August):1-13.
177. Fujii N, Jessen N, Goodyear LJ. AMP-activated protein kinase and the regulation of glucose transport. *Am J Physiol - Endocrinol Metab*. 2006;291(5).
178. Evans PL, McMillin SL, Weyrauch LA, Witczak CA. Regulation of skeletal muscle glucose

transport and glucose metabolism by exercise training. *Nutrients*. 2019;11(10):1-24.

179. Verheggen RJHM, Maessen MFH, Green DJ, Hermus ARMM, Hopman MTE, Thijssen DHT. A systematic review and meta-analysis on the effects of exercise training versus hypocaloric diet: distinct effects on body weight and visceral adipose tissue. *Obes Rev*. 2016;17(8):664-690.
180. Irving BA, Davis CK, Brock DW, et al. Effect of exercise training intensity on abdominal visceral fat and body composition. *Med Sci Sport Exerc*. 2008;40(11):1863-1872.
181. Konopka AR, Harber MP. Skeletal muscle hypertrophy after aerobic exercise training. *Exerc Sport Sci Rev*. 2014;42(2):53-61.
182. Baldwin KM, Haddad F. Skeletal muscle plasticity: cellular and molecular responses to altered physical activity paradigms. *Am J Phys Med Rehabil*. 2002;81(11 Suppl):S40-51.
183. Lee SH, Kim BJ, Park DR, Kim UH. Exercise induces muscle fiber type switching via transient receptor potential melastatin 2-dependent Ca2+ signaling. *J Appl Physiol*. 2018;124(2):364-373.
184. Cheng X, Yan J, Liu Y, Wang J, Taubert S. eVITTA: a web-based visualization and inference toolbox for transcriptome analysis. *Nucleic Acids Res*. 2021;49(W1):W207-W215.
185. Dent RM, Penwarden RM, Harris N, Hotz SB. Development and evaluation of patient-centered software for a weight-management clinic. *Obes Res*. 2002;10(7):651-656.
186. Pileggi CA, Blondin DP, Hooks BG, et al. Exercise training enhances muscle mitochondrial metabolism in diet-resistant obesity. *eBioMedicine*. Published online August 11, 2022:104192.
187. Mookerjee SA, Gerencser AA, Nicholls DG, Brand MD. Quantifying intracellular rates of glycolytic and oxidative ATP production and consumption using extracellular flux measurements. *J Biol Chem*. 2017;292(17):7189-7207.
188. Mookerjee SA, Gerencser AA, Nicholls DG, Brand MD. Erratum: Quantifying intracellular rates of glycolytic and oxidative ATP production and consumption using extracellular flux measurements (Journal of Biological Chemistry (2018) 293 (12649-12652) DOI: 10.1074/jbc.M116.774471). *J Biol Chem*. 2018;293(32):12649-12652.
189. Larsen S, Nielsen J, Hansen CN, et al. Biomarkers of mitochondrial content in skeletal muscle of healthy young human subjects. *J Physiol*. 2012;590(14):3349-3360.
190. Vigelsø A, Andersen NB, Dela F. The relationship between skeletal muscle mitochondrial citrate synthase activity and whole body oxygen uptake adaptations in response to exercise training. *Int J Physiol Pathophysiol Pharmacol*. 2014;6(2):84.
191. Nikolić N, Skaret Bakke S, Tranheim Kase E, et al. Electrical pulse stimulation of cultured human skeletal muscle cells as an in vitro model of exercise. *PLoS One*. 2012;7(3):e33203.
192. Chen J, Wong HS, Leong PK, Leung HY, Chan WM, Ko KM. Ursolic acid induces mitochondrial biogenesis through the activation of AMPK and PGC-1 in C2C12 myotubes: a possible mechanism underlying its beneficial effect on exercise endurance. *Food Funct*. 2017;8(7):2425-2436.
193. Yano M, Kanazawa M, Terada K, Takeya M, Hoogenraad N, Mori M. Functional analysis of human mitochondrial receptor Tom20 for protein import into mitochondria. *J Biol Chem*. 1998;273(41):26844-26851.
194. Sylow L, Kleinert M, Richter EA, Jensen TE. Exercise-stimulated glucose uptake —

regulation and implications for glycaemic control. *Nat Rev Endocrinol 2016 133*. 2016;13(3):133-148.

195. Berggren JR, Hulver MW, Dohm GL, Houmard JA. Weight loss and exercise: Implications for muscle lipid metabolism and insulin action. *Med Sci Sport Exerc*. 2004;36(7):1191-1195.
196. Widegren U, Wretman C, Lionikas A, Hedin G, Henriksson J. Influence of exercise intensity on ERK/MAP kinase signalling in human skeletal muscle. *Pflugers Arch Eur J Physiol*. 2000;441(2-3):317-322.
197. Aas V, Bakke SS, Feng YZ, et al. Are cultured human myotubes far from home? *Cell Tissue Res*. 2013;354(3):671-682.
198. Cha BS, Ciaraldi TP, Park KS, Carter L, Mudaliar SR, Henry RR. Impaired fatty acid metabolism in type 2 diabetic skeletal muscle cells is reversed by PPARγ agonists. *Am J Physiol - Endocrinol Metab*. 2005;289(1 52-1):151-159.
199. Ciaraldi TP, Ryan AJ, Mudaliar SR, Henry RR. Altered myokine secretion is an intrinsic property of skeletal muscle in type 2 diabetes. *PLoS One*. 2016;11(7).
200. Hansen ME, Simmons KJ, Tippetts TS, et al. Lipopolysaccharide disrupts mitochondrial physiology in skeletal muscle via disparate effects on sphingolipid metabolism. *Shock*. 2015;44(6):585-592.
201. Liang H, Hussey SE, Sanchez-Avila A, Tantiwong P, Musi N. Effect of lipopolysaccharide on inflammation and insulin action in human muscle. *PLoS One*. 2013;8(5):8-15.
202. Cani PD, Amar J, Iglesias MA, et al. Metabolic endotoxemia initiates obesity and insulin resistance. *Diabetes*. 2007;56(7):1761-1772.
203. Olesen J, Larsson S, Iversen N, Yousafzai S, Hellsten Y, Pilegaard H. Skeletal muscle PGC-1α is required for maintaining an acute LPS-induced TNFα response. *PLoS One*. 2012;7(2):1-9.
204. Loop T, Pahl HL. Activators and target genes of Rel/NF-B transcription factors. *Nucl Factor κB*. Published online 2003:1-48.
205. Remels AHV, Gosker HR, Verhees KJP, Langen RCJ, Schols AMWJ. TNF-α-induced NF-κB activation stimulates skeletal muscle glycolytic metabolism through activation of HIF-1α. *Endocrinology*. 2015;156(5):1770-1781.
206. Zentella A, Manogue K, Cerami A. Cachectin/TNF-mediated lactate production in cultured myocytes is linked to activation of a futile substrate cycle. *Cytokine*. 1993;5(5):436-447.
207. Kodama S, Saito K, Tanaka S, et al. Cardiorespiratory fitness as a quantitative predictor of all-cause mortality and cardiovascular events in healthy men and women: A meta-analysis. *JAMA*. 2009;301(19):2024-2035.
208. Kemmler W, von Stengel S, Engelke K, Häberle L, Mayhew JL, Kalender WA. Exercise, body composition, and functional ability: A randomized controlled trial. *Am J Prev Med*. 2010;38(3):279-287.
209. Stenholm S, Harris TB, Rantanen T, Visser M, Kritchevsky SB, Ferrucci L. Sarcopenic obesity: Definition, cause and consequences. *Curr Opin Clin Nutr Metab Care*. 2008;11(6):693-700.
210. Johns DJ, Hartmann-Boyce J, Jebb SA, Aveyard P. Diet or exercise interventions vs combined behavioral weight management programs: A systematic review and meta-analysis of directcom parisons. *J Acad Nutr Diet*. 2014;114(10):1557-1568.

211. Gaster M, Kristensen SR, Beck-Nielsen H, Schrøder HD. A cellular model system of differentiated human myotubes. *APMIS*. 2001;109(11):735-744.
212. Ukropcova B, McNeil M, Sereda O, et al. Dynamic changes in fat oxidation in human primary myocytes mirror metabolic characteristics of the donor. *J Clin Invest*. 2005;115(7):1934-1941.
213. Eisner V, Lenaers G, Hajnóczky G. Mitochondrial fusion is frequent in skeletal muscle and supports excitation-contraction coupling. *J Cell Biol*. 2014;205(2):179-195.
214. Abdelmoez AM, Puig LS, Smith JAB, et al. Comparative profiling of skeletal muscle models reveals heterogeneity of transcriptome and metabolism. *Am J Physiol - Cell Physiol*. 2020;318(3):C615-C626.
215. Andrzejewski S, Klimcakova E, Johnson RM, et al. PGC-1α promotes breast cancer metastasis and confers bioenergetic flexibility against metabolic drugs. *Cell Metab*. 2017;26(5):778-787.e5.
216. Sparks LM, Ukropcova B, Smith J, et al. Relation of adipose tissue to metabolic flexibility. *Diabetes Res Clin Pract*. 2009;83(1):32-43.
217. Lund J, Rustan AC, Løvsletten NG, et al. Exercise in vivo marks human myotubes in vitro: Training-induced increase in lipid metabolism. *PLoS One*. 2017;12(4).
218. Place N, Ivarsson N, Venckunas T, et al. Ryanodine receptor fragmentation and sarcoplasmic reticulum Ca2+ leak after one session of high-intensity interval exercise. *Proc Natl Acad Sci U S A*. 2015;112(50):15492-15497.
219. Gomez-Cabrera MC, Domenech E, Viña J. Moderate exercise is an antioxidant: Upregulation of antioxidant genes by training. *Free Radic Biol Med*. 2008;44(2):126-131.
220. Leeuwenburgh C, Hollander J, Leichtweis S, Griffiths M, Gore M, Ji LL. Adaptations of glutathione antioxidant system to endurance training are tissue and muscle fiber specific. *Am J Physiol - Regul Integr Comp Physiol*. 1997;272(1 41-1).
221. Marin E, Kretzschmar M, Arokoski J, Hännien O, Klinger W. Enzymes of glutathione synthesis in dog skeletal muscles and their response to training. *Acta Physiol Scand*. 1993;147(4):369-373.
222. Sen CK, Marin E, Kretzschmar M, Hanninen O. Skeletal muscle and liver glutathione homeostasis in response to training, exercise, and immobilization. *J Appl Physiol*. 1992;73(4):1265-1272.
223. Mattie S, Krols M, McBride HM. The enigma of an interconnected mitochondrial reticulum: new insights into mitochondrial fusion. *Curr Opin Cell Biol*. 2019;59:159-166.
224. Perry CGR, Lally J, Holloway GP, Heigenhauser GJF, Bonen A, Spriet LL. Repeated transient mRNA bursts precede increases in transcriptional and mitochondrial proteins during training in human skeletal muscle. *J Physiol*. 2010;588(Pt 23):4795.
225. Gregor MF, Hotamisligil GS. Inflammatory mechanisms in obesity. *Annu Rev Immunol*. 2011;29:415-445.
226. Beavers KM, Brinkley TE, Nicklas BJ. Effect of exercise training on chronic inflammation. *Clin Chim Acta*. 2010;411(11-12):785-793.
227. Inokuma D, Abe R, Fujita Y, et al. CTACK/CCL27 Accelerates Skin Regeneration via Accumulation of Bone Marrow-Derived Keratinocytes. *Stem Cells*. 2006;24(12):2810-2816.
228. Chodari L, Mohammadi M, Ghorbanzadeh V, Dariushnejad H, Mohaddes G. Testosterone

and Voluntary Exercise Promote Angiogenesis in Hearts of Rats with Diabetes by Enhancing Expression of VEGF-A and SDF-1a. *Can J Diabetes*. 2016;40(5):436-441.

229. Kitahara CM, Trabert B, Katki HA, et al. Body mass index, physical activity, and serum markers of inflammation, immunity, and insulin resistance. *Cancer Epidemiol Biomarkers Prev*. 2014;23(12):2840-2849.
230. Gallagher KA, Liu ZJ, Xiao M, et al. Diabetic impairments in NO-mediated endothelial progenitor cell mobilization and homing are reversed by hyperoxia and SDF-1α. *J Clin Invest*. 2007;117(5):1249-1259.
231. Yu M, Stepto NK, Chibalin A V., et al. Metabolic and mitogenic signal transduction in human skeletal muscle after intense cycling exercise. *J Physiol*. 2003;546(2):327-335.
232. Coffey VG, Zhong Z, Shield A, et al. Early signaling responses to divergent exercise stimuli in skeletal muscle from well-trained humans. *FASEB J*. 2006;20(1):190-192.
233. Groop LC, Bonadonna RC, Simonson DC, Petrides AS, Shank M, DeFronzo RA. Effect of insulin on oxidative and nonoxidative pathways of free fatty acid metabolism in human obesity. *Am J Physiol - Endocrinol Metab*. 1992;263(1 26-1).
234. Opie LH, Walfish PG. Plasma free fatty acid concentrations in obesity. *New English J Med*. 1963;268(14):757-760.
235. McInnis CM, Wang D, Gianferante D, et al. Response and habituation of pro- and anti-inflammatory gene expression to repeated acute stress. *Brain Behav Immun*. 2015;46:237-248.
236. Pellegrinelli V, Rouault C, Rodriguez-Cuenca S, et al. Human adipocytes induce inflammation and atrophy in muscle cells during obesity. *Diabetes*. 2015;64(9):3121-3134.
237. Widdrington JD, Gomez-Duran A, Pyle A, et al. Exposure of monocytic cells to lipopolysaccharide induces coordinated endotoxin tolerance, mitochondrial biogenesis, mitophagy, and antioxidant defenses. *Front Immunol*. 2018;9(September):1-13.
238. Tidball JG, Wehling-Henricks M. Macrophages promote muscle membrane repair and muscle fibre growth and regeneration during modified muscle loading in mice in vivo. *J Physiol*. 2007;578(1):327-336.
239. Cai D, Frantz JD, Tawa NE, et al. IKKβ/NF-κB Activation Causes Severe Muscle Wasting in Mice. *Cell*. 2004;119(2):285-298.
240. Talanian JL, Holloway GP, Snook LA, Heigenhauser GJF, Bonen A, Spriet LL. Exercise training increases sarcolemmal and mitochondrial fatty acid transport proteins in human skeletal muscle. *Am J Physiol - Endocrinol Metab*. 2010;299(2):180-188.
241. Phillips SM. A brief review of critical processes in exercise-induced muscular hypertrophy. *Sport Med*. 2014;44(SUPPL.1):71-77.

Contributions of Collaborators

I would like to acknowledge: Dr. Robert Dent (MD) from the Ottawa Hospital Weight Management Clinic and Dr. Ruth McPherson (MD, PhD) from the University of Ottawa Heart Institute for their expertise and collaboration, as well as for performing muscle biopsies; Dr. Denis Blondin (PhD) for his time and services helping with pre-lab participant analyses; and Dr. Miroslava Cuperlovic-Culf (PhD) for her help with analysis and presentation of transcriptomic and proteomic data. A special thank you and acknowledgement to Dr. Chantal Pileggi (PhD) for her expertise and assistance with all my training and troubleshooting, as well as coordinating schedules to optimize the timing and performance of several experiments and cell culture upkeep.

Appendix

Table S1. Baseline and post-exercise training anthropometric characteristics of DS and DR women with p-values. Anthropometric measurements were conducted on individuals at the time of pre- and post-intervention *vastus lateralis* muscle biopsies. *p<0.05 DS vs DR, #p<0.05 BL vs PET

	BL		***PET***		***Main Effect p-value***	
Variable	***DS***	***DR***	***DS***	***DR***	***Quintile***	***Exercise***
n	10	10				
Age (years)	53.9 ± 7.7	53.2 ± 9.3	-	-	0.578	-
Height (cm)	165.85 ± 7.34	158.55 ± 4.99*	-	-	0.046	-
Bodyweight (kg)	110.67 ± 28.86	96.87 ± 17.55	111.07 ± 29.30	96.27 ±17.68	0.033	0.831
BMI (kg/m^2)	39.92 ± 8.00	38.66 ± 7.56	40.03 ± 8.20	38.38 ± 7.66	0.334	0.638
Waist circumference (cm)	124.11 ± 19.54	116.05±11.45	121.67±16.06	112.69±10.46	0.042	0.052
Body composition by DEXA						
Fat mass (kg)	53.53 ±18.98	50.49 ± 13.56*	53.56 ± 19.30	49.55 ± 14.11*$^{\#}$	0.404	0.220
Lean mass (kg)	52.88 ± 6.47	43.75 ± 4.04*	52.57 ± 6.47	44.20 ± 4.87*	<0.001	0.871
% Body fat	49.23 ± 5.40	52.97 ± 4.66*	49.32 ± 5.57	52.00 ± 5.20*$^{\#}$	0.094	0.147
Fasting blood biochemistry						
Fasting glucose (mmol/L)	5.20 ± 0.49	5.02 ± 0.49	5.50 ± 0.72	5.24 ± 0.53	0.238	0.165
HbA1c (%)	5.79 ± 0.41	5.59 ± 0.28	5.63 ± 0.40$^{\#}$	5.49 ± 0.31	0.318	0.003
Fasting insulin (pmol/L)	91.20 ± 50.37	61.40 ± 24.31*	101.50 ± 58.52	60.4 ± 25.15*	0.029	0.526

HOMA-IR	3.06 ± 1.78	2.00 ± 0.89	3.65 ± 2.40	2.08 ± 1.01*	0.024	0.416
Fasting triglycerides (mmol/L)	1.38 ± 0.49	1.54 ± 0.52	1.25 ± 0.42	1.35 ± 0.58	0.511	0.076
Total cholesterol (mmol/L)	5.30 ± 0.87	5.09 ± 0.89	5.33 ± 0.83	5.26 ± 0.93	0.692	0.461
HDL-cholesterol (mmol/L)	1.54 ± 0.26	1.47 ± 0.36	1.54 ± 0.09	1.50 ± 0.39	0.800	0.998
LDL cholesterol (mmol/L)	3.13 ± 0.78	2.95 ± 0.72	3.36 ± 0.74	3.22 ± 0.86	0.557	0.121
White blood cell count ($x10^9$/L)	6.14 ± 1.05	7.25 ± 1.32*	6.20 ± 1.38	6.44 ± 1.48$^{\#}$	0.034	0.219
Creatine kinase (U/L)	127.80 ± 81.13	68.67 ± 21.97*	110.5 ± 37.34	72.90 ± 30.68*	0.048	0.300

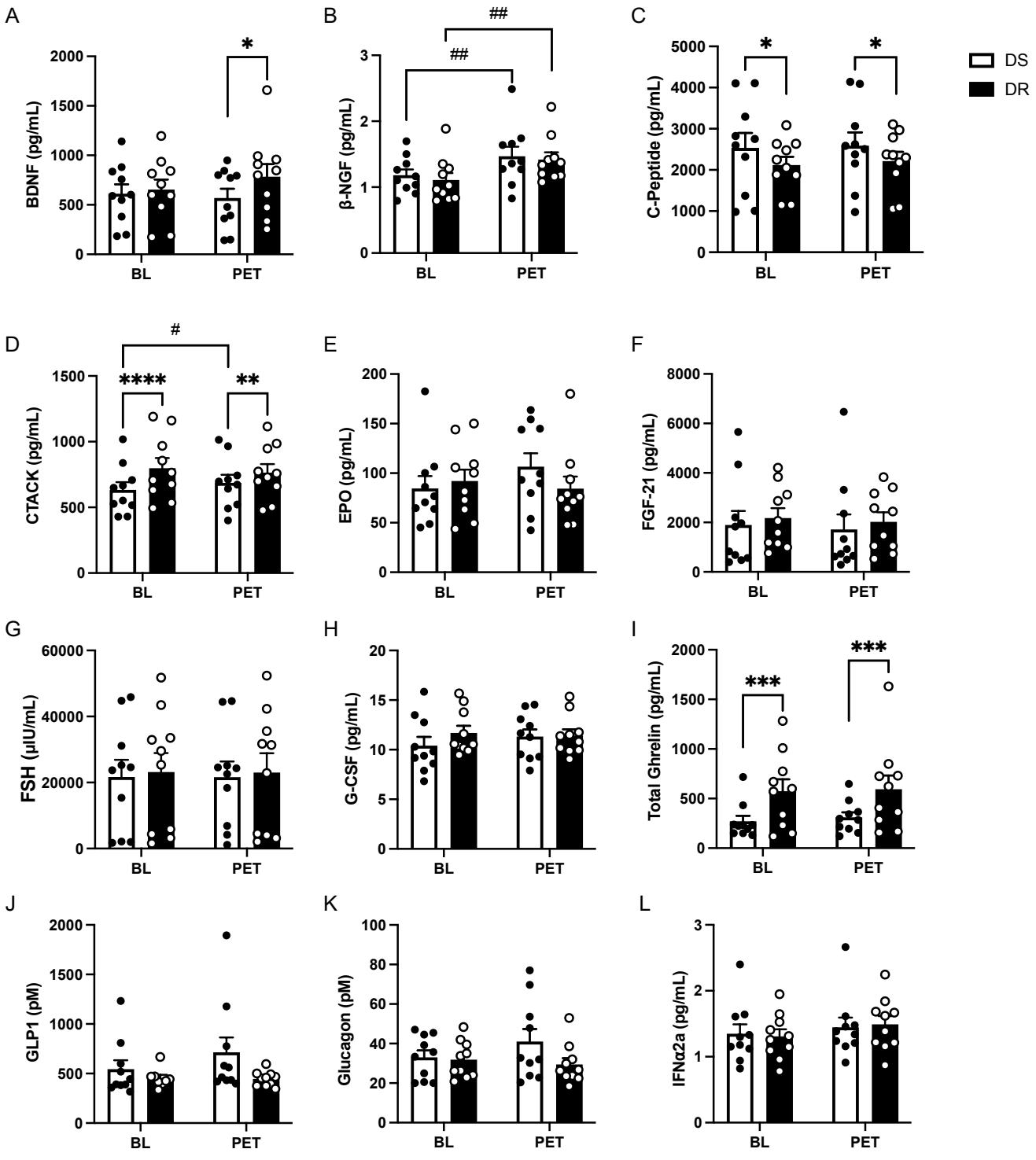
A
BDNF (pg/mL)
2000
1500
1000
500
0
*
BL
PET
B
β-NGF (pg/mL)
3
2
1
0
##
##
BL
PET
C
C-Peptide (pg/mL)
5000
4000
3000
2000
1000
0
*
*
BL
PET
DS
DR
D
CTACK (pg/mL)
1500
1000
500
0
#
****
**
BL
PET
E
EPO (pg/mL)
200
150
100
50
0
BL
PET
F
FGF-21 (pg/mL)
8000
6000
4000
2000
0
BL
PET
G
FSH (µIU/mL)
60000
40000
20000
0
BL
PET
H
G-CSF (pg/mL)
20
15
10
5
0
BL
PET
I
Total Ghrelin (pg/mL)
2000
1500
1000
500
0
***
***
BL
PET
J
GLP1 (pM)
2000
1500
1000
500
0
BL
PET
K
Glucagon (pM)
100
80
60
40
20
0
BL
PET
L
IFNα2a (pg/mL)
3
2
1
0
BL
PET

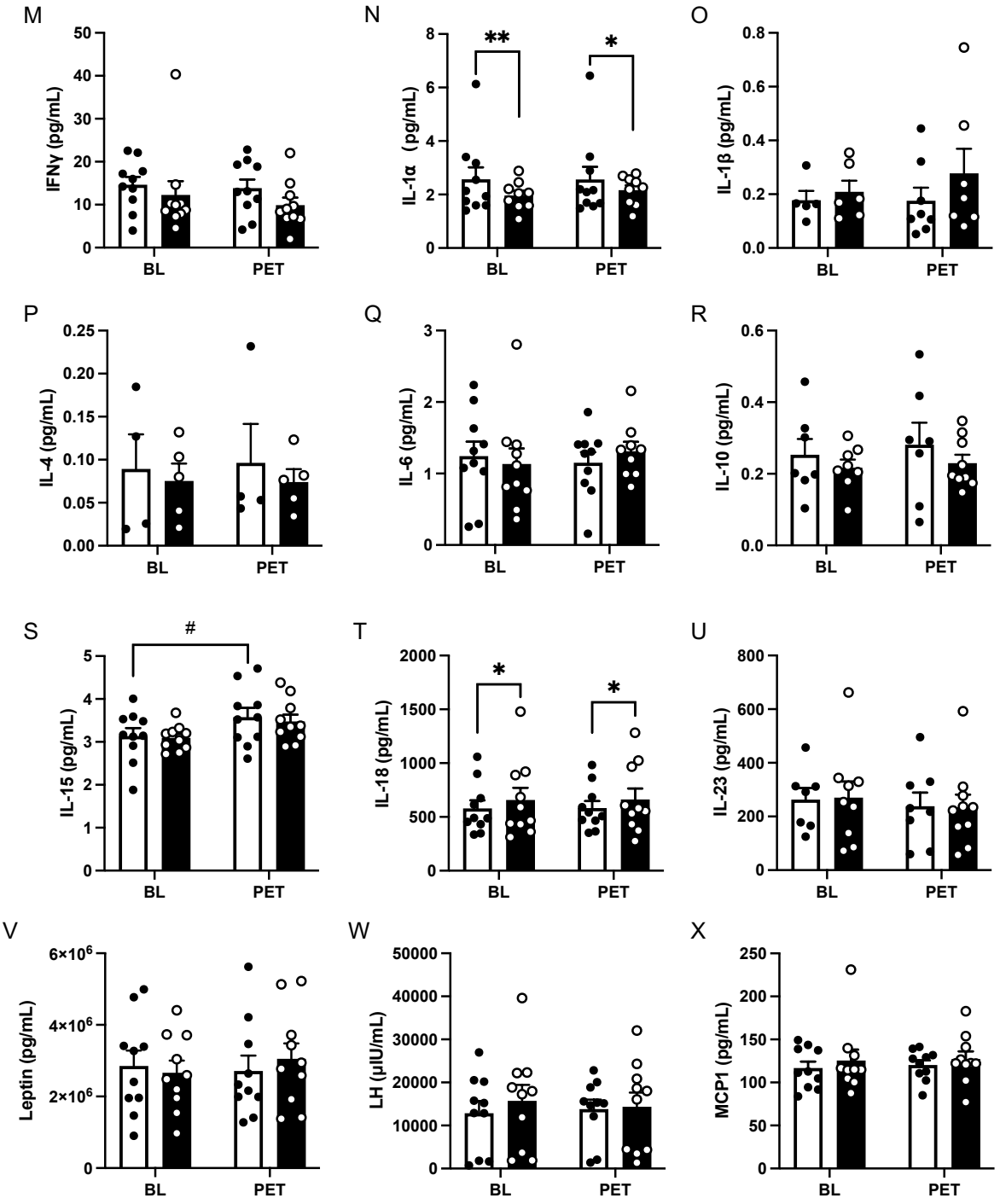
M
IFNγ (pg/mL)
50
40
30
20
10
0
BL
PET
N
IL-1α (pg/mL)
8
6
4
2
0
**
*
BL
PET
O
IL-1β (pg/mL)
0.8
0.6
0.4
0.2
0.0
BL
PET
P
IL-4 (pg/mL)
0.25
0.20
0.15
0.10
0.05
0.00
BL
PET
Q
IL-6 (pg/mL)
3
2
1
0
BL
PET
R
IL-10 (pg/mL)
0.6
0.4
0.2
0.0
BL
PET
S
IL-15 (pg/mL)
#
5
4
3
2
1
0
BL
PET
T
IL-18 (pg/mL)
2000
1500
1000
500
0
*
*
BL
PET
U
IL-23 (pg/mL)
800
600
400
200
0
BL
PET
V
Leptin (pg/mL)
6×10^6
4×10^6
2×10^6
0
BL
PET
W
LH (μIU/mL)
50000
40000
30000
20000
10000
0
BL
PET
X
MCP1 (pg/mL)
250
200
150
100
50
0
BL
PET

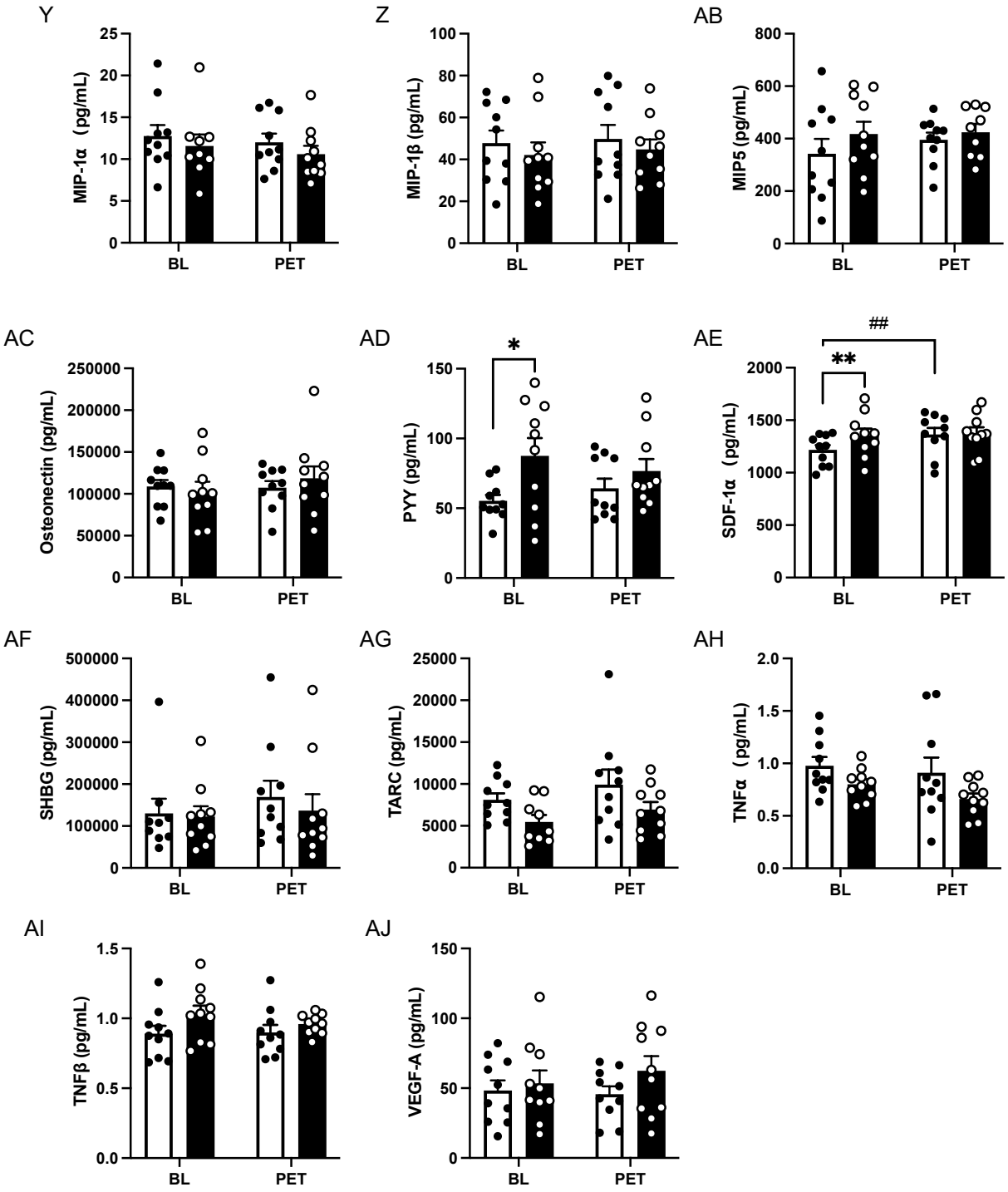
Y
MIP-1α (pg/mL)
25
20
15
10
5
0
BL
PET
Z
MIP-1β (pg/mL)
100
80
60
40
20
0
BL
PET
AB
MIP5 (pg/mL)
800
600
400
200
0
BL
PET
AC
Osteonectin (pg/mL)
250000
200000
150000
100000
50000
0
BL
PET
AD
PYY (pg/mL)
*
150
100
50
0
BL
PET
AE
##
**
SDF-1α (pg/mL)
2000
1500
1000
500
0
BL
PET
AF
SHBG (pg/mL)
500000
400000
300000
200000
100000
0
BL
PET
AG
TARC (pg/mL)
25000
20000
15000
10000
5000
0
BL
PET
AH
TNFα (pg/mL)
2.0
1.5
1.0
0.5
0.0
BL
PET
AI
TNFβ (pg/mL)
1.5
1.0
0.5
0.0
BL
PET
AJ
VEGF-A (pg/mL)
150
100
50
0
BL
PET

Figure S1. Effect of exercise training on the levels of various plasma cytokines. Expression of selected cytokines in fasted EDTA plasma samples from DS and DR women were analysed using U-PLEX assay including: **(A)** BDNF, **(B)** β-NGF, **(C)** C-peptide, **(D)** CTACK, **(E)** EPO, **(F)** FGF-21, **(G)** FSH, **(H)** G-CSF, **(I)** Total Ghrelin, **(J)** GLP1, **(K)** Glucagon, **(L)** IFNα2a, **(M)** IFNγ, **(N)** IL-1α, **(O)** IL-1β, (P) IL-4, **(Q)** IL-6, (R) IL-10, **(S)** IL-15, **(T)** IL-18, **(U)** IL-23, **(V)** Leptin, **(W)** LH, **(X)** MCP1, **(Y)** MIP-1α, **(Z)** MIP-1β, **(AB)** MIP5, **(AC)** Osteonectin, **(AD)** PYY, **(AE)** SDF1α, **(AF)** SHBG, **(AG)** TARC, **(AH)** TNFα, **(AI)** TNFβ, and **(AJ)** VEGF-A. Some of the cytokines (notably, IL-1β and IL-6) were below the limits of detection. Data are expressed as mean±SEM (n=10). Means were compared using a 2-way repeated-measures ANOVA. *$p<0.05$ DS vs DR, #$p<0.05$ BL vs PET

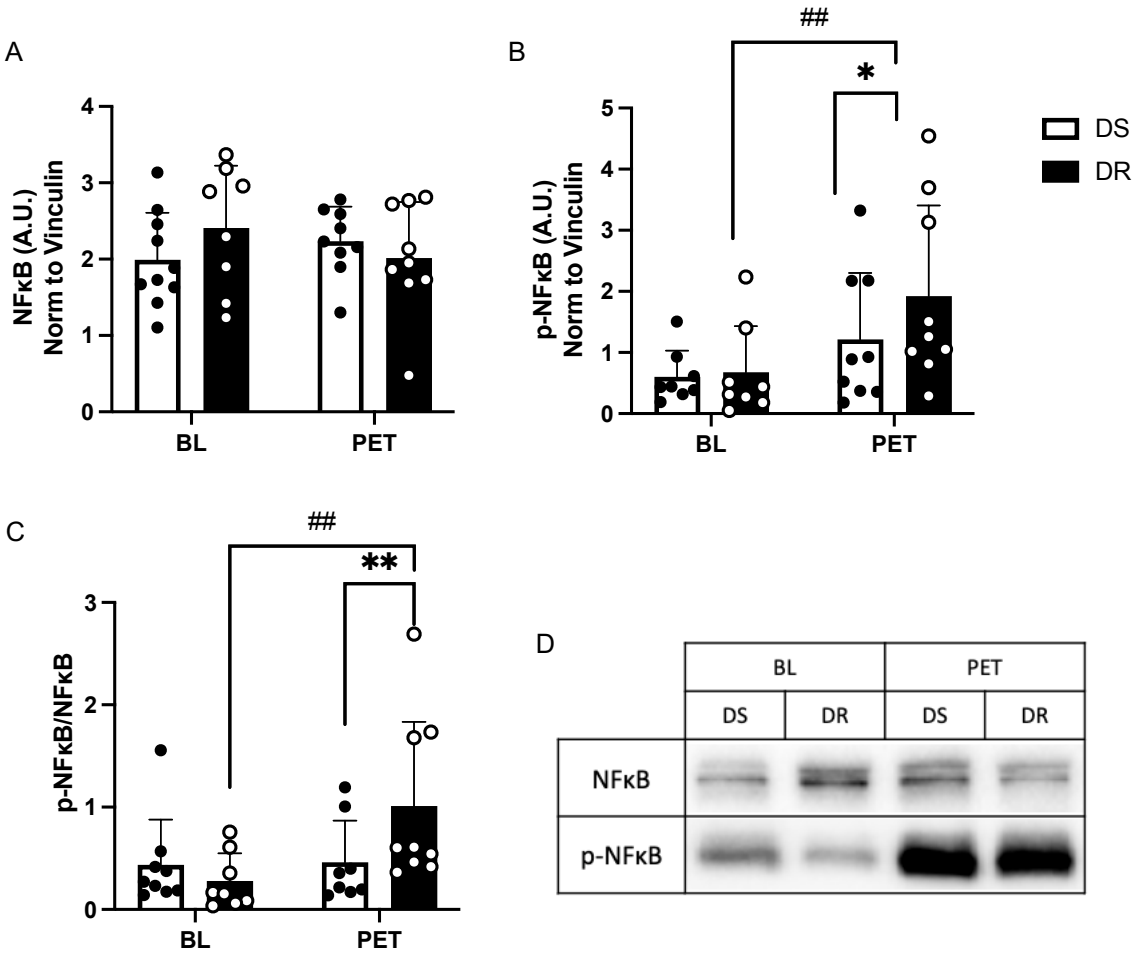

Figure S2. Phospho:total NFκB ratio is increased post-exercise training in DR muscle tissue. Western blots were performed on muscle homogenate and used to quantify: **(A)** the protein expression of NFκB, **(B)** the protein expression of p-NFκB, **(C)** the phospho:total NFκB ratio. **(D)** Representative western blot of the indicated proteins. Data are expressed as mean±SD relative to vinculin protein expression (n=9). *p<0.05 DS vs DR, #p<0.05 BL vs PET

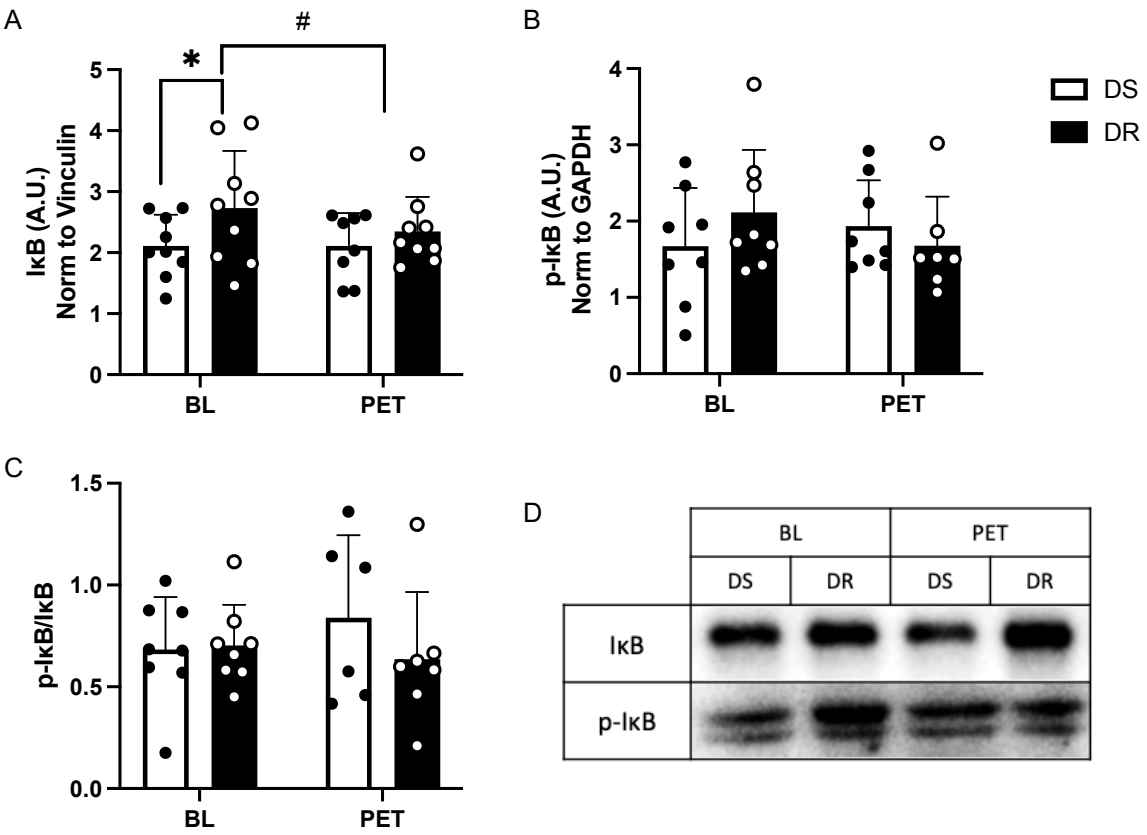

Figure S3. IκB is increased in muscle tissue from DR vs DS women. Western blots were performed on muscle homogenate and used to quantify: **(A)** the protein expression of IκB, **(B)** the protein expression of p-IκB, **(C)** the phospho:total IκB ratio. **(D)** Representative western blot of the indicated proteins. Data are expressed as mean±SD relative to vinculin or GAPDH protein expression as indicated (n=9). *p<0.05 DS vs DR, #p<0.05 BL vs PET

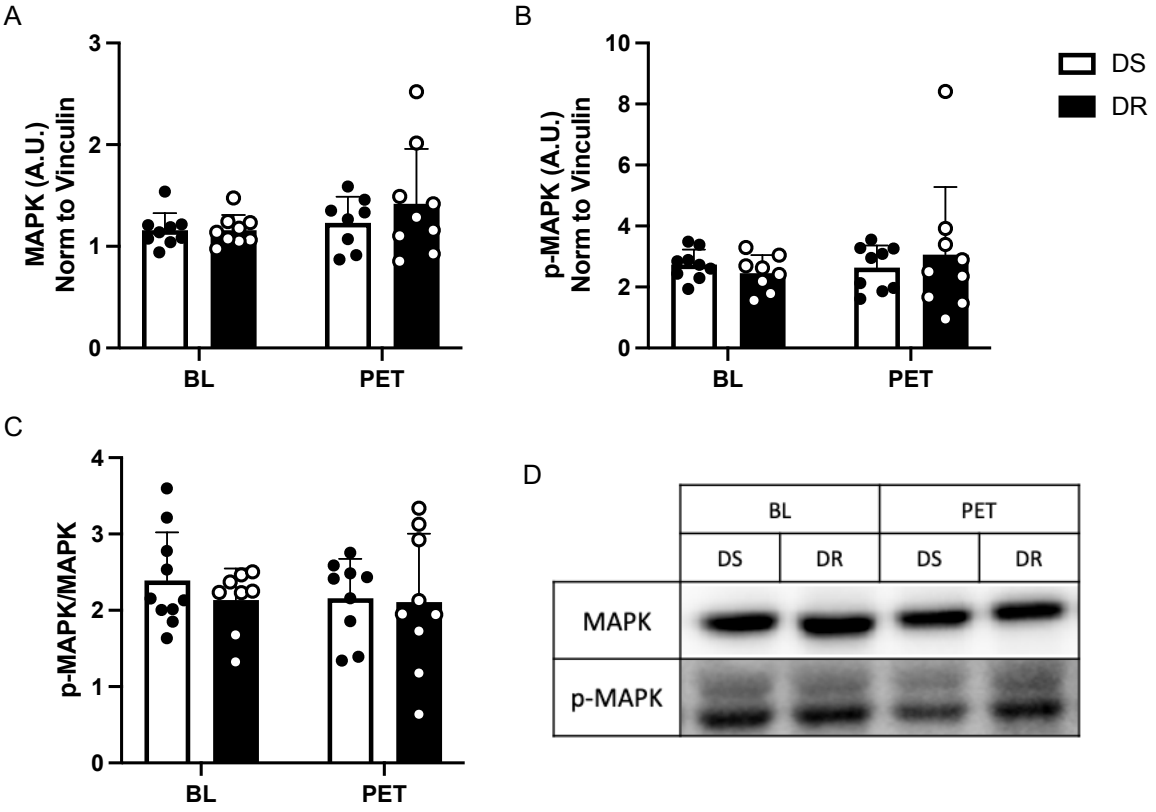

Figure S4. Phospho:total MAPK ratio is unaltered between groups in muscle tissue. Western blots were performed on muscle homogenate and used to quantify: **(A)** the protein expression of MAPK, **(B)** the protein expression of p-MAPK, **(C)** the phospho:total MAPK ratio. **(D)** Representative western blot of the indicated proteins. Data are expressed as mean±SD relative to vinculin protein expression (n=9).

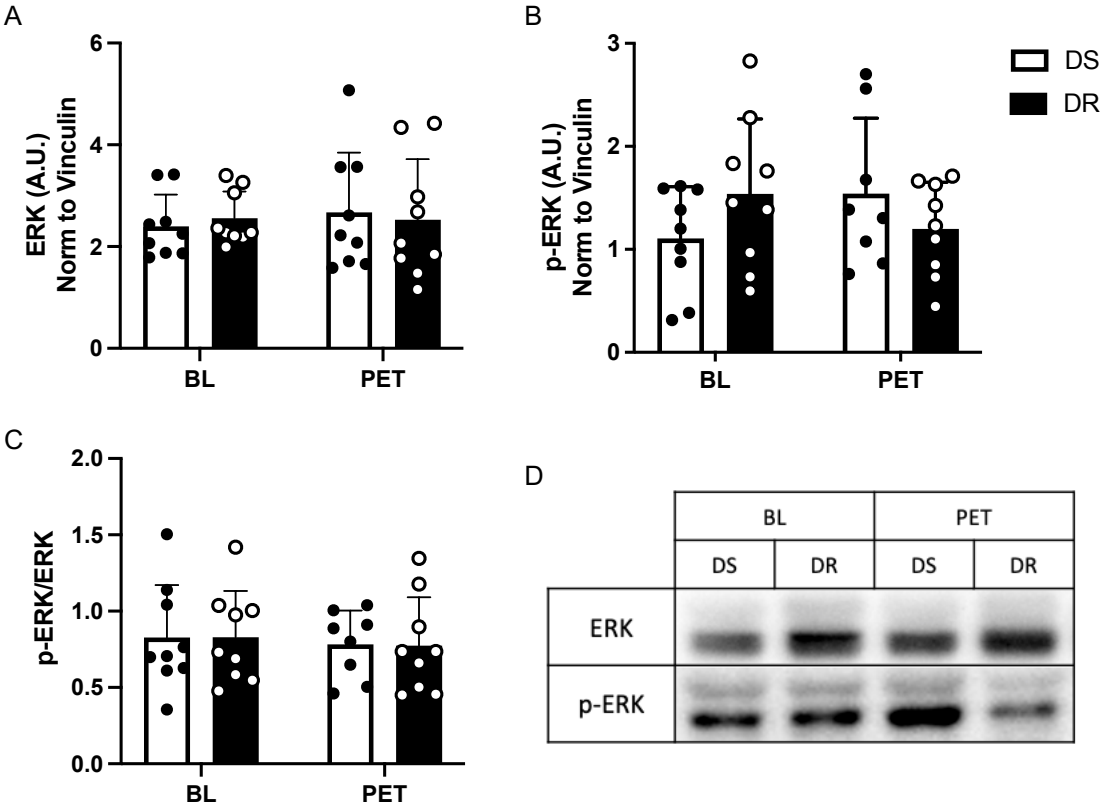

Figure S5. Expression of p-ERK is affected by exercise, dependent on quintile, in muscle tissue. Western blots were performed on muscle homogenate and used to quantify: **(A)** the protein expression of ERK, **(B)** the protein expression of p-ERK, **(C)** the phospho:total ERK ratio. **(D)** Representative western blot of the indicated proteins. Data are expressed as mean±SD relative to vinculin protein expression (n=9).

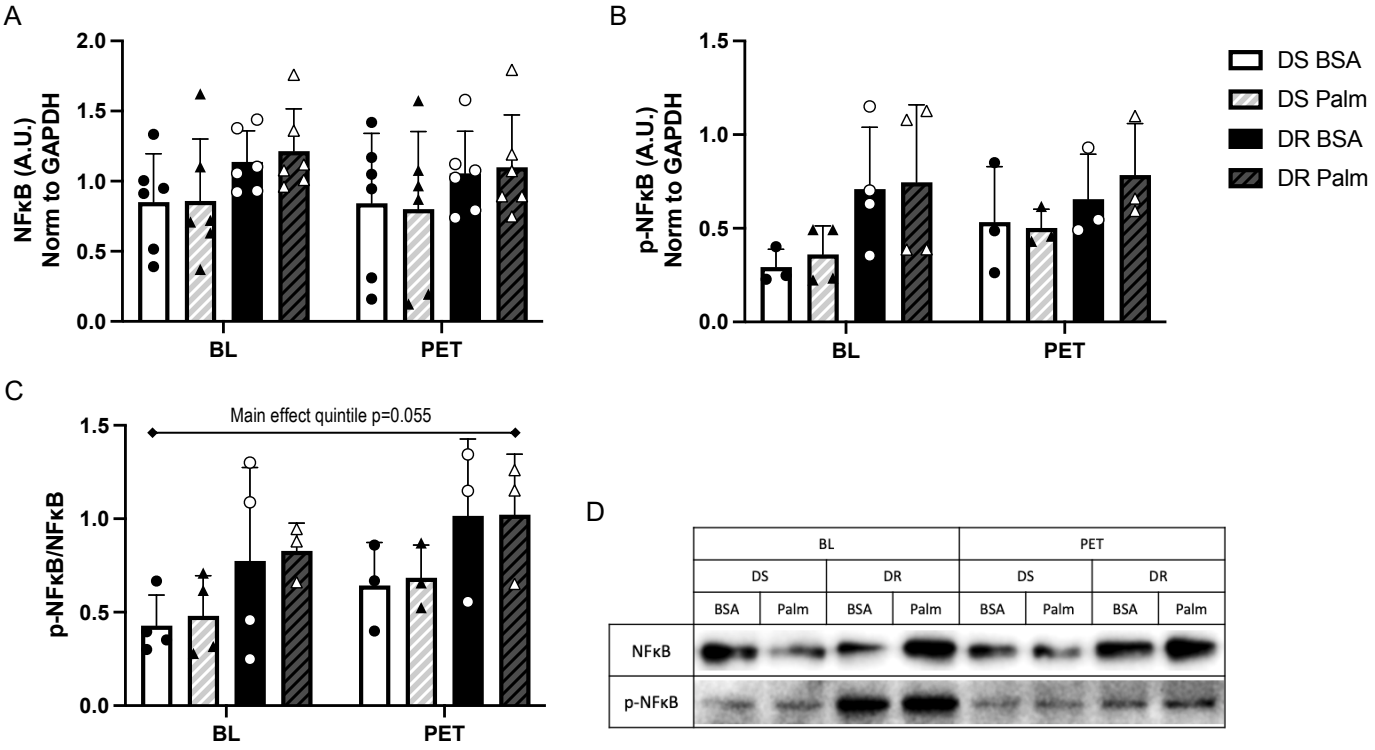

Figure S6. Phospho:total NFκB ratio is increased in DR vs DS primary myotubes. Differentiated myotubes were treated with 500 μM palmitate for 24 hours. Western blots were performed on treated cells and used to quantify: **(A)** the protein expression of NFκB, **(B)** the protein expression of p-NFκB, **(C)** the phospho:total NFκB ratio. **(D)** Representative western blot of the indicated proteins. Data are expressed as mean±SD relative to GAPDH protein expression (n=6 [NFκB], n=4 [p-NFκB]).

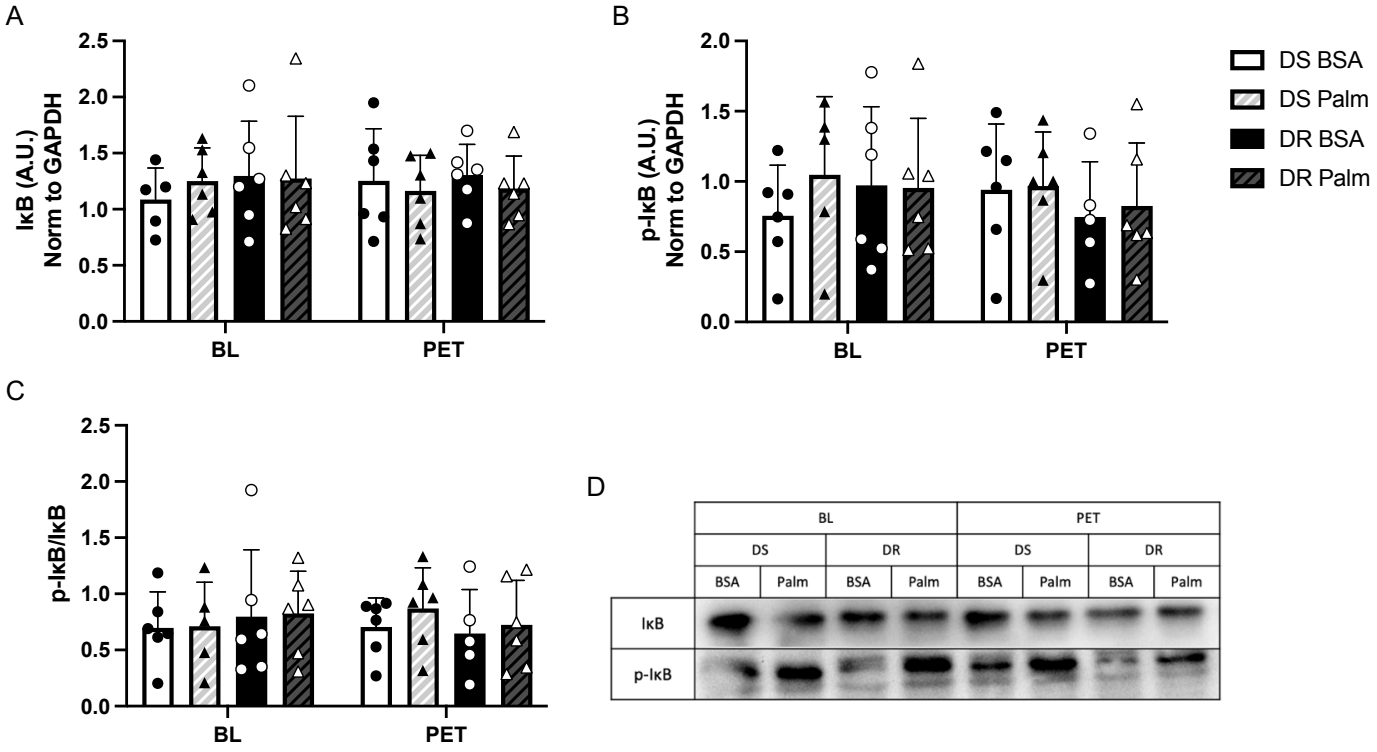

Figure S7. Phospho:total IκB ratio remains unaltered after a palmitate inflammatory challenge. Differentiated myotubes were treated with 500 μM palmitate for 24 hours. Western blots were performed on treated cells and used to quantify: **(A)** the protein expression of IκB, **(B)** the protein expression of p-IκB, **(C)** the phospho:total IκB ratio. **(D)** Representative western blot of the indicated proteins. Data are expressed as mean±SD relative to GAPDH protein expression (n=6).

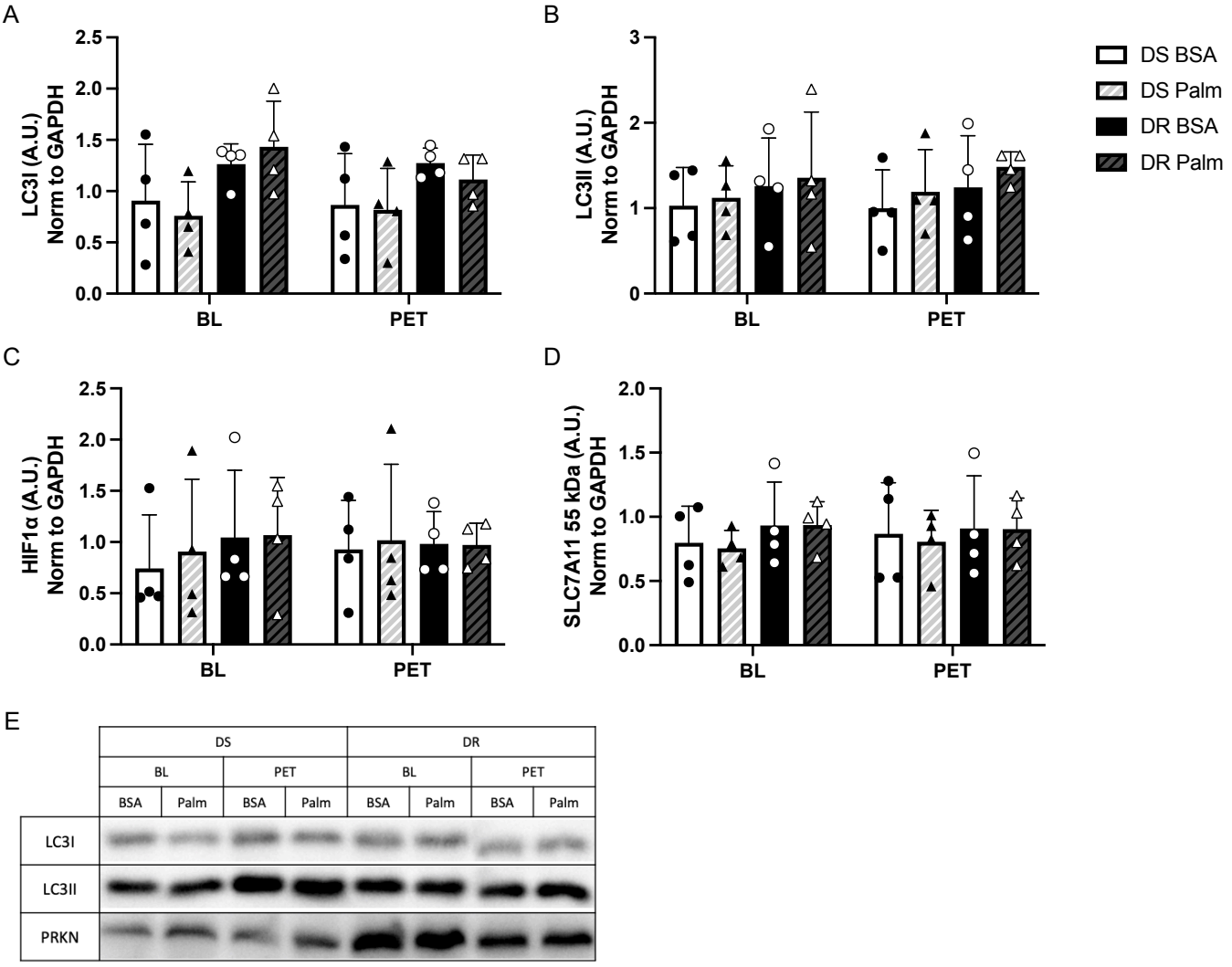

Figure S8. Expression of markers of autophagic flux after a palmitate inflammatory challenge. Differentiated myotubes were treated with 500 µM palmitate for 24 hours. Western blots were performed on treated cells and used to quantify: **(A)** the protein expression of LC3I, **(B)** the protein expression of LC3II, **(C)** the protein expression of HIF1α, **(D)** the protein expression of SLC7A11 (55 kDa). **(E)** Representative western blot of the indicated proteins. Data are expressed as mean±SD relative to GAPDH protein expression (n=4).

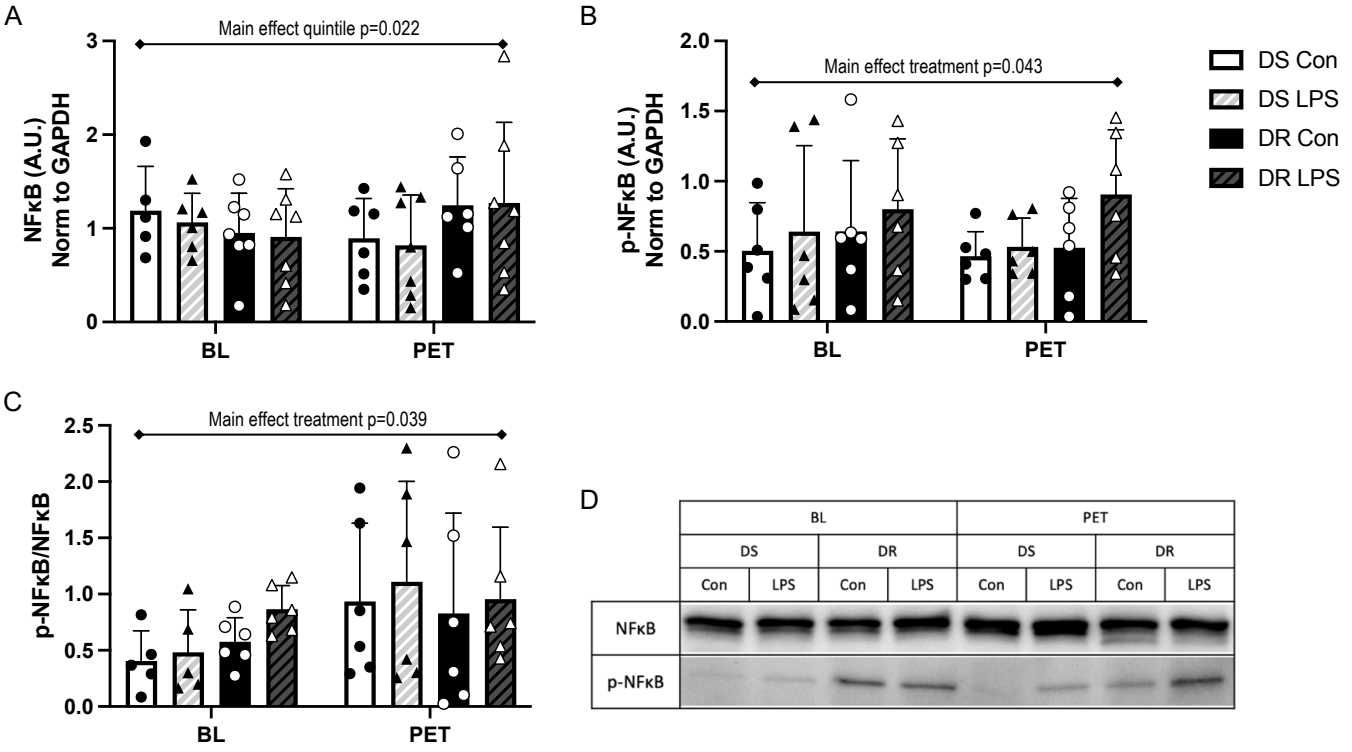

Figure S9. Phospho:total NFκB ratio is increased after an LPS inflammatory challenge. Differentiated myotubes were treated with 100 pg/mL LPS for 24 hours. Western blots were performed on treated cells and used to quantify: **(A)** the protein expression of NFκB, **(B)** the protein expression of p-NFκB, **(C)** the phospho:total NFκB ratio. **(D)** Representative western blot of the indicated proteins. Data are expressed as mean±SD relative to GAPDH protein expression (n=6).

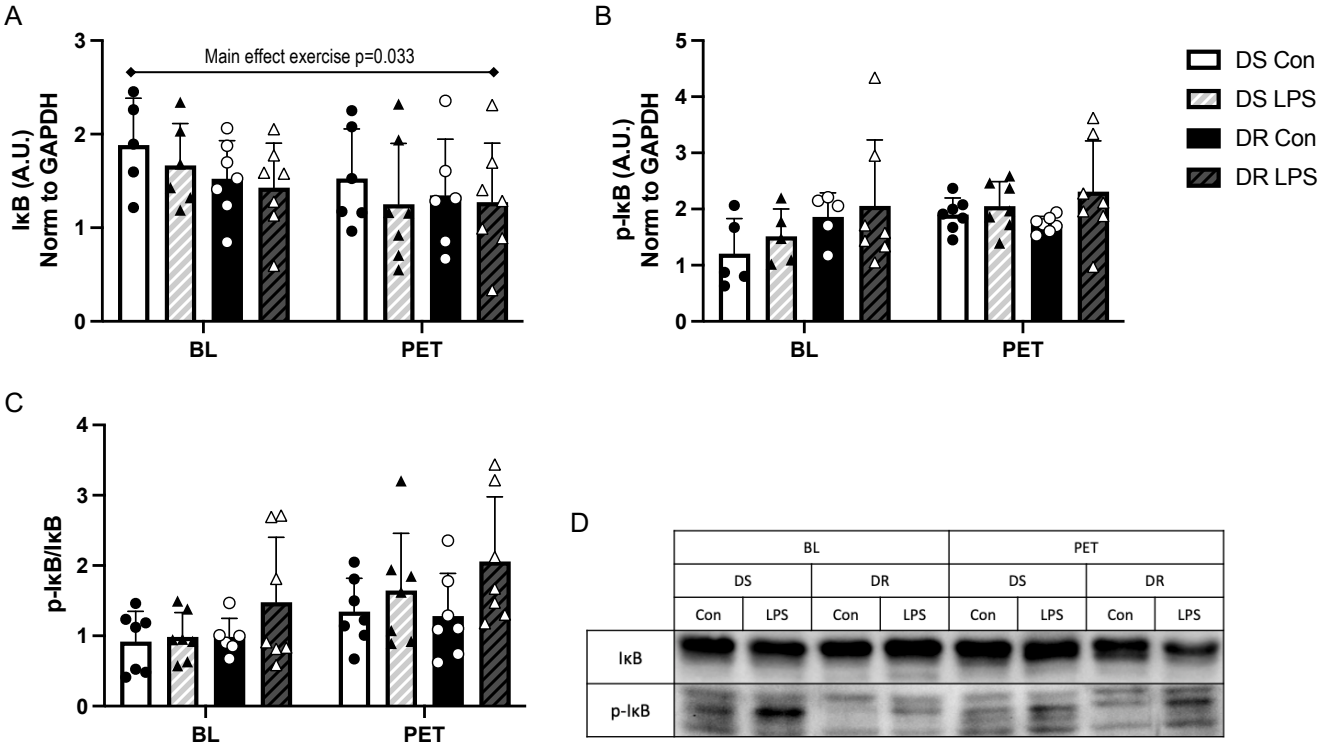

Figure S10. Phospho:total IκB ratio is increased post-exercise in both DS and DR primary myotubes. Differentiated myotubes were treated with 100 pg/mL LPS for 24 hours. Western blots were performed on treated cells and used to quantify: **(A)** the protein expression of IκB, **(B)** the protein expression of p-IκB, **(C)** the phospho:total IκB ratio. **(D)** Representative western blot of the indicated proteins. Data are expressed as mean±SD relative to GAPDH protein expression (n=7).

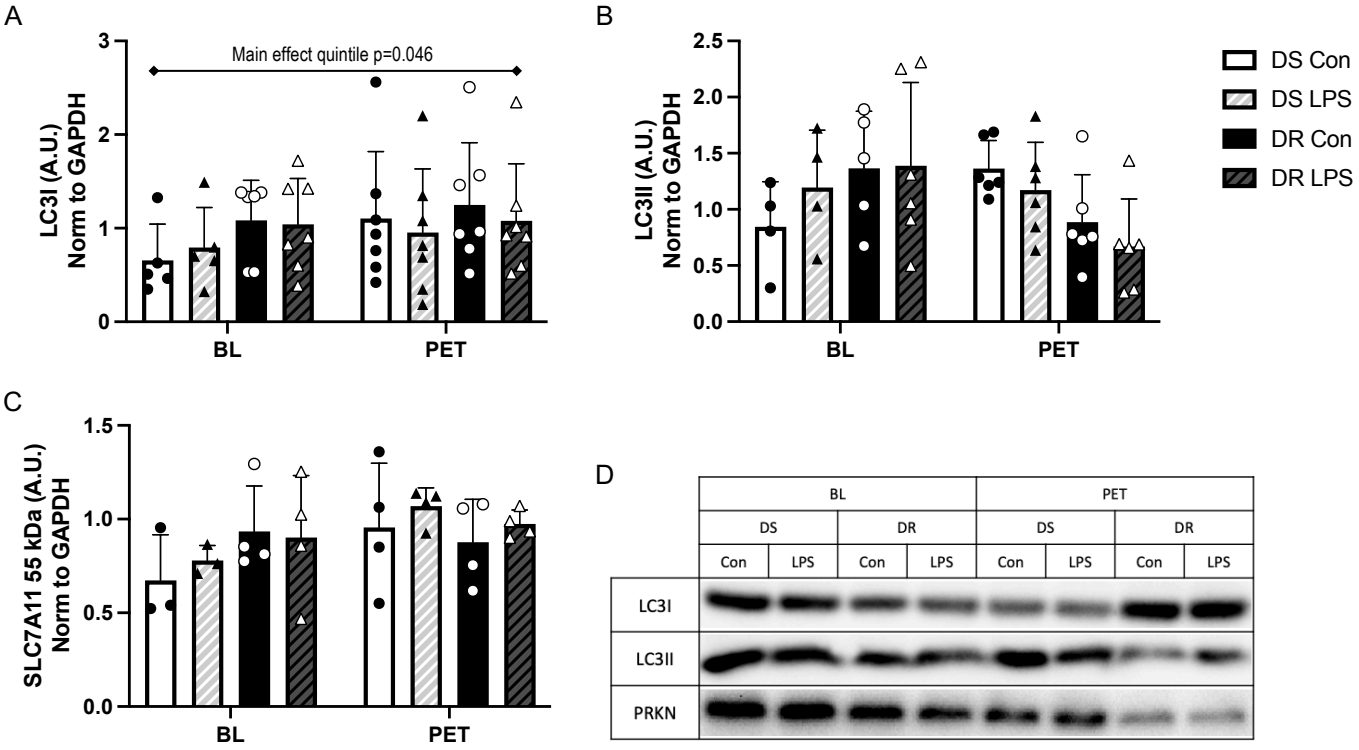

Figure S11. Marker of autophagic flux, LC3I, is preferentially expressed in DR vs DS primary myotubes. Differentiated myotubes were treated with 100 pg/mL LPS for 24 hours. Western blots were performed on treated cells and used to quantify: **(A)** the protein expression of LC3I, **(B)** the protein expression of LC3II, **(C)** the protein expression of SLC7A11 (55 kDa). **(D)** Representative western blot of the indicated proteins. Data are expressed as mean±SD relative to GAPDH protein expression (n=7 [LC3II/I], n=4 [SLC7A11]).